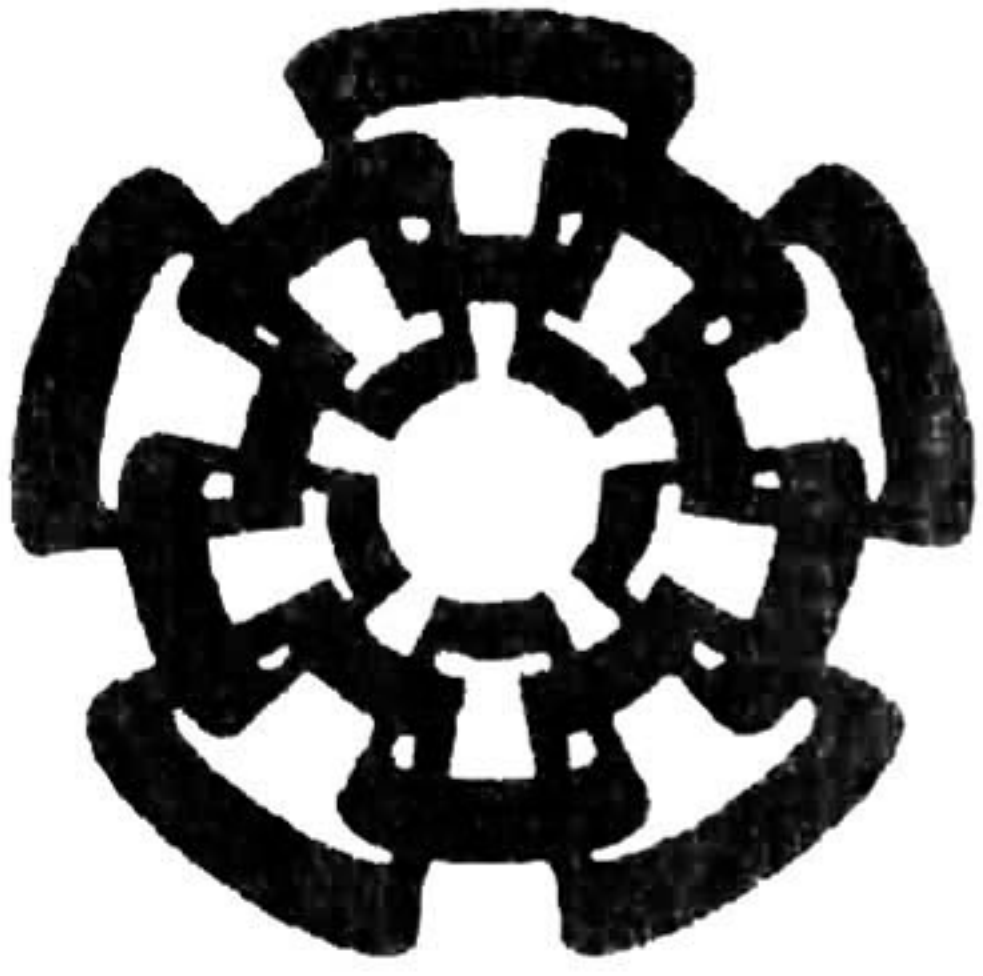


xx(147082.1)



Centro de Investigación y de Estudios Avanzados del I.P.N.
Unidad Guadalajara

Análisis de Sistemas de Potencia que Preservan la Estructura del Modelo Usando Formas Normales

Tesis que presenta:
Irma Martínez Carrillo

para obtener el grado de:
Doctor en Ciencias

en la especialidad de:
Ingeniería Eléctrica

Director de Tesis
Dr. Arturo Román Messina

**CINVESTAV
IPN
ADQUISICION
DE LIB**

Guadalajara, Jalisco, Enero de 2008.

CLASIF.: <u>TK16S.GB .H37</u>
ADQUIS.: <u>BC-505</u>
FECHA: <u>12-XI-2008</u>
PROCED.: <u>Don. - 2008</u>
\$ <u> </u>

2008

ID: 144214-1001

Análisis de Sistemas de Potencia que Preservan la Estructura del Modelo Usando Formas Normales

**Tesis de Doctorado en Ciencias
Ingeniería Eléctrica**

Por:

Irma Martínez Carrillo

Maestro en ciencias

Cinvestav Unidad Guadalajara 2001-2003

Becario de Conacyt, expediente no. 165236

Director de Tesis

Dr. Arturo Román Messina

CINVESTAV del IPN Unidad Guadalajara, Enero de 2008.



Centro de Investigación y de Estudios Avanzados
del I.P.N.

Unidad Guadalajara

A Structure-Preserving Approach to Normal Form Analysis of Power Systems

A thesis presented by:
Irma Martínez Carrillo

to obtain the degree of:
Doctor of Science

in the subject of:
Electrical Engineering

Thesis Advisor:
Dr. Arturo Román Messina

Guadalajara, Jalisco, January 2008.

A Structure-Preserving Approach to Normal Form Analysis of Power Systems

**Doctor of Science Thesis
In Electrical Engineering**

By:

Irma Martínez Carrillo

Master of Sciences in Electrical Engineer
Centro de Investigación y de Estudios Avanzados del I.P.N.,
Unidad Guadalajara
2001-2003

Scholarship granted by CONACYT, No. 165236

Thesis Advisors:
Dr. Arturo Román Messina

CINVESTAV del IPN Unidad Guadalajara, January, 2008.

Acknowledgments

My greater acknowledgment to my advisor Dr. Arturo Román Messina, for the wisdom and patience that led to this work.

With love to my parents, sisters, brothers, nephews and friends.

This thesis is dedicated to Carlos Juárez Toledo and my child Diego.

This work was supported in part by grants from the CONACYT of Mexico under Postgraduate National Program (165236).

Resumen

El comportamiento dinámico de los sistemas de potencia es no lineal y es comprendido por diversos procesos en diferentes escalas de tiempo. El tamaño y la complejidad de estos mecanismos han estimulado a la propuesta de métodos que reducen la dimensión original preservando características esenciales de la naturaleza del sistema. En esta investigación, se propone un método analítico no lineal basado en la teoría de formas normales y técnicas de perturbación singular para el análisis de oscilaciones de gran amplitud. Este enfoque permite que el método de formas normales alcance su máxima capacidad proporcionando una metodología general para su aplicación en una amplia variedad de sistemas no lineales en los diversos campos de la investigación.

Basados en la teoría de formas normales de los sistemas dinámicos, se propone un modelo que preserva la estructura del sistema, las características de la red y la carga. Aprovechando la separación que existe entre la dinámica lenta y rápida, originada por las diferentes escalas de tiempo; una eficiente técnica basada en perturbaciones singulares, es usada para obtener el comportamiento no lineal de los sistemas de potencia preservando exactamente la estructura de la red. Este método no requiere reducción de ecuaciones por lo que se puede obtener información adicional de interés directamente de la red y de la dinámica de la carga del sistema de potencia.

En este trabajo son desarrolladas expresiones analíticas que proporcionan una buena aproximación al comportamiento real del sistema, y además se proponen técnicas para interpretar estas soluciones en términos de funciones modales para designar áreas de control y ubicar dispositivos FACTS; así también se desarrollan criterios para caracterizar los efectos de la red sobre el comportamiento no lineal del sistema. Los procedimientos desarrollados son probados en dos sistemas reales de potencia.

Abstract

Power system dynamic behavior is inherently nonlinear and is driven by different processes at different time scales. The size and complexity of these mechanisms has stimulated the search for methods that reduce the original dimension but retain a certain degree of accuracy. In this dissertation, a novel nonlinear dynamical analysis method for the analysis of large amplitude oscillations that embraces ideas from normal form theory and singular perturbation techniques is proposed. This approach allows the full potential of the normal form method to be reached, and is suitably general for application to a wide variety of nonlinear systems.

Drawing on the formal theory of dynamical systems, a structure-preserving model of the system is developed that preserves network and load characteristics. By exploiting the separation of fast and slow time scales of the model, an efficient approach based on singular perturbation techniques, is then derived for constructing a nonlinear power system representation that accurately preserves network structure. The method requires no reduction of the constraint equations and gives therefore, information about the effect of network and load characteristics on system behavior.

Analytical expressions are then developed that provide approximate solutions to system performance near a singularity and techniques for interpreting these solutions in terms of modal functions are given. New insights into the nature of nonlinear oscillations are also offered and criteria for characterizing network effects on nonlinear system behavior are proposed. Theoretical insight into the behavior of dynamic coupling of differential-algebraic equations and the origin of nonlinearity is given, and implications for analyzing for design and placement of power system controllers in complex nonlinear systems are discussed. The extent of applicability of the proposed procedure is demonstrated by analyzing nonlinear behavior in two realistic test power systems.

Contents

Chapter 1 Introduction

1.1 Motivation and Background	1
1.2 Statement of the Problem	2
1.3 Review of the Previous Work	4
<i>1.3.1 Approaches Based on the Series Expansion of Nonlinear Models</i>	<i>5</i>
<i>1.3.2 Approaches Based on Perturbation Theory</i>	<i>5</i>
<i>1.3.2.1 Method of Normal Forms</i>	<i>6</i>
<i>1.3.2.2 Other Methods of Analysis</i>	<i>7</i>
1.4 Objectives of the Thesis	7
1.5 Contributions of the Thesis	8
1.6 Outline of the Thesis	9
1.7 Publications	10
<i>1.7.1 Refereed Papers in Journals</i>	<i>10</i>
<i>1.7.2 Papers in Conference Proceedings</i>	<i>10</i>
<i>1.7.3 Submitted Papers.</i>	<i>10</i>
References	11

Chapter 2 Power System Normal Form Theory: Theoretical Background

2.1 Introduction	15
2.2 General Concepts	16
2.2.1 Model Formulation	16
2.3 Review of Normal Forms Theory: Existing Approaches	18
2.3.1 Local Analysis and Normal Forms	18
2.3.2 The Jordan Canonical Form	18
2.3.3 Second-Order Normal Form Approximations	19
2.4 Extension to Higher Dimensional Systems	22
4.4.1 Higher Order Power System Representation	22
2.4.2 Nonlinear Coordinate Transformations	25
2.5 Approximate Normal Form Solutions	27
2.5.1 Third-Order Normal Form Approximation	27
2.5.2 Closed-Form Expressions for Second and Higher-Order Approximations	29
2.6 Numerical Example	31
2.6.1 Equations of Motion	32
2.6.2 Numerical Results	32
2.6.3 Linear Approximation	33
2.6.4 Normal Form Solutions	33
2.7 Discussion	38
References	39

Chapter 3 Normal Form of Complex System Models: A Structure-Preserving Approach

3.1 Introduction	42
3.2 Structure-Preserving Power System Model	43
3.2.1 Model Equations	43
3.2.2 Structure-Preserving Power System Model	46
3.3 Singular Perturbations Analysis Approach	48
3.3.1 Singularly Perturbed Dynamics	48
3.4 Normal Form Analysis of the Singularly Perturbed System	50
3.4.1 Second-Order Approximation	50
3.4.2 Jordan Form Representation	51
3.5 Reduction to Normal Form.	52
3.6 Numerical Implementation	53
3.7 Conclusions	54
References	54

Chapter 4 A Structure-Preserving Approach to Power System Normal Form Analysis

4.1 Background	57
4.2 Analytical Approach	57
4.2.1 Closed-Form Analytical Solutions	57
4.2.2 Time Evolution of Network Variables	59
4.2.3 Sensitivity to Parameter Variations	60
4.2.4 Effect of Load Characteristics	62
4.2.5 Transmission Line Participations	65
4.2.6 SVC Voltage Support	66
4.3 Network-Based Participation Factors	68

4.3.1 <i>Nonlinear Participation Factors</i>	68
4.4 Discussion	69
References	70

Chapter 5 Normal Form Analysis of DAE Systems: Application to a Small Test System

5.1 Test Results	72
5.1.1 <i>Modeling Assumptions</i>	72
5.1.2 <i>Modal Characteristics</i>	73
5.2 Numerical Issues	78
5.3 Model Validation	78
5.3.1 <i>Time Domain Simulations and Results</i>	78
5.4 Discussion	90
References	91

Chapter 6 Evaluation of Network Contribution to Global Behavior

6.1 The Test System	93
6.1.1 <i>Modeling Considerations</i>	93
6.2 Modal Analysis	94
6.2.1 <i>Dominant Modes</i>	94
6.2.2 <i>Perturbation-Based Nonlinear Participations</i>	96
6.3 Test Results: Effect of Load Characteristics on System Behavior	97
6.3.1 <i>Ranking of Load Participations: A Linear Analysis Approach</i>	97
6.3.2 <i>Nonlinear Analysis Approach</i>	98
6.3.3 <i>Evaluation of Critical Operating Conditions</i>	101
6.4 Voltage-Based Nonlinear Participation Factors	104

6.5 Conclusions	109
References	110

Chapter 7 General Conclusions and Suggestions for Future Work

7.1 General Conclusions	111
7.2 Suggestions for Future work	112
Appendix A	114
Appendix B	115

List of Figures

Figure 2.1.	Schematic representation of the method of normal forms	31
Figure 2.2.	One-line diagram of the test system	31
Figure 2.3.	Comparison of machine dynamic behavior for an initial perturbation $\Delta\delta^o=15^\circ, \Delta\omega=0$	35
Figure 2.4.	Comparison of machine dynamic behavior for an initial perturbation $\Delta\delta^o=30^\circ, \Delta\omega=0$	36
Figure 2.5.	Comparison of machine dynamic behavior for an initial perturbation $\Delta\delta^o=45^\circ, \Delta\omega=0$	37
Figure 3.1.	Structure-preserving power system representation	43
Figure 3.2.	Flow chart of the structure-preserving normal form analysis procedure	53
Figure 4.1.	Schematic diagram illustrating the derivation of analytical closed-form solutions in physical space	59
Figure 4.2.	Overview of the proposed algorithm for modal analysis	61
Figure 4.3.	Schematic of the adopted power modulation concept	64
Figure 4.4.	Conceptual representation of SVCs for sensitivity analysis	67
Figure 5.1.	Two-area, four-machine test system	72
Figure 5.2.	Comparison of relative rotor angle swings computed with conventional, and the structure preserving model. Case study 1	79

Figure 5.3.	Comparison of relative rotor speed swings computed with conventional, and the structure preserving model. Case study 1	80
Figure 5.4.	Comparison of relative rotor d -axis voltage swings computed with conventional, and the structure preserving model. Case study 1	80
Figure 5.5.	Comparison of relative rotor q -axis voltage swings computed with conventional, and the structure preserving model. Case study 1	81
Figure 5.6.	Comparison of field voltage computed with conventional, and structure preserving model. Case study 1	81
Figure 5.7.	Comparison of relative d -axis current swings computed with conventional, and the structure preserving model. Case study	82
Figure 5.8.	Comparison of relative q -axis current swings computed with conventional, and the structure preserving model. Case study 1	82
Figure 5.9.	Comparison of active output power computed with conventional, and the structure preserving model. Case study 1	83
Figure 5.10.	Comparison of reactive output power computed with conventional, and the structure preserving model. Case study 1	83
Figure 5.11.	Comparison of phase angles computed with conventional, and structure preserving model. Case study 1	84
Figure 5.12.	Comparison of bus voltage magnitude computed with conventional, and structure preserving model. Case study 1	84
Figure 5.13.	Comparison of relative rotor angle swings computed with conventional, and structure preserving model. Case study 2	85
Figure 5.14.	Comparison of relative rotor speed swings computed with conventional, and the structure preserving model. Case study 2	85
Figure 5.15.	Comparison of relative rotor d -axis voltage swings computed with conventional, and the structure preserving model. Case study 2	86
Figure 5.16.	Comparison of relative rotor q -axis voltage swings computed with conventional, and the structure preserving model. Case study 2	86
Figure 5.17.	Comparison of field voltage computed with conventional, and structure preserving model. Case study 2	87
Figure 5.18.	Comparison of relative rotor d -axis current swings computed with conventional, and the structure preserving model. Case study 2	87

Figure 5.19.	Comparison of relative rotor q -axis current swings computed with conventional, and the structure preserving model. Case study 2	88
Figure 5.20.	Comparison of active output power computed with conventional, and structure preserving model. Case study 2	88
Figure 5.21.	Comparison of reactive output power computed with conventional, and structure preserving model. Case study 2	89
Figure 5.22.	Comparison of phase angles computed with conventional, and structure preserving model. Case study 2	89
Figure 5.23.	Comparison of bus voltage magnitude computed with conventional, and structure preserving model. Case study 2.	90
Figure 6.1.	Sixteen-machine, five-area study system	93
Figure 6.2.	Linear participations to generators and dominant active load	98
Figure 6.3.	Location of sensitivity on load buses	100
Figure 6.4.	Interactions of nonlinear sensitivity of load buses	100
Figure 6.5.	Closed-form solutions of active load deviations	101
Figure 6.6.	Comparison of relative rotor speed swings computed with conventional, and the structure preserving model with δ_{16} as reference	.102
Figure 6.7.	Comparison of relative rotor speed swings computed with conventional, and the structure preserving model	.103
Figure 6.8.	Comparison of bus voltage magnitude computed with conventional, and structure preserving model.	.103
Figure 6.9.	Comparison of active power load bus computed with conventional, and structure preserving model	104
Figure 6.10.	Approximate location of dominant second-order participations	106
Figure 6.11.	Comparison of closed-form solutions of selected signals	109

List of Tables

Table 5.1.	Slow eigenvalues of the system for the case study 1 for different values of ε	74
Table 5.2.	Fast pseudo-eigenvalues of the system for the case study 1 for different values of ε	75
Table 5.3.	Slow eigenvalues of the system for the case study 2 for different values of ε	76
Table 5.4.	Fast pseudo-eigenvalues of the system for the case study 2 for different values of ε	77
Table 6.1.	Case 1. Inter-area modes of oscillation	95
Table 6.2.	Case 2. Inter-area modes of oscillation	95
Table 6.3.	Dominant load-based linear participation factors $p_k = u_{kl} v_{kl}$	97
Table 6.4.	Dominant first -order nonlinear participation factor, $P_{2L,\eta}$	99
Table 6.5.	Dominant load bus-based nonlinear participation factors , $P_{2L,kl}$	99
Table 6.6.	Evolutions of inter-area modes to $P_{Lo20} = 5.500$ p.u.	101
Table 6.7.	Evolutions of inter-area modes to $P_{Lo20} = -1.100$ p.u.	102

Table 6.8. Dominant voltage and load based nonlinear participation factors	105
Table 6.9. Dominant voltage-based nonlinear participation factors, P_{2Vqkl}	105

Chapter 1

Introduction

1.1 Motivation and Background

Many power system problems involve non-linear processes. Recently, the problem of nonlinear analysis of stressed power systems has received considerable attention owing to the need to accurately describe and predict the system response to various loading conditions. These techniques have been shown to give improved understanding of the fundamental nature of system nonlinear behavior and have the capability to help in the design and placement of power system controllers [1,2].

Research over the past decade on normal form analysis has led to enormous progress in the development and interpretation of analytical system representations. The main limitations of the above mentioned procedures are their reliance on reduced-order representations of the power system, and the lack of general techniques to explicitly represent network characteristics and the effects of control devices on the transmission system.

Reduced order mathematical models of the power systems have a firm mathematical underpinning and are relatively simple to implement. An important issue of current interest is that of incorporating network characteristics in the analysis procedure which reliably predict nonlinear system behavior. In recent years the incorporation of control characteristics into nonlinear power system stability analysis has received increased attention. Several approaches to represent the network equations explicitly have been described in the literature. These include the representation of dc transmission links and the representation of FACTS controllers [3,4].

Although normal form analysis may be extended to account for the inclusion of control devices on the transmission network, these approaches are limited in practice to simplified system representations, due to the inherent assumptions in the models [3,5]. In addition, the computational cost of evaluating modal characteristics may be prohibitive if the sparse nature of system interconnection is not taken into account. There is, therefore, a strong motivation to extend these approaches to account for both control elements on the transmission network and more realistic load characteristics.

Structure-preserving nonlinear models represented by differential algebraic equations (DAEs) are used in a variety of applications in different sciences such as medicine, mechanics, circuit theory, chemistry and more recently in transient energy function analysis and angle (voltage) stability analysis and control in power systems [6,7] and constitute an important tool for the analysis of the nonlinear characteristics of complex power system models. These approaches can be used to estimate the effect of machine and load characteristics on nonlinear behavior as well as to study structural characteristics. In addition, the network variables contain potentially valuable information for monitoring system behavior and designing wide-area system controllers.

In this thesis, we present a rigorous analytical approach to preserving network structure based on singular perturbation techniques and normal form theory. The method uses symbolic computing capabilities to permit the analysis of nonlinearity in various physical quantities and provides greater insight into the nature and extent of nonlinear behavior.

1.2 Statement of the Problem

Power system dynamics involves a multitude of phenomena occurring on multiple scales from transient processes to slow variations and nonlinear dynamics. The nonlinear behavior of the power systems is described by a set of differential and algebraic equations representing the network constraints.

This approach has several limitations:

- Reduction techniques are error-prone and time consuming
- The network variables contain potentially important information that is destroyed during the reduction process
- These methods are computationally demanding for large-scale problems

The differential-algebraic equations of motion a power system are inherently non-linear, especially under heavy stress or heavy loading conditions. A sound understanding of these characteristics can provide physical insight into

system dynamic performance or network and at the same time be helpful in the study of nonlinear attributes of oscillatory phenomena.

A number of recent studies have sought to identify such interactions and their associated time scales, by analyzing both observational record and the results of transient stability simulations. Recently, the problem of nonlinear analysis of stressed power systems has received considerable attention owing to the need to accurately describe and predict the system response to various loading conditions. Nonlinear effects of electromechanical origin arise in power system dynamic behavior when rotor angle deviations become too large. A problem of special importance arises when the motion of the system is sufficiently large to make the nonlinear terms of the Taylor expansion of the differential-algebraic equations significant.

The nature of these oscillations is complex and can include the interaction nonlinear of the fundamentals modes of oscillations as well as other nonlinear phenomena [8-10]. The complex properties of these oscillations have led to extensive investigation of the nonlinear dynamics. Analytical theories for the analysis of systems described by differential-algebraic systems remains an open problem, except for [11] where recent progress was made. Normal forms of large DAE systems have been studied by Martinez *et al.* Issues such as the effects of load characteristics and the potential for adverse interactions among the network variables have not been fully addressed.

Conventionally, the study of this phenomenon has been approached by assuming linearity in the underlying mechanism giving rise to the observed oscillations; Small signal analysis provides an understanding of the modal structure of a power system that is not clearly shown from time domain simulations. As power systems become more heavily loaded however, complex dynamics, involving interaction between the fundamental modes of the system may occur [12,13]. A clear understanding of this phenomenon is only emerging and techniques are required to assess its effect on various aspects of system performance.

Accurate modeling of power system phenomena that contain highly nonlinear behavior requires a method that takes system nonlinearities into account. Owing to the inherent complexity of nonlinear systems, most of analytical studies deal with linear power system representations. Linear models, however, are incapable of explaining important nonlinear phenomena and may lead to inaccurate system results, especially under stressed operating conditions.

The need for improved modeling and analysis procedures in the study of nonlinear inter-area oscillations has been recently pointed out by several investigators [8-12], [14]. Various approximations have been utilized in the modeling of weakly nonlinear systems. Among them, the method of normal

forms (MNF) has been used to aid in the understanding of the fundamental nature of inter-area oscillations as well as to predict the onset of nonlinear behavior. The method is particularly attractive for the study of nonlinear effects arising from the series expansion of the original non-linear power system representation and is amenable to computer implementation. Another area of interest has been in simulating and analytically approximating the behavior of power system models described by DAE equations.

Relatively little work has been done on modeling network and control system characteristics. Except for the work of Martinez *et al.* [11,15], dealing with structure-preserving models, all the above results were obtained on a reduced-order system representation.

In the brief account that follows, we review recent advances and challenges in modelling, understanding and controlling nonlinear processes. To provide a context for these, the following section begins with a description of the various physical models used in the study of nonlinear systems, then moves to a discussion of the distinction between existing approaches, and various methods for treating nonlinear models.

1.3 Review of the Previous Work

A number of alternative approaches have been proposed in the literature for the analysis and identification of nonlinear phenomena arising in dynamic oscillations. These methods, including direct numerical simulation, methods from dynamical systems theory and bifurcation theory have joined more classical perturbation methods for the study of various aspects of nonlinear dynamics. All currently available methods have some drawbacks.

The physical models used in treating nonlinear phenomena vary enormously in their complexity and range of applicability. Most of the existing system analysis methods are designed for linear processes. Yet, physical processes are seldom linear. In particular, power system behavior is known to exhibit nonlinear and non-stationary behavior.

This approach however, ignores many nonlinear terms and may predict inaccurate results. Further, these tools provide no means for identification or quantization of nonlinear effects and do not take into account any interaction between various modes of oscillation [5,6].

A relatively new perspective is that nonlinear oscillations may result from nonlinear interaction between the fundamental modes of the system. The study of this latter issue has been raised in the literature from diverse perspectives. Four basic approaches for studying several aspects of nonlinear behaviour exist:

1. Direct numerical simulation of the system model [12].

2. Analytical solutions of reduced system representations
3. Semi-analytical approaches based on the series expansion of the nonlinear system models [16-18].
4. Techniques based on perturbation theory

The discussion that follows briefly discusses the study of diverse aspects of power system nonlinear behaviour by other groups, with emphasis in the development and implementation of analytical models. We restrict ourselves to studies in which the same general approach is taken.

1.3.1 Approaches Based on the Series Expansion of Nonlinear Models

Several formulations have been recently developed based on semi-analytical formulations derived from the series expansion of the nonlinear power system representation. In these procedures, the nonlinear system model is expanded in a Taylor or MacLaurin series around an equilibrium point; the series coefficients can be found either numerically or from Taylor series expansions.

The method improves the usual linearization of the system about an equilibrium point and enables to identify nonlinear characteristics using standard linear analysis. In addition to providing a clearer characterization of the processes underlying oscillations, the proposed formulation have some advantages over conventional techniques, particularly for studying nonlinear interactions between modes in both, the frequency and time domain spaces.

In [16], Starret et. al. showed that the dynamic models based on the expansion in series of Taylor of third order can capture conditions of stability, particularly in condition of stress in the operation of the system. In a later work, Sobajic *et al.*, [17] used a similar approach to show the importance of the incorporation of effects of high order in the expansion in series of power of the model of the system and provided a physical interpretation of the mechanism of modal interaction. As observed by several researchers, however, the use of semi-analytical modes does not allow to study of precise form the amplitude of the oscillations as well as the conditions that lead to the loss of synchronism [18,19]. A further disadvantage of these formulations is derived fundamentally from their incapacity to provide analytical measures to identify the origin of nonlinear effects.

1.3.2 Approaches Based on Perturbation Theory

This type of methodologies provides a better understanding of the fundamental nature of the oscillating process and allows the study of various aspects of power system nonlinear behavior [8,9]. The standard procedure for determining the normal form representation requires that all algebraic equations are eliminated. This results in dense, nonlinear formulations that are not amenable

for computer analysis. Standard techniques such as dynamic model reduction can be employed to reduce the original model, but the resulting state space representations are, in general too large for practical computation of the basis linear functions.

The existing methods for the analysis of oscillations nonlinear in power systems are restricted to low-order dimensional representations [20-23]. Recent studies, suggest that the inclusion of effects high order can help to explain the nature of diverse nonlinear effects such as intermode coupling, the generation of harmonic effects and intermodulation, as well as to identify the limits and the mechanism leading to loss of stability [8,24].

Analytical evidences supporting this mechanism are given in a recent paper by the IEEE Task Force on Assessing the Need to include Higher Order Terms for Small-signal Analysis [4]. This work has become a cornerstone for many subsequent studies. One of the novelties of this work is that an attempt is made to compare analytical and numerical results. This is an aspect of the problem that has not been addressed before.

1.3.2.1 Method of Normal Forms

The method of normal form (MNF) is a powerful analytical tool that allows simplifying the study of physical processes described by equations ordinary differentials. The interest of the theory of normal forms like analytical tool for the study of diverse aspects of the behaviour nonlinear of the power system extensively has been recognized in the literature [9-18] and includes the study of the determination of interaction nonlinear mode interaction and the analysis of resonance between modes.

The theory of normal forms applies to the reduced dynamical system derived from center manifold theory. This approach has been successfully used to investigate various aspects of system performance and has resulted in production-grade software.

Nevertheless, few analytical works exist that investigate the effect of high-dimensional system representations. In [16], Starret *et. al.* showed that the dynamic response of the system can include combinations of the fundamental modes of oscillation. Recently, diverse investigators [10]-[16] have suggested the necessity to include terms of greater order in the dynamic response of the system.

Previous work using the MNF was usually concerned with the analysis of second-order effects in the power system representation [13-17]. For higher order systems, there exists no general, systematic procedure for constructing the power system representation and computing the associated normal form transformations [18]. The extension and generalization of these methods to

more complex system representations is an extremely complex problem for which little results have been reported [24]. Further, the required computational cost for its practical implementation can be prohibitive, especially for the study of realistic power system models.

1.3.2.2 Other Methods of Analysis

The study of alternate analytical representations with the ability to extract system dynamic information has recently attracted attention in the power system community. Much of the recent work has been driven by interest in nonlinear mode interaction and its relation to system nonlinear behavior. Arroyo *et al.* utilized a technique based on Carleman linearization to address the problem of nonlinear intermode coupling using a third-order system representation [24]. Another field of study which is currently of great interest is the control of chaos and bifurcations.

In reference [9] a fundamental revision of the characteristics of several methods for the study of the nonlinear behaviour of the power system is presented. The authors emphasize the use of the method of the multiple time scales (MTC), the theory of Floquet-Lyapunov and the spectral method of Galerkin.

These methods have been applied to the study of diverse aspects of power system nonlinear behaviour using simplified system representations. References [19], and [25-27] review some applications of this type of methodologies. The extension of this type of approaches to deal with complex systems, however, has not been reported in the literature.

1.4 Objectives of the Thesis

The primary objective of this dissertation is to extend and generalize the existing normal form analysis methodology to treat large power system models described by nonlinear differentials-algebraic equations (DAEs). This thesis extends the reduced order normal form analysis approach developed by several researchers with the primary goal of obtaining high order normal form representations of nonlinear power system models. To this end, a systematic procedure based in normal form theory and singular perturbation techniques is proposed to investigate nonlinear effects arising from the perturbation model of the power system dynamic representation. In particular, theoretical and computational approaches are combined to establish an efficient, structure-preserving model of the power system for analyzing nonlinear effects arising from the perturbation model of the power system dynamic representation.

A second objective is the development of a modeling framework based on normal form theory and singular perturbation techniques for analyzing the nonlinear behavior of power system that preserves system structure. In contrast

to previous work on normal form analysis of DAEs, this research introduces a new framework for characterization of nonlinear behavior.

A final objective is the extension and generalization of existing techniques to incorporate the effects of network variables into the normal form representation.

1.5 Contributions of the Thesis

The following aspects constitute original contributions in this work:

- The development of a generalized mathematical model of the power system dynamic representation for the study of nonlinear system response around an equilibrium conditions, with emphasis in the study of nonlinear modal interaction and its effect on the global behavior of the system.
- The development of a structure-preserving method for the analysis of system behaviour based on normal form theory and singular perturbation techniques. A perturbation technique based on normal form theory and singular perturbation techniques is developed and extended to, without simplifying assumptions, compute the normal forms of DAE models and the associated normal form transformations. First, the equivalence between the normal representation of the full system model and the reduced system representations is rigorously proved. Then, general solutions are established for the structure-preserving model and algorithms for computing the normal forms of large power system models are developed. Importantly, the dynamic and network variables are retained separately and efficiently in the model.
- The generalization of existing methods to determine the sensitivity of inter-area modes with respect to perturbations in the network parameters. A sensitivity-based method is used as a first approximation for describing and identifying the most disturbed load and buses involved in the oscillation.
- The derivation of an analytical framework to analyze the mapping between different coordinate systems.
- The evaluation of the accuracy of the model. Extensive numerical calculations are performed to support qualitative results.

1.6 Outline of the Thesis

The structure of this dissertation is as follows. In chapter 2, a brief review of classical methods used for the computation of the normal form of vector fields is presented. The Chapter begins by giving an introduction to the study of nonlinear system representations of second and higher-order normal form analysis. A survey of alternative techniques, both approximate and exact, is then provided for the computation of the normal form representation of system described by reduced-order representations. The errors of the approximate representations are reviewed and extensions to the basic algorithm are suggested.

In Chapter 3, a systematic procedure based in the theory of normal form and singular perturbation techniques is proposed for the study of systems described by DAEs. Analytical techniques to represent the effect of second and higher-order nonlinearities resulting from the Taylor series representation of the system model are introduced and methods to account for these effects in the normal form representation are suggested. Finally, issues concerning the implementation of the method and numerical calculations are discussed.

Chapter 4 is devoted to the generalization of existing normal form procedures to compute sensitivity relationships between states and arbitrary perturbations. In particular, an analytical procedure is given to approach the role of transmission network variables in system dynamic performance. Building on the connection between normal form theory and dynamical systems theory a method for identifying relevant disturbed loads and system buses is suggested and various local indices are defined to identify this behavior. Possible analytical procedures which draw upon our results, and which may enhance our understanding of power system nonlinear dynamics, are proposed.

The next two Chapters mainly address the application of normal form theory to the analysis and characterization of nonlinear processes in power systems. Chapter 5 discusses the application of the theory to the conventional study of DAE systems following large perturbations. As an illustrative example, a two-area test power system is employed to verify the accuracy of the developed algorithms. This new framework is further extended to incorporate the representation of nonlinear load characteristics and voltage control devices. The procedure may be easily generalized to deal with more complex system representations.

Chapter 6 presents the development and application of sensitivity based nonlinear participations to the identification of relevant disturbed load and buses.

Finally, Chapter 7 offers a critical interpretation of the results and discusses the limitations of the study as well as the future work.

1.7 Publications

1.7.1 Refereed Papers in Journals

1. Irma Martínez, A. R. Messina and E. Barocio, "Perturbation Analysis of Power systems: Effects of Second and- Third-Order Nonlinear Terms on system Dynamic Behavior" , Electric Power Systems Research, Volume 71, Issue 2, October 2004, Pages 159-167.
2. I. Martinez; A. R. Messina; E. Barocio, "Higher-Order Normal Form Analysis of stressed Power Systems: A Fundamental Study", Electric Power Components and systems, Volume 32, Issue 12 December 2004 , pages 1301 – 1317
3. Irma Martínez, A. R. Messina, and Vijay Vittal, "Normal Form Analysis of Complex System Models: A Structure-Preserving Approach", IEEE Transactions on Power Systems, vol. 22, no. 4, November 2007, pp. 1908-1915.

1.7.2 Papers in Conference Proceedings

1. I. Martínez C., A. R. Messina y E. Barocio, "A Structure-preserving Approach to Power System Normal Form Analysis", In Power Tech 2007, Lausanne, Switzerland, Suiza, July, 2007.
2. R.J. Betancourt, E. Barocio, I. Martinez, A.R. Messina, "Higher-Order Normal Forms analysis of Stressed Power Systems: A non-recursive approach", IEE Power System Conference and Computation 2005, Lieja, Belgica, August 16-20.
3. Betancourt, R.J., Martinez, I., Barocio, E., Roman, A. "Normal Mode Analysis of Inter-Area Oscillations" : Power Systems Conference and Exposition, 2006. PSCE '06. 2006 IEEE PES.

1.7.3 Submitted papers

1. R. J. Betancourt, I. Martínez, E. Barocio and A. R. Messina, "Modal Analysis of Inter-Area Oscillations Using the Theory of Normal Modes", submitted to Electric Power Systems Research, September 2007.
2. I. Martínez, A. R. Messina, "Effect of Load Dynamic Characteristics on System Power Behavior: Analysis of Network Contributions via normal Form", submitted to Journal of nonlinear science, June 2007

3. I. Martínez, A. R. Messina, "Analysis of Complex Power System Model with Multiple Time Scales Using Normal Form", submitted to *Journal of Nonlinear Mathematical Physics*, September 2007.

References

- [1] J.J. Sanchez Gasca, V. Vittal, M. J. Gibbard, A. R. Messina, D. J. Vowles, S. Liu and U. D. Annakkage, "Analysis of higher order terms for small signal stability analysis," *IEEE Power Engineering Society General Meeting*, San Francisco CA., Jun 2005
- [2] Y. X. Ni, V. Vittal and W. Kliemnan, "Nonlinear modal interaction in HVDC/AC power system with DC power modulation", *IEEE Trans. Power Systems*, vol. 11, pp. 2011-2017, Nov 1996
- [3] E. Barocio and A.R. Messina, "Normal form analysis of stressed power systems: incorporation of SVC models", *Electrical Power and Energy Systems*, vol. 25, pp. 79-90, Jan 2003
- [4] P. V. Kokotovic and P. W. Sauer, "Integral manifold as a tool for reduced order modeling of nonlinear systems: A synchronous machine case study", *IEEE Trans. Circuits and Systems*, vol. 36, pp. 403-410, Mar 1989
- [5] K. Read Nolan and W. H. Ray, "Application of nonlinear dynamic analysis in the identification and control of nonlinear system-I. Simple dynamics," *Elsevier Science Ltd*, vol. 8, pp. 1-15, 1988
- [6] J. Haueisen, L. Leistritz, T. Süsse, G. Curio and H. Witte, "Identifying mutual information transfer in the brain with differential-algebraic modeling: Evidence for fast oscillatory coupling between cortical somatosensory areas 3b and 1", *NeuroImage*, vol. 37, pp. 130-136, Aug 2007
- [7] P. W. Sauer and M. A. Pai, *Power System Dynamics and Stability*, Prentice Hall Upper Saddle River, NJ. 1998
- [8] "Nonlinear power system behavior-Extension of linear system analysis via higher order correction", *EPRI Report TR-107798*, Feb. 1997
- [9] "Nonlinear analysis methods for sustained inter-area oscillations", *EPRI Report TR-108821*, Sep 1997
- [10] J. J. Sanchez-Gasca, V. Vittal, M. J. Gibbard, A. R. Messina, D. J. Vowles, S. Liu, and U. D. Annakkage, "Inclusion of higher order terms for small-signal (modal) analysis: committee report-task force on assessing the need to include higher order terms for small-signal (modal) analysis", *IEEE Power Systems*, vol. 20, pp. 1886-1904, Nov 2005

- [11] I. Martínez, A. R. Messina, and V. Vittal, "Normal Form Analysis of Complex System Models: A Structure-Preserving Approach", ", *IEEE Transactions on Power Systems*, vol. 22, pp. 1908-1915, Nov 2007
- [12] P Kundur, *Power System Control and Stability*, McGraw-Hill , 1994
- [13] CIGRE, Task Force 07, "Analysis and Control of Power System Oscillations", *Final Report*, Dec 1996
- [14] P M. Anderson, *Power System Control and Stability*, McGraw-Hill, 1994
- [15] I. Martínez, A. R. Messina, and V. Vittal, "Normal Form Analysis of Complex System Models: A Structure-Preserving Approach", ", *IEEE Transactions on Power Systems*, vol. 22, pp. 1908-1915, Nov 2007
- [16] S. K Starret, W. Klieman, V. Vittal and A.A. Fouad, "Power system modal behavior: Significance of second and third order nonlinear terms", *North America Power Symposium*, Washington D.C., Oct 1993
- [17] D. J. Sobajic, "An introduction to normal forms of vector fields: New framework for assessing stability of highly stressed power systems", *Electrotechnical Conference MELECON'96.*, 8th Mediterranean, vol. 1, pp. 13-16, May 1996
- [18] E. Barocio, "Normal form analysis of stressed power systems using normal forms", PhD Thesis, The Center for Research and Advanced Studies of the National Polytechnic Institute of Mexico, Guadalajara, 2003
- [19] M. Y Vaiman and D. J. Sobajic "A novel approach to compute characteristics of sustained inter-area oscillations", *IEEE Power Engineering Review*, vol. 18, pp. 52-54, Jan 1998
- [20] V. Vittal, N. Bhatia and A.A. Fouad, "Analysis of the inter-area mode phenomenon in power systems following large disturbances, *IEEE Power Systems*, vol. 6, pp. 1515-1521, Nov 1991
- [21] J. Thapar, V. Vittal, W. Kliemann and A. A. Fouad, "Application of the normal form of vector fields to predict interarea separation in power systems" *IEEE Trans. on Power Systems*, Vol. 12pp. 844-850, May 1997
- [22] A. R. Messina and E. Barocio, "Assessment of non-linear modal interaction in stressed power networks using the method of normal forms" *Electrical Power & Energy Systems*, vol. 25, pp. 21-29, Jan 2003

- [23] J. Gilsoo, V. Vittal and W. Kliemann, "Effect of nonlinear modal interaction on control performance: Use of normal forms technique in control design, Part I: General theory and procedure", *IEEE Trans. on Power Systems*, vol. 13, pp. 401-407, May 1998
- [24] A. R. Messina, E. Barocio and J. Arroyo, "Analysis of modal interaction in power systems with FACTS controllers using normal forms", *IEEE General Meeting, Toronto, Canada*, Jul 2003
- [25] Y. Tamura and N. Yorino, "Possibility of auto-and hetero parametric resonances in power systems and their relationship with long term dynamics", *IEEE trans. Power Systems*, pp. 890-897, May 2001
- [26] N. Yorino, H. Sasaki, Y. Tamura and R. Yokoyama "A generalized analysis method of auto- parametric resonances in power systems" *IEEE Trans. on Power Systems*, vol. 4, pp. 1057-1064, Aug 1989
- [27] T. Watanabe, J. Ohishi and K. Yasuda, "Robust damping control of power oscillation incorporating parametric resonance", *Electrical Engineering in Japan*, vol. 142, pp. 42-49, 2003

Chapter 2

Power System Normal Form Theory: Theoretical Background

Normal form theory is one of the most useful and important tools in local analysis of nonlinear dynamical systems in the neighborhood of equilibria. In this chapter a systematic procedure based on normal form theory is proposed to investigate nonlinear effects arising from the perturbation model of the power system dynamic representation.

Using this method, a high-order model of the power systems is proposed in which weak system nonlinearities are explicitly represented. Analytical expressions are then obtained that provide approximate solutions to system performance near a singularity, and techniques for interpreting these solutions in terms of modal functions are given. New insights into the nature of nonlinear oscillations are offered and criteria for characterizing nonlinear effects are discussed. Attention is also focused on assessing the effect of system stress on nonlinear dynamic performance.

The conventional normal form analysis methods are extended to allow for a rigorous treatment of higher order effects. The notation utilized throughout the dissertation is also summarized. We begin by giving a brief overview of the normal form method and the corresponding model governing this problem. A single-machine infinite-bus system (SMIB) system is analyzed as illustrative example.

2.1 Introduction

Recently, the problem of nonlinear analysis of stressed power systems has received considerable attention owing to the need to accurately describe and predict the system response to various loading conditions [1-4]. Nonlinear effects of electromechanical origin arise in power system dynamic behavior when rotor angle deviations become too large. A problem of special importance arises when the motion of the system is sufficiently large to make the nonlinear terms of the Taylor expansion of the differential equations of motion significant. Although the dynamic response of many systems can be described by linear-ordinary-differential or algebraic equations, there also exists many physical phenomena that may not be accurately modeled by linear means.

Perturbation techniques as the method of multiple scales, the harmonic balance method particularly the normal form method (NFM) have found wide acceptance as valuable tools in the analysis of nonlinear system behavior. These methods consist of a first-order or linear approximation for the solution upon which are superimposed correction terms in the forms of a truncated power series [5,6].

Nonlinear analysis techniques based on normal form (NF) theory have been shown to give an improved understanding of the fundamental nature of system nonlinear behavior and have the capability to provide accurate solutions over a wider range of operating conditions [2],[7]. Existing analytical methods for the analysis of nonlinear oscillations in power systems have traditionally been restricted to low-dimensional system representations [3-7]. Recent studies, however, suggest that nonlinearities of higher-order play an important role in determining relevant performance characteristics such as nonlinear modal interaction among modes [8]. Further, a complete understanding of the role of these nonlinearities in determining system behavior is lacking.

This Chapter extends the normal forms method proposed by [1] to explore the effects of higher-order nonlinear terms arising from the series representation of the nonlinear system representation. A general nonlinear analysis technique based on normal form theory is first proposed in which weak system nonlinearities are represented explicitly.

Using this method, a high-order model of the power system is then developed that provides approximate solutions to system performance near a singularity, and techniques for interpreting these solutions in terms of modal functions are given. Attention is focused on assessing the effect of system stress on nonlinear dynamic response.

First, the behavior of a power system model in the vicinity of a point of interest is studied is analytically obtained in terms of the series power expansion of the system model and an equivalent higher-order approximation is reviewed.

Then, the generalization of the technique to derive closed-form analytical approximations to system behavior is discussed.

Several assumptions are introduced in order to formulate practical system representations. These assumptions are consistent with those used in power system nonlinear analysis.

2.2 General Concepts

2.2.1 Model Formulation

The behavior of many dynamical processes in power systems is simulated by nonlinear differential equations describing the underlying process. To introduce the notation and describe the interpolation problem more precisely, we briefly outline the conventional analysis process.

More specifically, suppose the governing equations of the system under consideration is modeled by a high-dimensional set of nonlinear differential equations, of the form

$$\dot{x}_j = f_j(x_1, x_2, \dots, x_n), \quad j = 1, 2, \dots, n \quad (2.1)$$

with initial conditions $x_j(0) = x_j^0$ where n is the number of states. Using vector-matrix notation, (2.1) can be written as

$$\dot{\mathbf{x}} = \mathbf{f}(\mathbf{x}), \quad \mathbf{x} \in \mathcal{R}^n, \quad \mathbf{f} : \mathcal{R}^n \rightarrow \mathcal{R}^n \quad (2.2)$$

where

$$\mathbf{x} = \begin{bmatrix} x_1 \\ x_2 \\ \dots \\ x_n \end{bmatrix} \quad \text{and} \quad \mathbf{f}(\mathbf{x}) = \begin{bmatrix} f_1(\mathbf{x}) \\ f_2(\mathbf{x}) \\ \dots \\ f_n(\mathbf{x}) \end{bmatrix}$$

In Eq. (2.2), \mathbf{x} is an n -dimensional vector of system states, and \mathbf{f} is an autonomous, real n -dimensional vector field in which linear and nonlinear terms are contained [9].

Let \mathbf{x}_{sep} be a stationary or stable equilibrium point (*sep*) such that $\mathbf{f}(\mathbf{x}_{sep}) = \mathbf{0}$ at $t=0$. Assuming that the vector field, $\mathbf{f}(\mathbf{x})$, is continuous and differentiable, the power series expansion of Eq. (2.2) about \mathbf{x}_{sep} up to k th order results in

$$\dot{\mathbf{x}} = \mathbf{A}\mathbf{x} + \sum_{i=2}^k \mathbf{f}_i(\mathbf{x}) \quad (2.3)$$

where matrix \mathbf{A} contains the real part of the original vector field and each $\mathbf{f}_i(\mathbf{x})$ is a real vector-valued polynomial vector of degree i in \mathbf{x} that represents non-linear effects of second order.

A common approach for interpretation and nonlinear analysis has been to assume that (2.3) can be approximated by a low order approximation (i.e $k=2$) [10]. Restricting (2.3) to second order, allows the deviation of system states to be expressed in component form as

$$\dot{x}_j = A_j x + \frac{1}{2!} \mathbf{x}^T \mathbf{H}' \mathbf{x}, \quad j = 1, 2, \dots, n \quad (2.4)$$

where matrix \mathbf{A} contains the Jacobian of the original vector field, and \mathbf{H}' is the j th Hessian matrix, with elements

$$\mathbf{H}_{lm}' = \frac{\partial^2 f_j}{\partial x_l \partial x_m}$$

Equation (2.4) can be written in compact form as

$$\dot{\mathbf{x}} = \mathbf{A}\mathbf{x} + \frac{1}{2!} \begin{bmatrix} \mathbf{x}^T \mathbf{H}^1 \mathbf{x} \\ \mathbf{x}^T \mathbf{H}^2 \mathbf{x} \\ \dots \\ \mathbf{x}^T \mathbf{H}^n \mathbf{x} \end{bmatrix} \quad (2.5)$$

This formulation forms the basis of existing power system normal form approaches [11].

A suitable choice of truncation order r will depend upon the properties of the original equation and the power system operating condition and structure.

In the following section we review the theory behind exiting normal form theory and present new results and extension which will be useful in the context of power system nonlinear analysis. Before going on to the general high-dimensional formulation

2.3 Review of Normal Forms Theory: Existing Approaches

The normal form method is an important tool for studying the behavior of dynamic systems described by differential equations near singularities. In this section, the classical normal form theory of Poincaré is briefly discussed.

2.3.1 Local Analysis and Normal Forms

Consider an n -dimensional nonlinear dynamic system characterized by the first-order differential equation

$$\dot{\mathbf{x}} = \mathbf{f}(\mathbf{x}) = \mathbf{f}_1(\mathbf{x}) + \sum_{k=2}^r \mathbf{f}_k(\mathbf{x}) + O(|\mathbf{x}|^{r+1}) \quad , \mathbf{x}_{sep} = \mathbf{0} \quad (2.6)$$

where \mathbf{x} is an n -dimensional vector of system states; $\mathbf{f}_1(\mathbf{x})$ contains the linear part of the original vector field; $\mathbf{f}_k(\mathbf{x}), k = 2, \dots, r$, contain the nonlinear part, and \mathbf{x}_{sep} is an isolated stable equilibrium point (*sep*); r is the order chosen for the process [6]. For each stable equilibrium point, move the origin to the *sep* such that $\mathbf{x} = \hat{\mathbf{x}} - \mathbf{x}_{sep}$ and consider the modified system $\dot{\mathbf{x}} = \mathbf{f}(\mathbf{x})$. In the above, $O(|\mathbf{x}|^{r+1})$ denotes terms of order $r + 1$.

The basic idea behind the MNF is to use a sequence of non-linear coordinate transformations to construct a form of the original differential equations which is as simple as possible, and keeps the dynamical properties of the original system unchanged. This process usually involves two preliminary steps [12,13]: a) the stable equilibrium point is moved to the origin, so that $\mathbf{f}(\mathbf{0}) = \mathbf{0}$, and b) the linear vector field is transformed to its Jordan canonical form by a linear change of coordinates, initiating with the terms of second order.

2.3.2 The Jordan Canonical Form

Let the matrix $D\mathbf{f}(\mathbf{0}) = \mathbf{A}$ have an eigenvalue set $\{\lambda_1 \ \lambda_2 \ \dots \ \lambda_n\}$ with associated eigenvectors $\mathbf{U} = \text{col}(\mathbf{u}_1, \mathbf{u}_2, \dots, \mathbf{u}_n)$ and reciprocal eigenvectors $\mathbf{V} = (\mathbf{v}_1, \mathbf{v}_2, \dots, \mathbf{v}_n)$. Then, the linear change of coordinates $\mathbf{x} = \mathbf{U}\mathbf{y}$ transforms the system in Eq. (2.2) into its complex Jordan canonical form:

$$\dot{\mathbf{y}} = \mathbf{\Lambda}\mathbf{y} + \mathbf{U}^{-1} \left[\sum_{k=2}^r \mathbf{f}_k(\mathbf{U}\mathbf{y}) \right] = \mathbf{\Lambda}\mathbf{y} + \sum_{k=2}^r \mathbf{F}_k(\mathbf{U}\mathbf{y}) + O(|\mathbf{y}|^{r+1}) \quad (2.7)$$

where $\mathbf{y} \in C^n$ is the vector of Jordan form coordinates, matrix $\mathbf{\Lambda} = \mathbf{U}^{-1}\mathbf{A}\mathbf{U}$ is the diagonal matrix of system eigenvalues and the vectors $\mathbf{F}_j(\mathbf{y}) = \mathbf{U}^{-1}\mathbf{f}_j(\mathbf{U}\mathbf{y}), j = 2, \dots, n$. are complex-valued polynomials vector of order j

in \mathbf{y} , and $\mathbf{F}_k(\mathbf{y}) = [F_k^1(\mathbf{y}) \ F_k^2(\mathbf{y}) \ \dots \ F_k^n(\mathbf{y})]^T$ in which the nonlinear terms are defined to be

$$\begin{aligned}
 F_2^j &= \sum_{k=1}^n \sum_{l=k}^n C_{2_{kl}}^j y_k y_l, & \text{for } k=2 \\
 F_3^j &= \sum_{k=1}^n \sum_{l=k}^n \sum_{m=l}^n C_{3_{klm}}^j y_k y_l y_m, & \text{for } k=3 \\
 & \dots
 \end{aligned} \tag{2.8}$$

for $j=1, \dots, n$, in which the $C_{2_{kl}}^j, C_{3_{klm}}^j, \dots$ are the second and higher-order Jordan-form coefficients. The underlying idea of NF theory is to find an analytical change of coordinates with the origin as a fixed point, such that the vector field $\mathbf{f}(\mathbf{x})$ becomes simpler to study in terms of the new variables [5]. The calculation of coefficients can be done recursively in a computationally efficient manner as discussed below.

2.3.3 Second-Order Normal Form Approximations

In the analysis of complex, high-dimensional systems, a common approximation is to ignore higher order terms in the Taylor series representation (2.6). Intuitively, the errors of the low-dimensional representation should be small if nonlinear effects are small.

Assume in order to introduce these concepts, that the system is truncated at second order. We seek a near identity coordinate change of the form [12,13]

$$\mathbf{y} = \mathbf{z} + \mathbf{h}_2(\mathbf{z}) \tag{2.9}$$

where $\mathbf{z} = (z_1 \ z_2 \ \dots \ z_n) \in C^n$ represents the new space or coordinate system, and $\mathbf{h}_i(\mathbf{z}) \geq 2$ represents polynomials vectors of order i which must be determined. Substitution of (2.6) into (2.6) and use of the chain rule yields

$$\dot{\mathbf{z}} = \mathbf{Lz} + \mathbf{g}(\mathbf{z}) = [\mathbf{I} + D\mathbf{h}_2(\mathbf{z})]^{-1} [\mathbf{\Lambda}(\mathbf{z} + \mathbf{h}_2(\mathbf{z})) + \mathbf{f}_2(\mathbf{z} + \mathbf{h}_2(\mathbf{z}))] \tag{2.10}$$

or at order $|\mathbf{z}|^2$,

$$\dot{\mathbf{z}} = \mathbf{\Lambda z} + \mathbf{g}(\mathbf{z}) = \mathbf{\Lambda z} + \mathbf{\Lambda h}_2(\mathbf{z}) - D\mathbf{h}_2(\mathbf{z}) + \mathbf{\Lambda h}_2(\mathbf{z}) + O(|\mathbf{z}|^3) + \mathbf{g}(\mathbf{z}) \tag{2.11}$$

where

$$D\mathbf{h}_2(\mathbf{z}) = \begin{bmatrix} \frac{\partial h_1(\mathbf{z})}{\partial z_1} & \frac{\partial h_1(\mathbf{z})}{\partial z_2} & \dots & \frac{\partial h_1(\mathbf{z})}{\partial z_n} \\ \frac{\partial h_2(\mathbf{z})}{\partial z_1} & \frac{\partial h_2(\mathbf{z})}{\partial z_2} & \dots & \frac{\partial h_2(\mathbf{z})}{\partial z_n} \\ \vdots & \vdots & \ddots & \vdots \\ \frac{\partial h_n(\mathbf{z})}{\partial z_1} & \frac{\partial h_n(\mathbf{z})}{\partial z_2} & \dots & \frac{\partial h_n(\mathbf{z})}{\partial z_n} \end{bmatrix}$$

If $\mathbf{h}_2(\mathbf{z})$ can be chosen so that the commutator or Lie bracket $\Lambda\mathbf{h}_2(\mathbf{z}) - D\mathbf{h}_2(\mathbf{z}) = [\Lambda\mathbf{z}, \mathbf{h}_2(\mathbf{z})]$ cancels every term in $\mathbf{f}_2(\mathbf{z})$, we have transformed all quadratic terms in (2.10) into cubic and higher order terms. The terms $\mathbf{g}_i(\mathbf{z}) \geq 2$ are called resonant terms that cannot be eliminated by the transformations in (2.6) and contain the essential part of the dynamic system; The system in Eq. (2.11) is called the normal form of the equations (2.2). If no resonant conditions $\mathbf{g}(\mathbf{z})$ are met, this system reduces to $\dot{\mathbf{z}} = \Lambda\mathbf{z}$.

The following theorems and definitions provide the theoretical basis of the method of normal forms.

Definition 2.1. A vector field $\mathbf{f}(\mathbf{x}), \mathbf{f}(\mathbf{0}) = \mathbf{0}$ has a resonant normal form if $\mathbf{f}(\mathbf{x}) = \mathbf{J}\mathbf{x} + \mathbf{f}_2(\mathbf{x})$, where \mathbf{J} has the normal form of Jordan and the nonlinear part of $\mathbf{f}_2(\mathbf{x})$ consists, exclusively, of resonant terms.

In other words, the series $\mathbf{f}_2^j(\mathbf{x})$ contains only monomials $x_1^{m_1} x_2^{m_2} \dots x_n^{m_n}$, where m_1, m_2, \dots, m_n satisfy the relations

$$\lambda_j = (m, \lambda) = \sum_{i=1}^n m_i \lambda_i \tag{2.12}$$

$$m = (m_1 \quad m_2 \quad \dots \quad m_n) \quad , \quad m_k \geq 0 \quad , \quad \sum_{i=1}^n m_i \geq 2$$

between the eigenvalues of \mathbf{J} . In addition, the condition assures that the nonlinear terms in $x_1^{m_1} x_2^{m_2} \dots x_n^{m_n}$ are purely nonlinear.

Theorem 2.1 [14,15]. If the eigenvalues of \mathbf{J} are not resonant, then the system described in Eq. (2.14), can be reduced to the linear equation

$$\dot{\mathbf{z}}_2 = \Lambda\mathbf{z}_2 \tag{2.13}$$

by means of a formal change of variables or nonlinear transformations of the form (2.6). This is referred to as the Theorem of Poincaré-Dulac.

It then follows that, if the eigenvalues of \mathbf{J} are not resonant, the nonlinear vectorial field in Eq. (2.3) can be transformed to a linear vector field.

As a first step toward determining the normal form representation, consider the second-order nonlinear transformation (2.13). Introducing this transformation in Eq. (2.6) and making use of Eq. (2.14) results in

$$\dot{\mathbf{z}}_2 = [\mathbf{I} + D\mathbf{h}_2(\mathbf{z}_2)]^{-1} \{ \Lambda \mathbf{z}_2 + \Lambda \mathbf{h}_2(\mathbf{z}_2) + \mathbf{F}_2(\mathbf{z}_2) \} \quad (2.14)$$

A convenient method for solving Eq. (2.15) consists of approximating the matrix $[\mathbf{I} + D\mathbf{h}_2(\mathbf{z}_2)]^{-1}$ by the first few terms of the Taylor expansion [2]. It can be easily proved that for small enough values of \mathbf{z}_2 , the Taylor series expansion of $[\mathbf{I} + D\mathbf{h}_2(\mathbf{z}_2)]^{-1}$ with respect to $D\mathbf{h}_2$ exists and is given by

$$[\mathbf{I} + D\mathbf{h}_2(\mathbf{z}_2)]^{-1} \approx \mathbf{I} - D\mathbf{h}_2(\mathbf{z}_2) + (D\mathbf{h}_2(\mathbf{z}_2))^2 - (D\mathbf{h}_2(\mathbf{z}_2))^3 + \dots \quad \text{as } |\mathbf{z}| \rightarrow 0 \quad (2.15)$$

since

$$[\mathbf{I} - D\mathbf{h}_2(\mathbf{z}_2) + (D\mathbf{h}_2(\mathbf{z}_2))^2 - (D\mathbf{h}_2(\mathbf{z}_2))^3 + \dots][\mathbf{I} - D\mathbf{h}_2(\mathbf{z}_2)] = \mathbf{I} \quad (2.16)$$

Carrying out the operations indicated in Eq. (2.15), the second-order system behavior may be approximated by

$$\dot{\mathbf{z}}_2 = \Lambda \mathbf{z}_2 + \hat{\mathbf{F}}_2(\mathbf{z}_2) + O(|\mathbf{z}|^{k+1}) \quad (2.17)$$

where the second order terms are given by

$$\hat{\mathbf{F}}_2 = \mathbf{F}_2(\mathbf{z}_2) + \Lambda \mathbf{h}_2(\mathbf{z}_2) - D\mathbf{h}_2(\mathbf{z}_2)\Lambda \mathbf{z}_2 \quad (2.18)$$

We refer to Eq. (2.18) as the second-order normal form system. The analysis of (2.19) suggests that in order to remove second order terms, the nonlinear transformation vector $\mathbf{h}_2(\mathbf{z}_2)$ may be determined from the solution of the homological equations

$$[\mathbf{h}_2(\mathbf{z}_2), \Lambda] = D\mathbf{h}_2(\mathbf{z}_2)\Lambda \mathbf{z}_2 - \Lambda \mathbf{h}_2(\mathbf{z}_2) = \hat{\mathbf{F}}_2(\mathbf{z}_2) \quad (2.19)$$

where $L_A(\mathbf{h}_2(\mathbf{z}_2)) = [\mathbf{h}_2(\mathbf{z}_2), \Lambda]$ is the Lie or Poisson bracket [6].

It can readily be proved that if no resonance conditions are found, all nonlinear terms of second order can be annihilated and the vectors $\mathbf{h}_2(\mathbf{z}_2)$ are obtained from

$$\mathbf{h}_2(\mathbf{z}_2) = \mathbf{L}_A^{-1} \hat{\mathbf{F}}_2(\mathbf{z}_2) \quad (2.20)$$

Solving (2.21) for the normal form transformation coefficients yields [6]

$$h_{2,kl}^j = \frac{C_{2,kl}^j}{(\lambda_k + \lambda_l - \lambda_j)}, \quad j, k, l = 1, 2, \dots, n \quad (2.21)$$

for $j = 1, 2, \dots, n$, provided that $\lambda_k + \lambda_l - \lambda_j \neq 0$ where the $C_{2,kl}^j$ are defined in Eq. (2.12) and higher order terms are neglected.

At second-order, the approximate normal form representation for the system in Eq. (2.6) may then be written as

$$\dot{\mathbf{z}}_2 \approx \Lambda \mathbf{z}_2 + O(3) \quad (2.22)$$

where $\Lambda = \text{diag}[\lambda_1 \ \lambda_2 \ \dots \ \lambda_n]$ and $O(3)$ denotes third and higher order terms that can not be eliminated or canceled by the non-linear transformation. Eq. (2.22) simplifies to the linear system $\dot{\mathbf{z}} = \Lambda \mathbf{z}$, if higher order terms $O(3)$ are neglected.

With this approach, a nonlinear system can be approximated to any arbitrary degree of accuracy over a wider range of operating conditions [2],[7].

Although acceptable for very small problems, this strategy has a number of defects:

- (i). Recursive computations result in neglected terms that are not accounted for
- (ii). These missing effects can cause significant model errors, such as overlooking internal resonances or ignoring critical mode interactions

2.4 Extension to Higher Dimensional Systems

The extension of the above approach to the higher dimensional case has been recently considered by Martínez *et al.* [16]. We next briefly review this approach.

2.4.1 Higher Order Power System Representation

Consider a non-linear dynamical system described by the differential equation in (2.2). Let now the series expansion of higher order of a scalar function of a vector \mathbf{x} , $f_k(\mathbf{x})$, about \mathbf{x}^0 be written as

$$\begin{aligned}
f_k(\mathbf{x}) = & f_k(\mathbf{x}^o) + \left[\frac{\partial f_k(\mathbf{x}^o)}{\partial \mathbf{x}^o} \right] (\mathbf{x} - \mathbf{x}^o) + \frac{1}{2} (\mathbf{x} - \mathbf{x}^o)^T \left[\frac{\partial}{\partial \mathbf{x}^o} \left(\frac{\partial f_k(\mathbf{x}^o)}{\partial \mathbf{x}^o} \right) \right]^T (\mathbf{x} - \mathbf{x}^o) + \\
& \frac{1}{6} (\mathbf{x} - \mathbf{x}^o)^T \left\{ (\mathbf{x} - \mathbf{x}^o)^T \frac{\partial}{\partial \mathbf{x}^o} \left(\frac{\partial}{\partial \mathbf{x}^o} \left[\frac{\partial f_k(\mathbf{x}^o)}{\partial \mathbf{x}^o} \right] \right)^T \right\} (\mathbf{x} - \mathbf{x}^o) + \dots
\end{aligned} \tag{2.23}$$

for $k = 1, \dots, n$.

For consistency, and in order to see the recursive relationships between successive order, we rewrite the series expansion as a vector matrix relationship.

Substituting this expression into Eq. (2.2) yields the perturbed model

$$\dot{\mathbf{x}} = \mathbf{f}_1(\mathbf{x}) + \mathbf{f}_2(\mathbf{x}) + \mathbf{f}_3(\mathbf{x}) + \mathbf{f}_4(\mathbf{x}) + \dots \tag{2.24}$$

where $\mathbf{f}_1(\mathbf{x}) = \mathbf{A}\mathbf{x}$, and

$$\mathbf{A} = D\mathbf{f}(\mathbf{0}) = \begin{bmatrix} \frac{\partial f_1}{\partial x_1} & \frac{\partial f_1}{\partial x_2} & \frac{\partial f_1}{\partial x_n} \\ \frac{\partial f_2}{\partial x_1} & \frac{\partial f_2}{\partial x_2} & \frac{\partial f_2}{\partial x_n} \\ \vdots & \vdots & \vdots \\ \frac{\partial f_n}{\partial x_1} & \frac{\partial f_n}{\partial x_2} & \frac{\partial f_n}{\partial x_n} \end{bmatrix}_{\mathbf{x}=\mathbf{x}_{sep}} ;$$

$$\mathbf{f}_2(\mathbf{x}) = \frac{1}{2!} \begin{bmatrix} \mathbf{x}^T \mathbf{H}_2^1 \mathbf{x} \\ \mathbf{x}^T \mathbf{H}_2^2 \mathbf{x} \\ \vdots \\ \mathbf{x}^T \mathbf{H}_2^n \mathbf{x} \end{bmatrix} ;$$

$$\mathbf{f}_3(\mathbf{x}) = \frac{1}{3!} \begin{bmatrix} \mathbf{x}^T \mathbf{H}_3^1 \begin{bmatrix} \mathbf{x} & \mathbf{0} \\ \mathbf{0} & \mathbf{x} \end{bmatrix} \mathbf{x} \\ \mathbf{x}^T \mathbf{H}_3^2 \begin{bmatrix} \mathbf{x} & \mathbf{0} \\ \mathbf{0} & \mathbf{x} \end{bmatrix} \mathbf{x} \\ \vdots \\ \mathbf{x}^T \mathbf{H}_3^n \begin{bmatrix} \mathbf{x} & \mathbf{0} \\ \mathbf{0} & \mathbf{x} \end{bmatrix} \mathbf{x} \end{bmatrix}; \quad \mathbf{f}_4(\mathbf{x}) = \frac{1}{4!} \begin{bmatrix} \mathbf{x}^T \mathbf{H}_4^1 \begin{bmatrix} \begin{bmatrix} \mathbf{x} & \mathbf{0} \\ \mathbf{0} & \mathbf{x} \end{bmatrix} \mathbf{x} & \begin{bmatrix} \mathbf{0} \\ \mathbf{0} \end{bmatrix} \\ \begin{bmatrix} \mathbf{0} \\ \mathbf{0} \end{bmatrix} & \begin{bmatrix} \mathbf{x} & \mathbf{0} \\ \mathbf{0} & \mathbf{x} \end{bmatrix} \mathbf{x} \end{bmatrix} \mathbf{x} \\ \mathbf{x}^T \mathbf{H}_4^2 \begin{bmatrix} \begin{bmatrix} \mathbf{x} & \mathbf{0} \\ \mathbf{0} & \mathbf{x} \end{bmatrix} \mathbf{x} & \begin{bmatrix} \mathbf{0} \\ \mathbf{0} \end{bmatrix} \\ \begin{bmatrix} \mathbf{0} \\ \mathbf{0} \end{bmatrix} & \begin{bmatrix} \mathbf{x} & \mathbf{0} \\ \mathbf{0} & \mathbf{x} \end{bmatrix} \mathbf{x} \end{bmatrix} \mathbf{x} \\ \vdots \\ \mathbf{x}^T \mathbf{H}_4^n \begin{bmatrix} \begin{bmatrix} \mathbf{x} & \mathbf{0} \\ \mathbf{0} & \mathbf{x} \end{bmatrix} \mathbf{x} & \begin{bmatrix} \mathbf{0} \\ \mathbf{0} \end{bmatrix} \\ \begin{bmatrix} \mathbf{0} \\ \mathbf{0} \end{bmatrix} & \begin{bmatrix} \mathbf{x} & \mathbf{0} \\ \mathbf{0} & \mathbf{x} \end{bmatrix} \mathbf{x} \end{bmatrix} \mathbf{x} \end{bmatrix}$$

...

where $\mathbf{f}_3, \mathbf{f}_4$ are a real vector-valued polynomial vectors of degree i in \mathbf{x} that represent non-linear effects and the $\mathbf{H}_2^j, \mathbf{H}_3^j, \mathbf{H}_4^j, j=1,2,\dots,n$ are constant matrices given by

$$\mathbf{H}_2^j = \begin{bmatrix} \frac{\partial^2 f_j}{\partial x_1^2} & \frac{\partial^2 f_j}{\partial x_1 \partial x_2} & \frac{\partial^2 f_j}{\partial x_1 \partial x_n} \\ \frac{\partial^2 f_j}{\partial x_1 \partial x_2} & \frac{\partial^2 f_j}{\partial x_2^2} & \frac{\partial^2 f_j}{\partial x_2 \partial x_n} \\ \frac{\partial^2 f_j}{\partial x_1 \partial x_n} & \frac{\partial^2 f_j}{\partial x_2 \partial x_n} & \frac{\partial^2 f_j}{\partial x_n^2} \end{bmatrix}_{\mathbf{x}=\mathbf{x}_{cp}}; \quad \mathbf{H}_3^j = \begin{bmatrix} \frac{\partial^3 f_j}{\partial x_1^3} & \frac{\partial^3 f_j}{\partial x_1^2 \partial x_2} & \dots & \frac{\partial^3 f_j}{\partial x_1 \partial x_n^2} \\ \frac{\partial^3 f_j}{\partial x_2 \partial x_1^2} & \frac{\partial^3 f_j}{\partial x_2^2 \partial x_1} & \dots & \frac{\partial^3 f_j}{\partial x_2 \partial x_n^2} \\ \frac{\partial^3 f_j}{\partial x_n \partial x_1^2} & \frac{\partial^3 f_j}{\partial x_n \partial x_1 \partial x_2} & \dots & \frac{\partial^3 f_j}{\partial x_n^3} \end{bmatrix}_{\mathbf{x}=\mathbf{x}_{cp}}$$

Analogous results to those described above, can be shown to hold for higher-order representations.

Then, the linear change of coordinates $\mathbf{x} = \mathbf{U}\mathbf{y}$ transforms the system in Eq. (2.2) into its complex Jordan canonical form:

$$\dot{\mathbf{y}} = \Lambda \mathbf{y} + \mathbf{U}^{-1} \left[\sum_{k=2}^r \mathbf{f}_k(\mathbf{U}\mathbf{y}) \right] = \Lambda \mathbf{y} + \sum_{k=2}^r \mathbf{F}_k(\mathbf{U}\mathbf{y}) + O(|\mathbf{y}|^{r+1}) \quad (2.25)$$

where $\mathbf{y} \in \mathbb{C}^n$ is the vector of Jordan form coordinates, matrix $\Lambda = \mathbf{U}^{-1} \mathbf{A} \mathbf{U}$ is the diagonal matrix of system eigenvalues and the vectors

$\mathbf{F}_j(\mathbf{y}) = \mathbf{U}^{-1} \mathbf{f}_j(\mathbf{U}\mathbf{y})$, $j = 2, \dots, n$. are complex-valued polynomials vector of order j in \mathbf{y} , and $\mathbf{F}_k(\mathbf{y}) = [F_k^1(\mathbf{y}) \ F_k^2(\mathbf{y}) \ \dots \ F_k^n(\mathbf{y})]^T$ in which the nonlinear terms are defined to be

$$\begin{aligned} F_2^j &= \sum_{k=1}^n \sum_{l=k}^n C_{2kl}^j y_k y_l, & \text{for } k = 2 \\ F_3^j &= \sum_{k=1}^n \sum_{l=k}^n \sum_{m=l}^n C_{3klm}^j y_k y_l y_m, & \text{for } k = 3 \\ & \dots \end{aligned} \quad (2.26)$$

for $j = 1, \dots, n$, in which the $C_{2kl}^j, C_{3klm}^j, \dots$ are the second and higher-order Jordan-form coefficients.

2.4.2 Nonlinear Coordinate Transformations

Let $s \geq 2$. Consider a formal nonlinear transformation [5,6]

$$\mathbf{y} = \mathbf{z}_s + \mathbf{h}_s(\mathbf{z}_s) \quad (2.27)$$

where the $\mathbf{h}_s(\mathbf{z}_s)$ are undefined complex-valued polynomial vectors to be determined so that the terms of order s will be simplified or eliminated; the vectors $\mathbf{z}_s \in C^n$, $s = 3, 4, \dots, r$ denote the new coordinate systems.

Introducing these transformations in Eq. (2.29) results in

$$\begin{aligned} \dot{\mathbf{z}}_k &= [\mathbf{I} + D\mathbf{h}_k(\mathbf{z}_k)]^{-1} [\mathbf{I} + D\mathbf{h}_{k-1}(\mathbf{z}_{k-1})]^{-1} \dots \\ & [\mathbf{I} + D\mathbf{h}_2(\mathbf{z}_2)]^{-1} \left\{ \Lambda \mathbf{z}_k + \Lambda \mathbf{h}_k(\mathbf{z}_k) + \sum_{m=2}^r \hat{\mathbf{F}}_m(\mathbf{z}_k) \right\} \end{aligned} \quad (2.28)$$

It can be proved that for $|\mathbf{z}|$ sufficiently small, $[\mathbf{I} + D\mathbf{h}_k(\mathbf{z}_k)]^{-1}$ is invertible, and may be approximated by

$$\begin{aligned} [\mathbf{I} + D\mathbf{h}_k(\mathbf{z}_k)]^{-1} &\approx \mathbf{I} - D\mathbf{h}_k(\mathbf{z}_k) + (D\mathbf{h}_k(\mathbf{z}_k))^2 + \dots = \\ &\mathbf{I} - D\mathbf{h}_k(\mathbf{z}_k) + O(|\mathbf{y}|^{2k-2}) \end{aligned}$$

where $D\mathbf{h}_k(\mathbf{z}_k)$ is the Jacobian matrix of $\mathbf{h}(\mathbf{z}_k)$ with respect to \mathbf{z}_k , and $O(|\mathbf{z}_k|^{2k-2})$ represents terms of order $\geq 2k - 2$.

Alternatively, the normal form of order k can be obtained by expanding Eq. (2.32) order by order. Successive substitution of Eq. (2.16) into Eq. (2.32) yields the recursive relationships [17]

$$\begin{aligned}
\dot{\mathbf{z}}_2 &= \Lambda \mathbf{z}_2 + \hat{\mathbf{F}}_2(\mathbf{z}_3) + \left[\hat{\mathbf{F}}_3(\mathbf{z}_3) + \Lambda \mathbf{h}_3(\mathbf{z}_3) - D\mathbf{h}_3(\mathbf{z}_3)\Lambda \mathbf{z}_3 \right] + \sum_{m=3}^k \hat{\mathbf{F}}_m(\mathbf{z}_3) \\
\dot{\mathbf{z}}_3 &= \Lambda \mathbf{z}_3 + \hat{\mathbf{F}}_2(\mathbf{z}_3) + \left[\hat{\mathbf{F}}_3(\mathbf{z}_3) + \Lambda \mathbf{h}_3(\mathbf{z}_3) - D\mathbf{h}_3(\mathbf{z}_3)\Lambda \mathbf{z}_3 \right] + \sum_{m=4}^k \hat{\mathbf{F}}_m(\mathbf{z}_3) \\
&\dots \\
\dot{\mathbf{z}}_k &= \Lambda \mathbf{z}_k + \sum_{m=2}^{k-1} \hat{\mathbf{F}}_m(\mathbf{z}_4) + \left[\hat{\mathbf{F}}_k(\mathbf{z}_k) + \Lambda \mathbf{h}_k(\mathbf{z}_k) - D\mathbf{h}_k(\mathbf{z}_k)\Lambda \mathbf{z}_k \right] + O(|\mathbf{z}|^{k+1})
\end{aligned} \tag{2.29}$$

where the first four nonlinear coefficients are given by

$$\begin{aligned}
\hat{\mathbf{F}}_2 &= \mathbf{F}_2(\mathbf{z}_2) - D\mathbf{h}_2(\mathbf{z}_2)\Lambda \mathbf{h}_2(\mathbf{z}_2) \\
\hat{\mathbf{F}}_3 &= \mathbf{F}_3(\mathbf{z}_2) - D\mathbf{h}_2(\mathbf{z}_2)\Lambda \mathbf{h}_2(\mathbf{z}_2) - D\mathbf{h}_2(\mathbf{z}_2)\mathbf{F}_2(\mathbf{z}_2) \\
&\quad + (D\mathbf{h}_2(\mathbf{z}_2))^2 \Lambda \mathbf{z}_2 \\
\hat{\mathbf{F}}_4 &= \mathbf{F}_4(\mathbf{z}_3) - D\mathbf{h}_2(\mathbf{z}_2)\Lambda \mathbf{h}_2(\mathbf{z}_2) - D\mathbf{h}_2(\mathbf{z}_2)\mathbf{F}_2(\mathbf{z}_2) \\
&\quad + (D\mathbf{h}_2(\mathbf{z}_2))^2 \Lambda \mathbf{z}_2 \\
&\dots
\end{aligned}$$

In the equations above, the $\hat{\mathbf{F}}_m$ represent terms of order m that have been modified by the nonlinear transformation. A recursive pattern is beginning to become discernible.

The analysis above suggests that in order to remove terms of order s , the nonlinear transformation vectors $\mathbf{h}(s)$ may be determined from the solution of the homological equations [5]

$$L_A(\mathbf{h}_s(\mathbf{z}_s)) - [\mathbf{h}_s(\mathbf{z}_s), \Lambda \mathbf{z}_s] = D\mathbf{h}_s \Lambda \mathbf{z}_s - \Lambda \mathbf{h}_s = \hat{\mathbf{F}}_s \tag{2.30}$$

for $s = 2, 3, \dots, r-1$, where the notation, $L_A(\mathbf{h}_s(\mathbf{z}_s)) = [\mathbf{h}_s(\mathbf{z}_s), \Lambda]$ denotes the Lie bracket operation of vectors $\mathbf{h}_s(\mathbf{z}_s)$ and $\Lambda \mathbf{z}_s$ [6], and the $\hat{\mathbf{F}}_s$ represent terms of order s that have been affected by the transformation of order $s-1$. Assuming L_A is invertible, and solving for $\mathbf{h}_s(\mathbf{z}_s)$ yields

$$\mathbf{h}_s(\mathbf{z}_s) = L_A^{-1} \hat{\mathbf{F}}_s(\mathbf{z}_s) \tag{2.31}$$

It can readily be proved, that if the eigenvalues of \mathbf{A} are not resonant of order s , the coefficients of the second and third-order normal form transformation are given by [13]

$$\begin{aligned} h_{2_{kl}}^j &= \frac{C_{2_{kl}}^j}{(\lambda_k + \lambda_l - \lambda_j)} \\ h_{3_{klm}}^j &= \frac{C_{3_{klm}}^j}{(\lambda_k + \lambda_l + \lambda_m - \lambda_j)} \\ &\dots \end{aligned} \tag{2.32}$$

for $j = 1, 2, \dots, n$, provided that $\lambda_k + \lambda_l - \lambda_j \neq 0, \lambda_k + \lambda_l + \lambda_m - \lambda_j \neq 0$ where the $C_{2_{kl}}^j, C_{3_{klm}}^j$ are defined in Eq. (2.30).

At k th-order, the approximate normal form representation for the system in Eq. (6) may be written as

$$\dot{\mathbf{z}}_k \approx \mathbf{\Lambda} \mathbf{z}_k + \mathbf{f}_k^r + O(|\mathbf{z}|^{k+1}) \tag{2.33}$$

where $\mathbf{\Lambda} = \text{diag}[\lambda_1 \ \lambda_2 \ \dots \ \lambda_n]$. The functions \mathbf{f}_k^r are called the resonant or secular terms that can not be eliminated by the transformations (2.27) and contain the essential part of the dynamic system.

This approach allows for the rigorous analysis of a wide variety of nonlinear systems, including systems with linear and nonlinear characteristics.

2.5 Approximate Normal Form Solutions

2.5.1 Third-Order Normal Form Approximation

For ease of discussion, and without loss of generality, the normal form analysis presented in this section is restricted to third-order, but the procedure is general and can be used to study higher-dimensional systems.

Let the system behavior be represented by Eq. (2.26). By the linear transformation $\mathbf{x} = \mathbf{U}\mathbf{y}$, Eq. (2.2) can be reduced to the Jordan-canonical form

$$\dot{\mathbf{y}} = \mathbf{\Lambda}\mathbf{y} + \mathbf{F}_2(\mathbf{y}) + \mathbf{F}_3(\mathbf{y}) + O(\|\mathbf{y}\|^4) \tag{2.34}$$

where

$$\mathbf{F}_2(\mathbf{y}) = \frac{1}{2} \mathbf{U}^{-1} \begin{bmatrix} (\mathbf{Uy})^T \mathbf{H}_2^1 \mathbf{U} \\ (\mathbf{Uy})^T \mathbf{H}_2^2 \mathbf{U} \\ \dots \\ (\mathbf{Uy})^T \mathbf{H}_2^n \mathbf{U} \end{bmatrix} = \frac{1}{2} \begin{bmatrix} \sum_{k=1}^n \sum_{l=k}^n C_{2_{kl}}^1 y_k y_l \\ \sum_{k=1}^n \sum_{l=k}^n C_{2_{kl}}^2 y_k y_l \\ \dots \\ \sum_{k=1}^n \sum_{l=k}^n C_{2_{kl}}^n y_k y_l \end{bmatrix} \quad (2.35)$$

$$\mathbf{F}_3(\mathbf{y}) = \frac{1}{6} \mathbf{U}^{-1} \begin{bmatrix} (\mathbf{Uy})^T \mathbf{H}_3^1 \begin{bmatrix} \mathbf{Uy} & \hat{\mathbf{0}} \\ \hat{\mathbf{0}} & \mathbf{Uy} \end{bmatrix} \mathbf{Uy} \\ (\mathbf{Uy})^T \mathbf{H}_3^2 \begin{bmatrix} \mathbf{Uy} & \hat{\mathbf{0}} \\ \hat{\mathbf{0}} & \mathbf{Uy} \end{bmatrix} \mathbf{Uy} \\ \dots \\ (\mathbf{Uy})^T \mathbf{H}_3^j \begin{bmatrix} \mathbf{Uy} & \hat{\mathbf{0}} \\ \hat{\mathbf{0}} & \mathbf{Uy} \end{bmatrix} \mathbf{Uy} \end{bmatrix} = \frac{1}{6} \begin{bmatrix} \sum_{k=1}^n \sum_{l=k}^n \sum_{m=k}^n C_{3_{klm}}^1 y_k y_l y_m \\ \sum_{k=1}^n \sum_{l=k}^n \sum_{m=k}^n C_{3_{klm}}^2 y_k y_l y_m \\ \dots \\ \sum_{k=1}^n \sum_{l=k}^n \sum_{m=k}^n C_{3_{klm}}^j y_k y_l y_m \end{bmatrix} \quad (2.36)$$

where the $C_{2_{kl}}^j$, and $C_{3_{klm}}^j$, $j=1,2$ are the second-order and third-order coefficients respectively of the Jordan form variables defined by Eqs. (2.35) and (2.36).

To remove second-order terms in Eq. (2.34), let now the second-order nonlinear transformation be introduced next

$$\mathbf{y} = \mathbf{z}_2 + \mathbf{h}_2(\mathbf{z}_2) \quad (2.37)$$

in which $\mathbf{z}_2 = [z_{2_1} \ z_{2_2} \ \dots \ z_{2_n}]^T$, and $\mathbf{h}_2(\mathbf{z}_2)$ is a complex-valued polynomial vector of order two defined as

$$\mathbf{h}_2(\mathbf{z}_2) = \begin{bmatrix} \sum_{k=1}^n \sum_{l=k}^n h_{2_{kl}}^1 z_{2_k} z_{2_l} \\ \sum_{k=1}^n \sum_{l=k}^n h_{2_{kl}}^2 z_{2_k} z_{2_l} \\ \dots \\ \sum_{k=1}^n \sum_{l=k}^n h_{2_{kl}}^n z_{2_k} z_{2_l} \end{bmatrix} \quad (2.38)$$

Substituting Eq. (2.37) into Eq. (2.34) results in

$$\dot{\mathbf{z}}_2 = \Lambda \mathbf{z}_2 + \hat{\mathbf{F}}_3(\mathbf{z}_2) + O(|\mathbf{z}_2|^4) \quad (2.39)$$

where the term $\hat{\mathbf{F}}_3(\mathbf{z}_2)$ indicates third-order terms that have been affected by the transformation in Eq. (2.38) and the terms $O(|\mathbf{z}_2|^4)$ represent fourth-order and higher terms introduced by the nonlinear transformation.

In an analogous fashion, third-order terms are removed by using the nonlinear transformation

$$\mathbf{z}_2 = \mathbf{z}_3 + \mathbf{h}_3(\mathbf{z}_3) \quad (2.40)$$

where,

$$\mathbf{h}_3(\mathbf{z}_3) = \begin{bmatrix} \sum_{k=1}^n \sum_{l=k}^n \sum_{m=k}^n h_{3_{klm}}^1 z_{3_k} z_{3_l} z_{3_m} \\ \sum_{k=1}^n \sum_{l=k}^n \sum_{m=k}^n h_{3_{klm}}^2 z_{3_k} z_{3_l} z_{3_m} \\ \dots \\ \sum_{k=1}^n \sum_{l=k}^n \sum_{m=k}^n h_{3_{klm}}^n z_{3_k} z_{3_l} z_{3_m} \end{bmatrix}$$

Substitution of (2.40) into Eq. (2.39) and neglecting residual terms above third-order, yields the approximate normal form system

$$\dot{\mathbf{z}}_3 \approx \Lambda \mathbf{z}_3 \quad (2.41)$$

where $\Lambda = \text{diag}[\lambda_1 \ \lambda_2 \ \dots \ \lambda_n]$. The details of these computations are given below.

2.5.2 Closed-Form Expressions for Second and Higher-Order Approximations

A more insightful analysis into the nature of system oscillations can be attained from the study of approximate time domain solutions. Let the system dynamic behavior in \mathbf{z}_3 -coordinates be given by Eq. (2.41) with initial conditions

$\mathbf{z}_3(t^0) = \mathbf{z}_3^0 = [z_{3_1}^0 \ z_{3_2}^0 \ \dots \ z_{3_n}^0]^T$ Solution of this equation for $\mathbf{z}_3(t)$ gives

$$z_{3_i}(t) = z_{3_i}^0 e^{\lambda_i t} \quad (2.42)$$

where λ_l and the initial conditions $z_{3_l}^o$ have to be determined from the initial conditions, \mathbf{x}^o , in the original coordinates. The following approach is used to compute initial conditions in the \mathbf{z}_3 coordinates.

Starting with any feasible \mathbf{x}_{sep} it can be readily shown that the solution of the inverse transformations can be recast as an optimization problem of the form:

1. Given an initial stable equilibrium point of interest $\mathbf{x}^o = \mathbf{x}_{sep}$, calculate initial condition in Jordan coordinates from $\mathbf{y}^o = \mathbf{U}^{-1}\mathbf{x}^o$
2. Compute \mathbf{z}_2 and \mathbf{z}_3 by solving the nonlinear optimization problems $\mathbf{f}_2(\mathbf{z}_2^o) = \mathbf{y}^o - \mathbf{z}_2^o - \mathbf{h}_2(\mathbf{z}_2^o) = \mathbf{0}$ and $\mathbf{f}_3(\mathbf{z}_3^o) = \mathbf{z}_2^o - \mathbf{z}_3^o - \mathbf{h}_3(\mathbf{z}_3^o) = \mathbf{0}$

Normal form solutions in Eq. (2.39) are then transformed back into the original physical domain by using the inverse transformations

$$\begin{cases} \mathbf{z}_2(t) = \mathbf{z}_3(t) + \mathbf{h}_3(\mathbf{z}_3(t)) \\ \mathbf{y}(t) = \mathbf{z}_2(t) + \mathbf{h}_2(\mathbf{z}_2(t)) \\ \mathbf{x}(t) = \mathbf{U}\mathbf{y}(t) \end{cases} \quad (2.43)$$

Making use of Eq. (2.43), time-domain closed-form solutions can be expressed in terms of modal components as follows

$$z_{2_j}(t) = z_{3_j}^o e^{\lambda_{j_l} t} + \sum_{k=1}^n \sum_{l=k}^n \sum_{m=k}^n h_{3_{klm}}^j z_{3_k}^o z_{3_l}^o z_{3_m}^o e^{(\lambda_k + \lambda_l + \lambda_m)t} \quad (2.44)$$

$$y_j(t) = z_{2_j}(t) + \sum_{k=1}^n \sum_{l=k}^n h_{2_{kl}}^j z_{2_k}(t) z_{2_l}(t) \quad (2.45)$$

and

$$x_j(t) = \sum_{i=1}^n u_{ji} z_{2_i} + \sum_{i=1}^n u_{ji} \left[\sum_{k=1}^n \sum_{l=k}^n h_{2_{kl}}^j z_{2_k}(t) z_{2_l}(t) \right] \quad (2.46)$$

Figure 2.1 provides a conceptual representation of the adopted model illustrating the different coordinated frames.

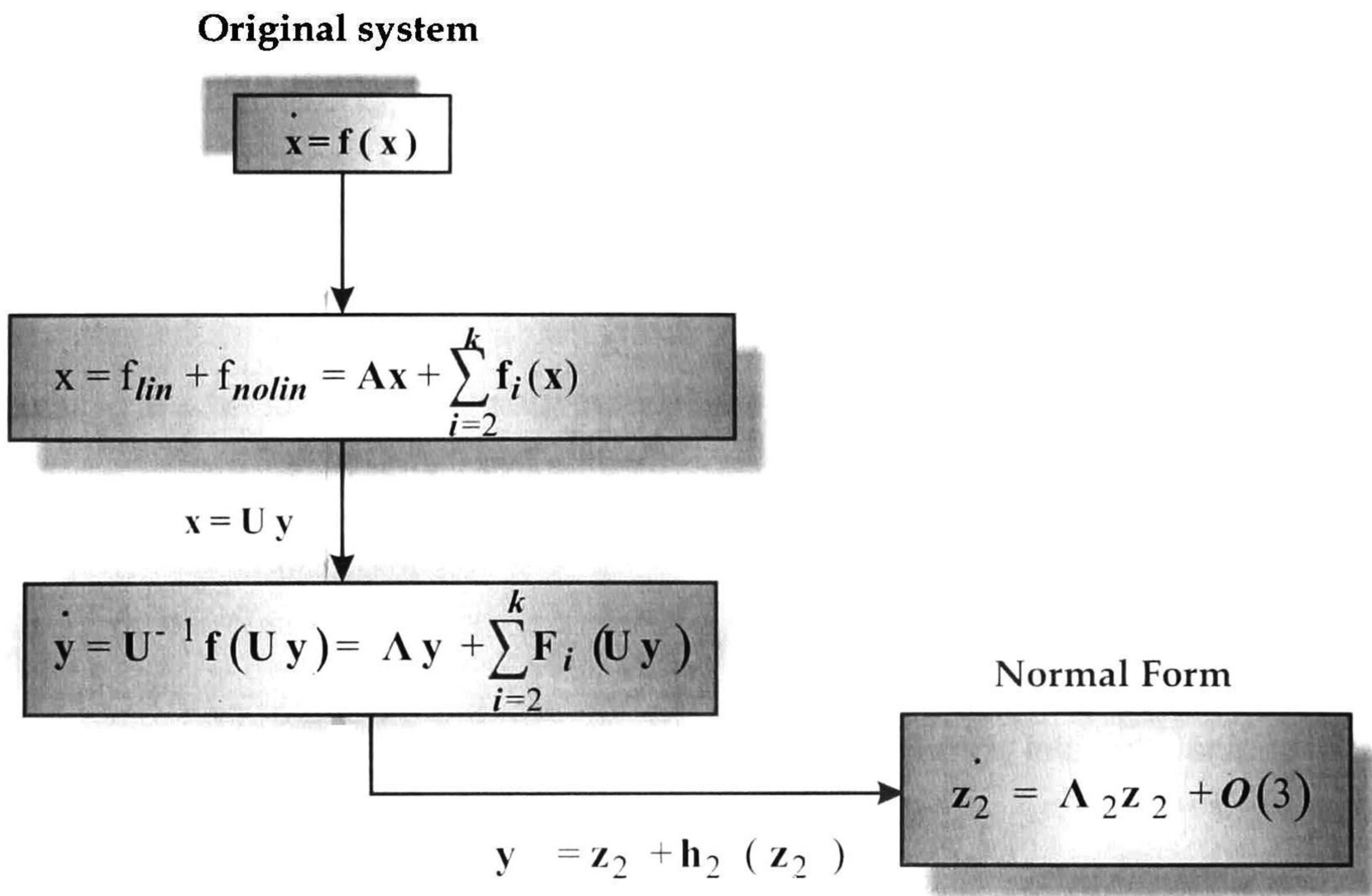


Figure 2.1. Schematic representation of the method of normal forms

For simplicity, a simple one-machine infinite-bus test power systems is used to address the computation of high-dimensional normal forms.

2.6 Numerical Example

The case under consideration is a single-machine infinite-bus system adapted from Ref. [18]. In deriving the system equations, resistances are neglected and the generator is represented by a classical model as a constant voltage source behind a transient reactance.

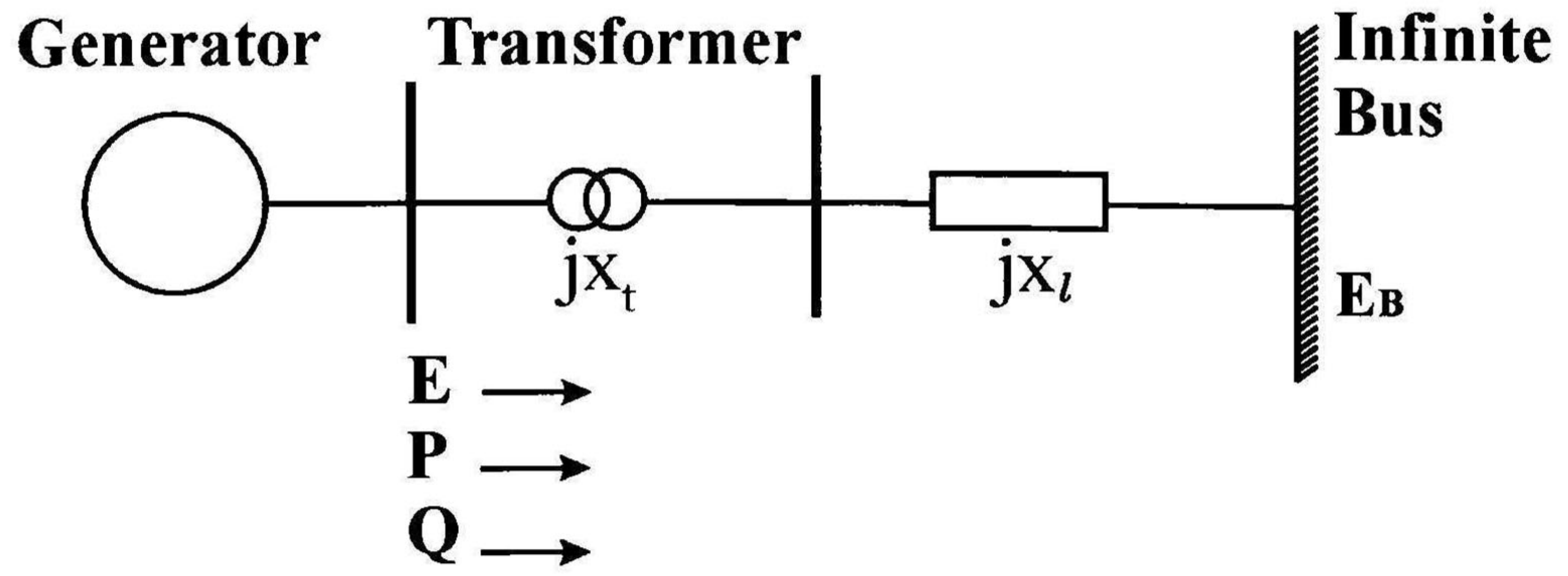


Figure 2.2. One-line diagram of the test system

2.6.1 Equations of Motion

The differential equations of motion of this system are thus

$$\frac{d\delta}{dt} = \omega \quad (2.47)$$

$$\frac{d\omega}{dt} = \frac{1}{2H} [P_m - D\omega - P_{\max} \sin \delta] \quad (2.48)$$

where δ is the angular position of the rotor in electrical radians with respect to the infinite system, ω is the angular velocity of the rotor in electrical rad/s, P_m is the mechanical input power in p.u., D is the generator damping coefficient in p.u torque/p.u. speed, and H is the inertia constant in MWs/MVA.

Introducing the two-dimensional vector $\mathbf{x} = [x_1 \ x_2]^T = [\delta \ \omega]^T$, the equation of motion can be described by the two-dimensional non-linear system

$$\dot{\mathbf{x}} = \mathbf{f}(\mathbf{x}) = \begin{bmatrix} f_1(x_1, x_2) \\ f_2(x_1, x_2) \end{bmatrix} \quad (2.49)$$

where

$$f_1(x_1, x_2) = \omega,$$

and

$$f_2(x_1, x_2) = \frac{1}{2H} [P_m - D\omega - P_{\max} \sin \delta]$$

with associated equilibrium points at $\left(\sin^{-1}\left(\frac{P_m}{P_{\max}}\right) - k\pi, 0 \right)$ where k is any integer.

2.6.2 Numerical Results

Normal form analyses were finally carried out to investigate the influence of perturbations on the system nonlinear behavior as well as to validate the developed procedures.

Emphasis is placed on the analysis of the effects of perturbations in the initial conditions, $\Delta\delta^0, \Delta\omega^0$ on system dynamic performance. The parameters used in the analysis are given in the Appendix A.

Two system representations were considered in the studies, namely: 1) a second-order system representation obtained by expanding Eq. (2.24) up to order two ($k = 2$ in the developed procedure), and 2) a third-order system representation ($k = 3$).

In both cases approximate normal form solutions were obtained using the procedures in section 2.6. These solutions are referred to in this chapter, as the second order NF solution and the third order NF solutions, respectively. For completeness, the full non-linear system behavior was obtained by integrating numerically the system nonlinear model using the ode routine in Matlab.

2.6.3 Linear Approximation

To gain additional insight into the nature of system behavior, linear approximations were obtained from the first-order system representation.

Let $\lambda_{1,2} = -0.7143 \pm j6.346$ be the complex conjugate eigenvalues of matrix \mathbf{A} at \mathbf{x}_{sep} (refer to Appendix A). For small disturbances, the general solution of the system $\dot{\mathbf{x}} = \mathbf{A}\mathbf{x}$, with initial conditions $\Delta\delta(0) = \Delta\delta^0, \Delta\omega(0) = 0$ at $t=0$ is:

$$\Delta\delta(t) = 1.008 \left[e^{-0.714t} \cos(6.35t - 0.112) \right] (\Delta\delta^0) \text{ rad.} \quad (2.50)$$

and

$$\Delta\omega(t) = -0.015 \left[e^{-0.714t} \text{sen}(6.35t) \right] (\Delta\delta^0) \text{ p.u.} \quad (2.51)$$

Equations (2.50) and (2.51) describe a damped harmonic motion with frequency $\omega = 6.35$ rad/s, and a decay time constant of $1/0.714$ s. Comparison of these expressions with those for the approximate normal form system in Eqs. (2.44) through (2.46) reveals the non-linear contributions that are not accounted for by linear analysis.

2.6.4 Normal Form Solutions

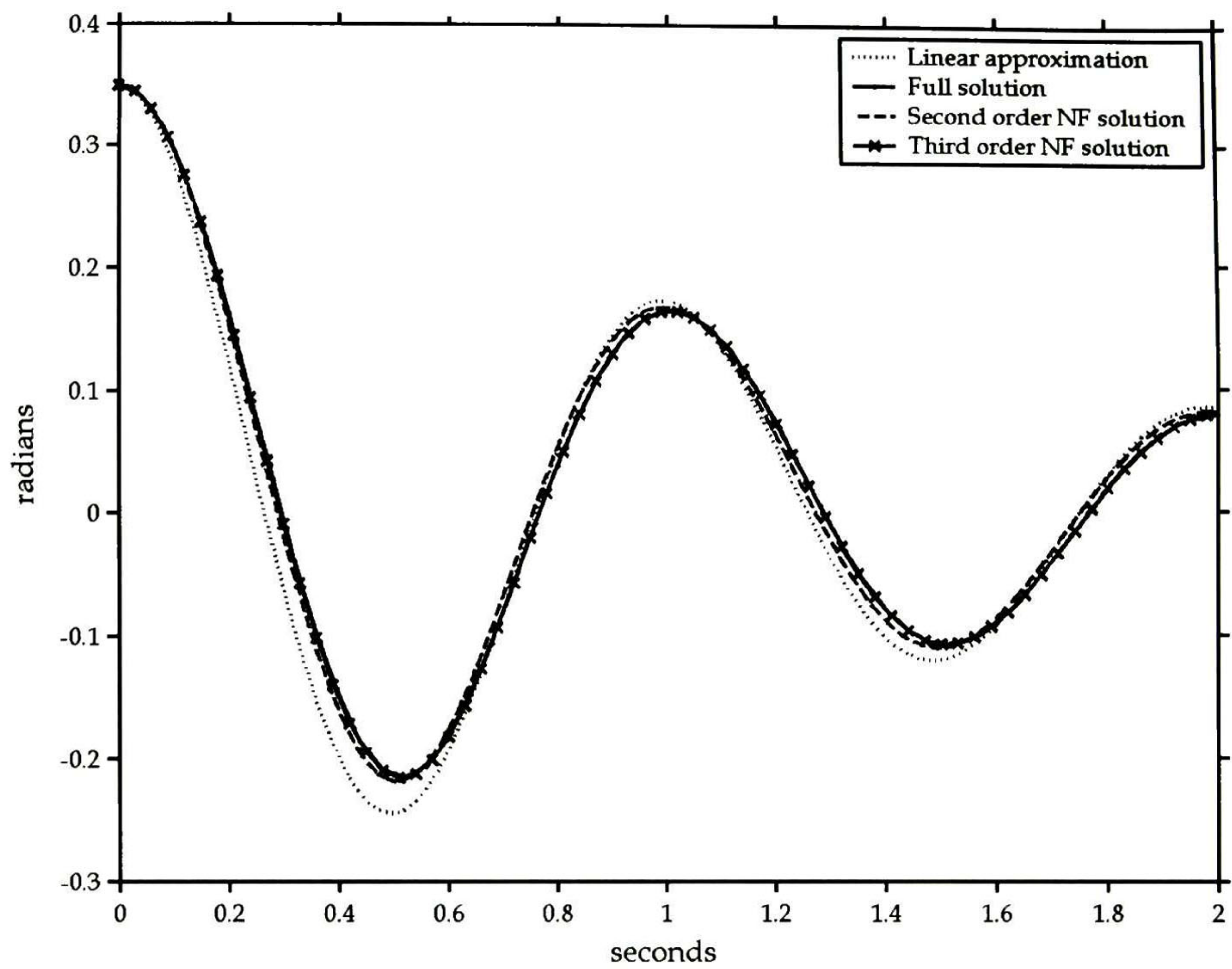
Figures 2.3 through 2.5 provide a comparison of the full system solution with the solution from the second and third-order normal forms for three different initial perturbations in the initial machine angle, namely: $\Delta\delta^0 = 15^\circ, \Delta\delta^0 = 30^\circ$, and $\Delta\delta^0 = 45^\circ$. For comparison, the linear solutions obtained from Eqs. (2.50) and (2.51) are also presented.

It can be seen in figure 2.3 that for small perturbations, the normal form approximations and the full system solution agree very well, while the linear approximation shows some deviation with respect to them. Further, all solutions remain practically in phase. As the initial system perturbation is increased from 15° to 45° in figures 3 and 4, however, the linear approximation and the second-order normal form solution are unable to approximate the full system response.

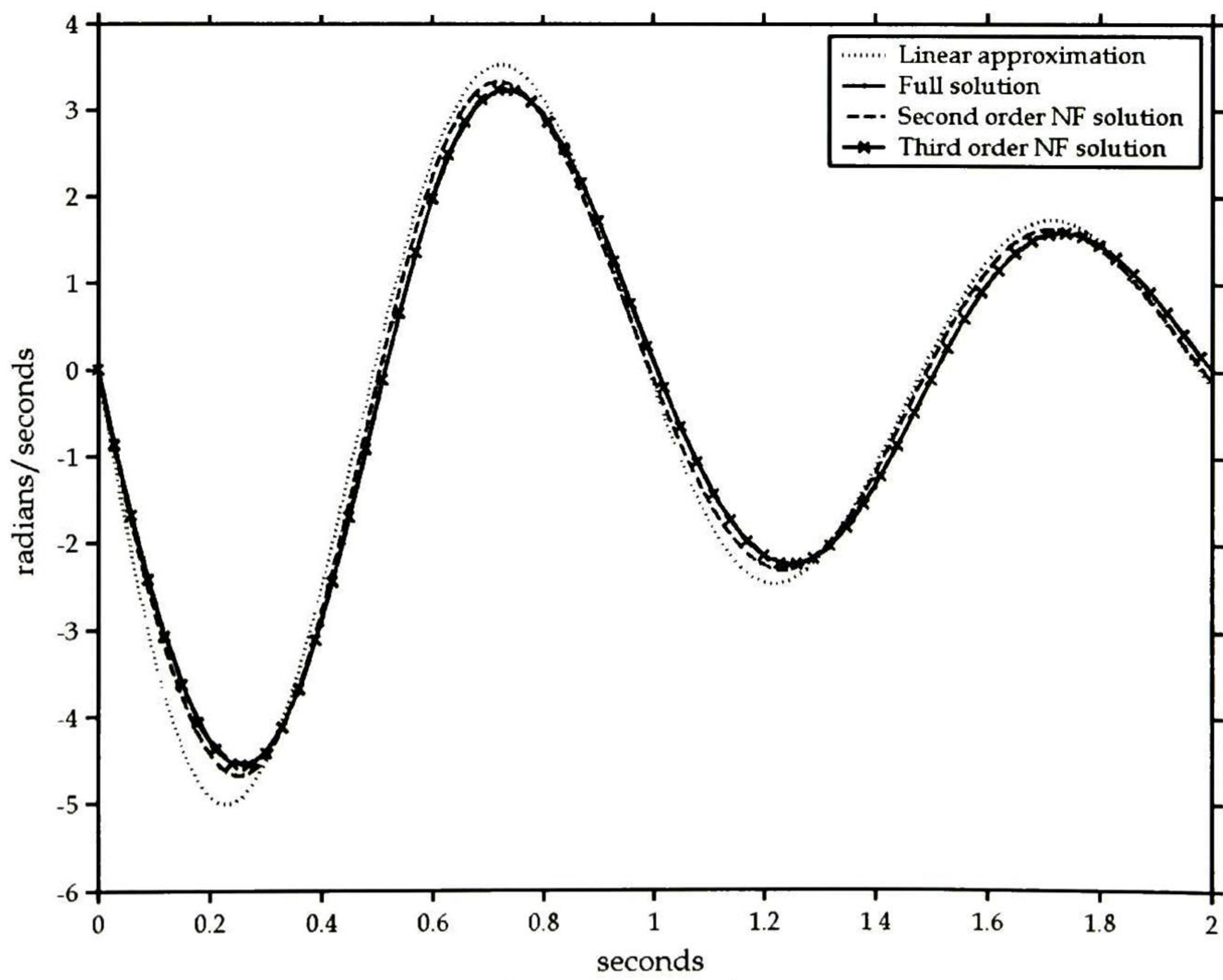
The following general conclusions can be drawn from this analysis:

- Normal form solutions provide a more accurate approximation for the full system solution over longer times than the approximations given by linear analysis.
- The degree of accuracy is a function of both, the magnitude of the initial perturbation and the level of stress in the system. The analysis also suggests that nonlinear effects arise in the system when the perturbation becomes large.

The linear approximation and the second order NF solution become less accurate as time increases. As expected from physical considerations, the addition of second and third-order effects is seen to improve the accuracy of the solution.



a) rotor angle deviation



b) speed deviation

Figure 2.3. Comparison of machine dynamic behavior for an initial perturbation $\Delta\delta'' = 15^\circ, \Delta\omega = 0$

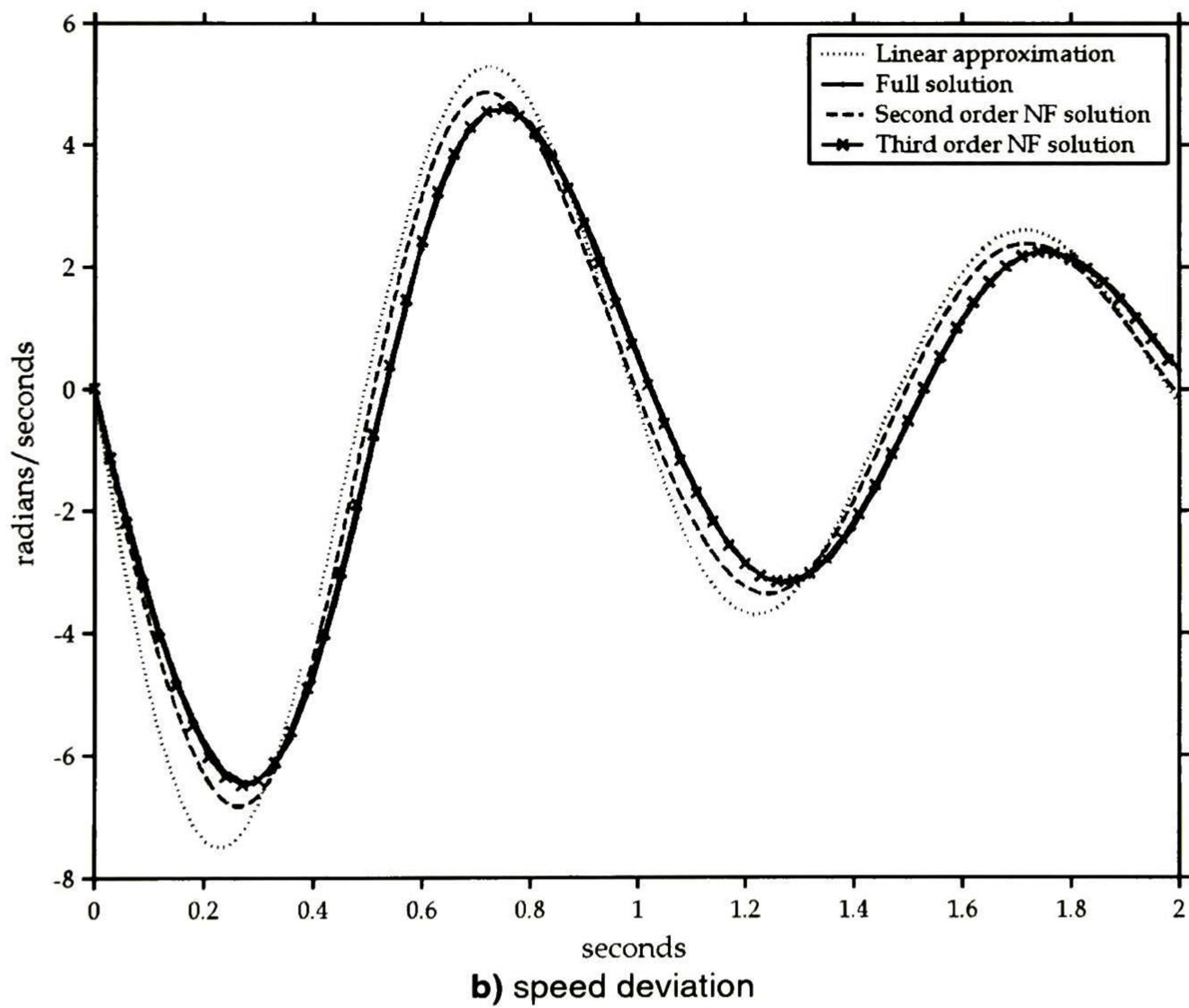
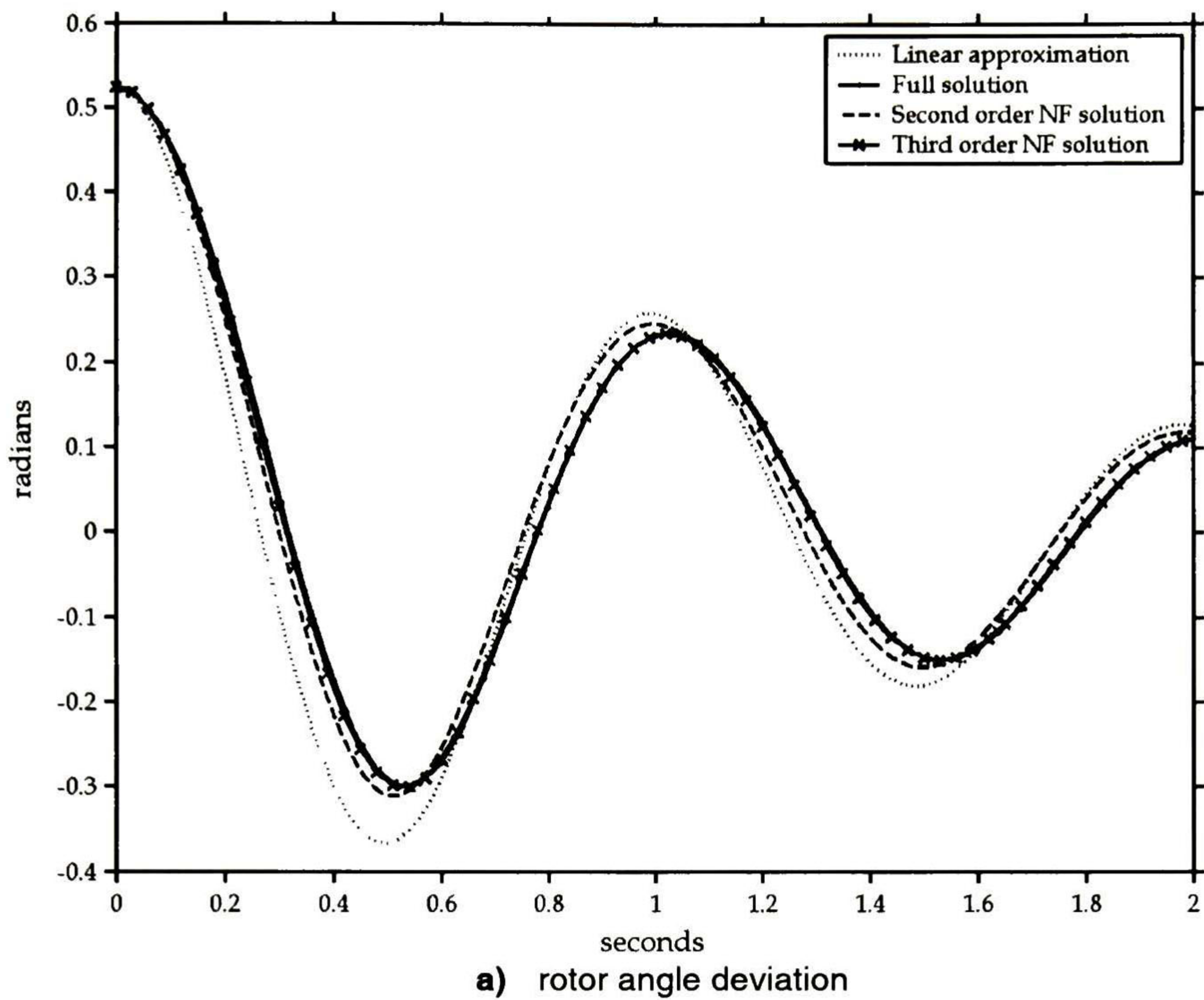
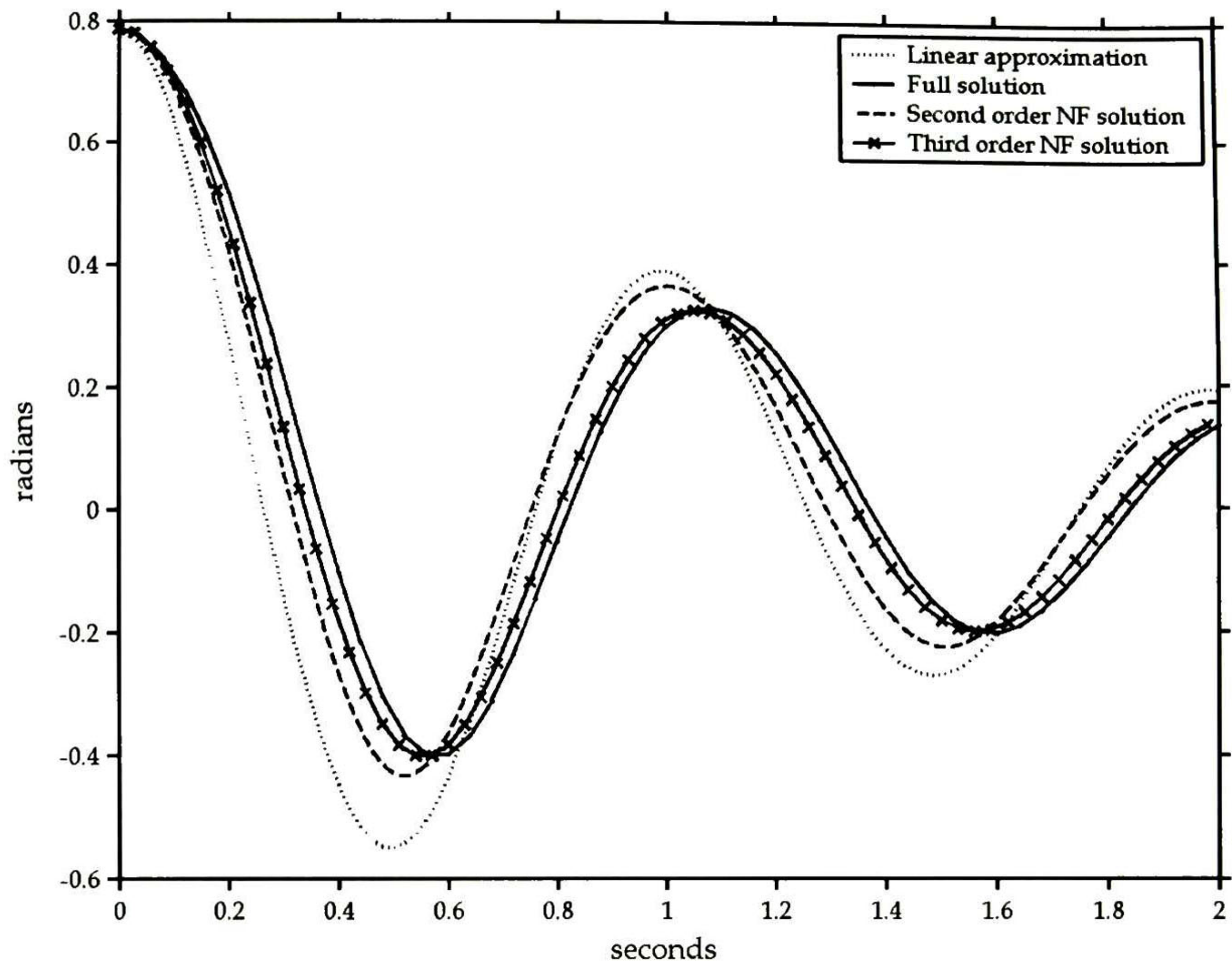
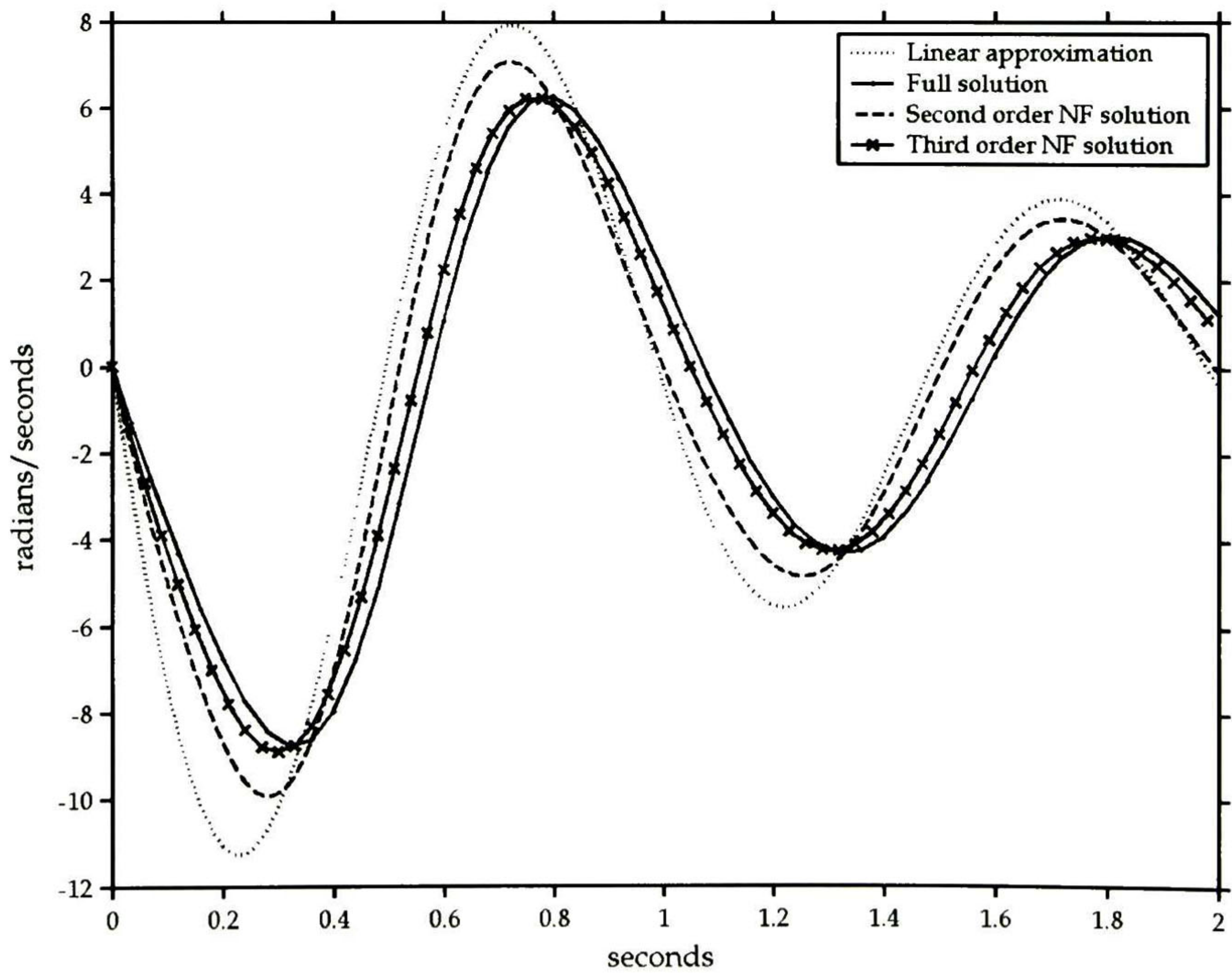


Figure 2.4. Comparison of machine dynamic behavior for an initial perturbation $\Delta\delta'' = 30^\circ, \Delta\omega = 0$



a) rotor angle deviation



b) speed deviation

Figure 2.5. Comparison of machine dynamic behavior for an initial perturbation $\Delta\delta'' = 45^\circ, \Delta\omega = 0$

These results suggest the potential for application of high-dimensional analysis to more complex systems.

2.7 Discussion

In this chapter, a brief review of conventional power system normal form analysis has been presented. A systematic methodology based on normal form theory is introduced for determining the effect of third –and higher-order terms of the power system representation on system performance. The conceptual framework developed provides a rigorous base for determining the effects of weak nonlinearities on system response. Moreover, the proposed procedure is general and can be extended to higher dimensional systems.

This theory has proved very successful and agrees well with a wide range of analytical results. However, several of the assumptions make the application of these approaches impractical for large, complex high-dimensional nonlinear systems. Additionally, its range of validity to assure accuracy within a given range of operating conditions has not been fully studied.

There are a number of issues regarding an accurate model of power system behavior. These include:

- The high-dimensionality and complexity of the resulting model. Conventional normal form analysis requires reduction to the internal nodes of generators.
- Accuracy issues. The extension of normal form analysis to high-dimensional systems is required, especially when the system operates closer to its stability limits.

These issues are fully addressed in subsequent sections of this dissertation. An improvement to the above formulation for determining the normal form representation is discussed. This improvement provides a means of determining higher-dimensional representations and enables the network structure to be preserved. There are a number of avenues for productive future work.

Studies of the effects of perturbations on system performance show that accurate modeling of system behavior is necessary if the detailed system response is to be successfully predicted. From the studies performed, third-order normal form solutions have been found to accurately predict system behavior even for large system perturbations.

References

- [1] V. Vittal, N. Bhatia and A.A. Fouad, "Analysis of the inter-area mode phenomenon in power systems following large disturbances, *IEEE Power Systems*, vol. 6, pp. 1515-1521, Nov 1991
- [2] J. Thapar, V. Vittal, W. Kliemann and A. A. Fouad, "Application of the normal form of vector fields to predict interarea separation in power systems". *IEEE Trans. on Power Systems*, Vol. 12pp. 844-850, May 1997
- [3] C. M. Ling, V. Vittal, W. Kliemann, and A.A. Fouad, "Investigation of modal interaction and its effects on control performance in stressed power systems using normal forms of vector fields", *IEEE Transactions on Power Systems*, vol. 11, pp. 781-787, May 1996
- [4] A. R. Messina and E. Barocio, "Assessment of non-linear modal interaction in stressed power networks using the method of normal forms" *Electrical Power & Energy Systems*, vol. 25, pp. 21-29, Jan 2003
- [5] A. H. Nayfeh, *Method of Normal Forms*, Wiley Series in Nonlinear Science, John Wiley & Sons, 1993
- [6] D.K. Arrowsmith, and C. M. Place, *An introduction to Dynamical Systems*, London: Cambridge University Press, 1994
- [7] N. Yorino, H. Sasaki, Y Tamura and R. Yokoyama "A generalized analysis method of auto-parametric resonances in power systems" *IEEE Trans. on Power Systems*, vol. 4, pp. 1057-1064, Aug 1989
- [8] S. K Starret, W. Klieman, V. Vittal and A.A. Fouad, "Power system modal behavior: Significance of second and third order nonlinear terms", *North America Power Symposium*, Washington D.C., Oct 1993
- [9] P. B. Kahn and Y Zarmi, "Nonlinear dynamics : a tutorial on the method of normal forms ", *American Journal of Physics*, vol. 68, pp. 907-919, Oct 2000
- [10] V. I. Arnold, *Geometrical methods in the theory of ordinary differential equations*, Springer Verlag, New York ,1998
- [11] V. F Edneral, "A symbolic approximation of periodic solutions of the Henon-Heiles system by the normal form method", *Mathematics and Computers in Simulation*, vol. 45, pp. 445-463, Mar 1998
- [12] S. Wiggins, *Introduction to applied nonlinear dynamical systems and chaos*, Text in Applied Mathematics, Springer Verlag, New York, vol. 2, 2003

- [13] E. Barocio, Normal form analysis of stressed power systems using normal forms, PhD Thesis, The Center for Research and Advanced Studies of the National Polytechnic Institute of Mexico, Guadalajara, 2003
- [14] P. Yu, "Computation of normal forms via a perturbation technique", *Journal of sound and Vibration*, vol. 211, pp. 19-38, Mar 1998
- [15] Lawrence Perko, Differential equations and dynamical systems, Springer Verlag. Nova York, 1991
- [16] A. H. Nayfe and D. T. Mook, Nonlinear Oscillations, Wiley-IEEE in Nonlinear Theories, 1979
- [17] I. Martinez, A. R. Messina and E. Barocio, "Higher-Order Normal Form Analysis of stressed Power Systems: A Fundamental Study", *Electric Power Components and systems*, vo. 32, pp. 1301-1317, Dec 2004
- [18] Z. Weiyi and K. Huseyin, "On the relations between the methods of averaging and normal forms", *Applied Mathematical Modelling*, vol. 24 , pp. 279-295, 2000
- [19] P Kundur, Power System Control and Stability, McGraw-Hill , 1994

Chapter 3

Normal Form of Complex System Models: A Structure-Preserving Approach

Large, sparse power system models arise naturally as dynamic models of a wide range of power system applications.

In this chapter, a modeling framework based on normal form theory and singular perturbation techniques is proposed for analyzing the nonlinear behavior of power system models described by nonlinear Differential-Algebraic Equations (DAEs). The method exploits the time scale separation of power system dynamic processes, to avoid reduction of the original DAE model and may therefore be used to assess control effects and network characteristics on system behavior. This approach allows the full use of the normal form formulation to be reached, and is applicable to a wide variety of nonlinear phenomena described by DAEs.

Using a control theory framework, a constructive approach is outlined for transforming a system of DAEs to a state space approximation that is suitable for normal form analysis. By casting the problem in the context of singular perturbation theory, a structure-preserving nonlinear mathematical model of the power system is established for the study of nonlinear behavior.

Criteria for this representation are derived and implementation issues are discussed.

3.1 Introduction

In recent years there has been significant interest in normal form analysis of detailed power system models. The primary advantage of this approach is its ability to express the complicated dynamics of the original nonlinear system in terms of modal interactions between modes [1]. This technique has been shown to give improved understanding of the fundamental nature of system nonlinear behavior and has the capability to help in the design of power system controllers [2-4].

Several analytical formulations using normal form theory have been proposed for assessing aspects of power system nonlinear behavior [4-6]. This has led to significant progress in the development and interpretation of analytical system representations and has highlighted the need to understand more fully the role of network and control characteristics in system performance. Characterization of transmission network effects is required for both, detailed understanding of the mechanisms of intersystem oscillations, insight into model structure, especially concerning nonlinear paths created by supplemental modulation [7], and addressing the key questions of how nonlinear effects control performance and system behavior.

Standard normal form analysis, however, rests upon reduced order representations in which the algebraic equations representing the network behavior are included in the set of differential equations. These models offer a compact description of the system dynamics, and are especially useful for the study of electromechanical oscillations since they preserve the essential features of system behavior in terms of the dynamic states of the system. Although normal form analysis has been extended in several ways in order to account for control effects, these approaches are difficult to implement due to the complexity of the nonlinear interactions between components created by the reduction process [6,8]. Further research is also necessary to address other issues such as the assessment of closed-loop effects arising from the use of supplementary controllers, the effect of loads on the oscillatory process and the loss of physical significance of system variables.

In this chapter, a structure-preserving approach to power system normal form analysis is presented. The key idea is to approximate the behavior of the original system by a singularly perturbed system in which the structure and physical meaning of the original variables is preserved. The method exploits the time scale separation property of power system processes, to accurately approximate system behavior and provides essential information for control design and parameter estimation.

3.2 Structure-Preserving Power System Model

3.2.1 Model Equations

A general, dynamic model of the power system is considered in the analysis which preserves network structure and load characteristics. Figure 3.1 provides a schematic illustration of the adopted model. Assume the power system under consideration consists of nb buses and ng generators, for the objectives of this study, each machine is modeled by a fourth order model equipped with a fast excitation system.

The voltage dependency of the loads is represented by a general exponential model. Flexible AC system controllers are represented by nonlinear constraint equations and included in the system model. The modeling framework, however, is general and can be used to accommodate more complex system representations.

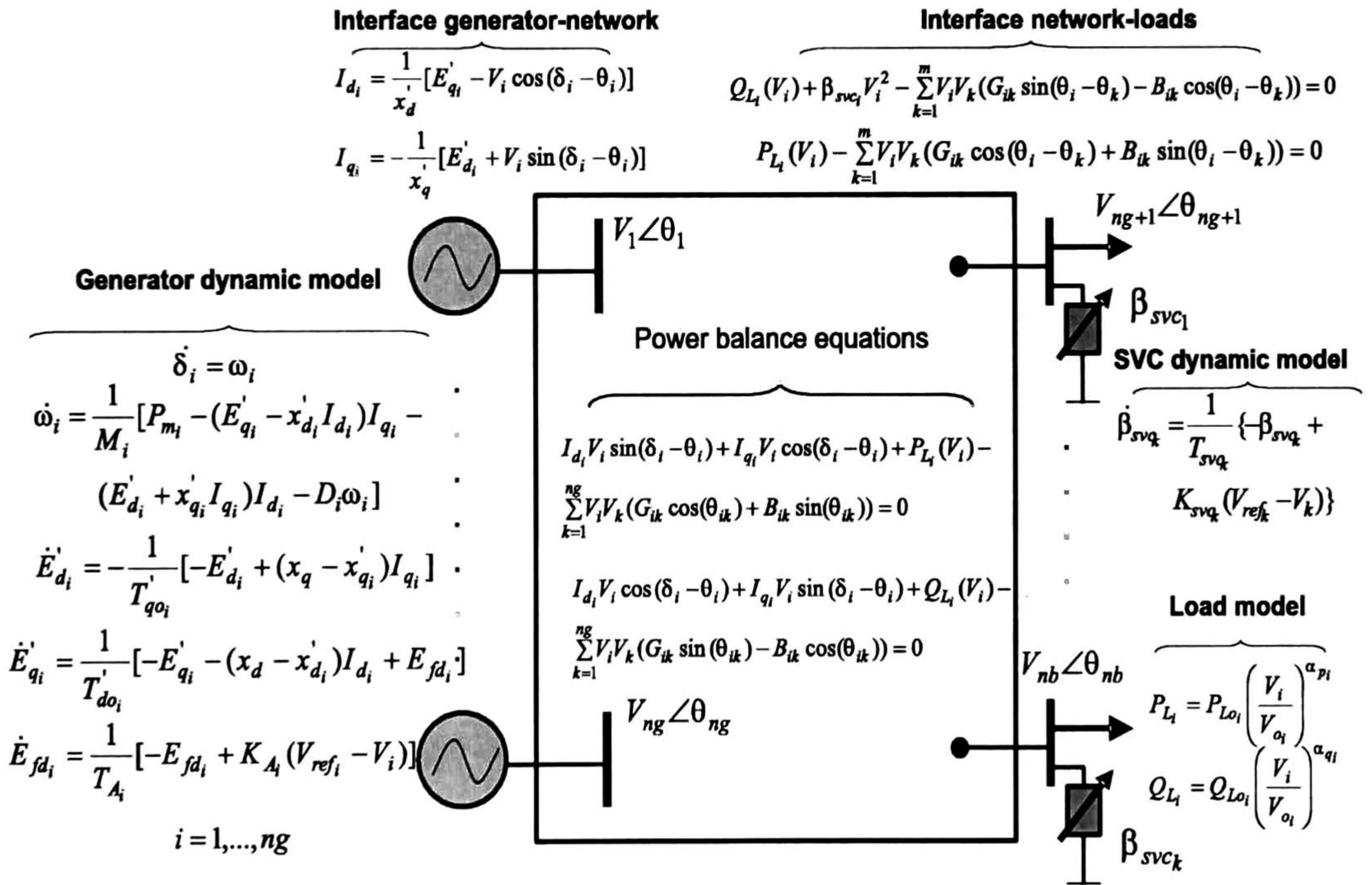


Figure 3.1. Structure-preserving power system representation

Under the above simplifying assumptions, the nonlinear system behavior is given by [8]

a) Rotor swing

$$\dot{\delta}_i = f_{\delta_i} = \omega_i \quad (3.1.a)$$

$$\dot{\omega}_i = f_{\omega_i} = \frac{1}{2H_i} [P_{m_i} - (E_{d_i} I_{d_i} + E_{q_i} I_{q_i}) - D_i \omega_i] \quad (3.1.b)$$

$$\dot{E}'_{d_i} = f_{epd_i} = \frac{1}{T'_{qo_i}} [-E'_{d_i} + (X_{q_i} - X'_{q_i}) I_{q_i}] \quad (3.1.c)$$

$$\dot{E}'_{q_i} = f_{epq_i} = \frac{1}{T'_{do_i}} [-E'_{q_i} - (X_{d_i} - X'_{d_i}) I_{d_i} + E_{fd_i}] \quad (3.1.d)$$

$$\dot{E}_{fd_i} = f_{fd_i} = \frac{1}{T_{A_i}} [-E_{fd_i} + K_{A_i} (V_{ref_i} - V_i)] \quad (3.1.e)$$

$$\dot{\beta}_{svc_i} = f_{\beta_{svc_i}} = \frac{(V_{ref_svc} - V_i) k_{r_i} - \beta_{svc_i}}{T_{r_i}} \quad (3.1.f)$$

b) Interface generator-network equations

$$0 = g_{d_i} = -I_{q_i} X'_{q_i} + R_{a_i} I_{d_i} - E'_{d_i} + V_i \sin(\delta_i - \theta_i) \quad (3.2)$$

$$0 = g_{q_i} = -I_{d_i} X'_{d_i} - R_{a_i} I_{q_i} + E'_{q_i} - V_i \cos(\delta_i - \theta_i) \quad (3.3)$$

$$0 = g_{p_i} = -P_{g_i} + I_{d_i} V_i \sin(\delta_i - \theta_i) + I_{q_i} V_i \cos(\delta_i - \theta_i) \quad (3.4)$$

$$0 = g_{g_i} = -Q_{g_i} + I_{d_i} V_i \cos(\delta_i - \theta_i) - I_{q_i} V_i \sin(\delta_i - \theta_i) \quad (3.5)$$

c) Load flow mismatches at generation and load buses

$$0 = g_{pg_i} = -P_{g_i} + \sum_{k=1}^{ng} V_i V_k (G_{ik} \cos(\theta_{ik}) + B_{ik} \sin \theta_{ik}) \quad (3.6)$$

$$0 = g_{pl_i} = -P_{L_i} + \sum_{k=ng+1}^n V_i V_k (G_{ik} \cos(\theta_{ik}) + B_{ik} \sin(\theta_{ik})) \quad (3.7)$$

$$0 = g_{qg_i} = -Q_{g_i} + \sum_{k=1}^{ng} V_i V_k (G_{ik} \sin(\theta_{ik}) - B_{ik} \cos(\theta_{ik})) \quad (3.8)$$

$$0 = g_{ql_i} = -Q_{l_i} + \sum_{k=ng+1}^n V_i V_k (G_{ik} \sin(\theta_{ik}) - B_{ik} \cos(\theta_{ik})) \quad (3.9)$$

with

$$0 = g_{pr_i} = -P_{l_i} + P_{l_i}(V_i) \quad (3.10)$$

$$0 = g_{qr_i} = -Q_{l_i} + Q_{l_i}(V_i) \quad (3.11)$$

where

$$P_{l_i}(V_i) = P_{Lo_i} \left[k_{p1_i} + k_{p2_i} \left(\frac{V_i}{V_{o_i}} \right) + k_{p3_i} \left(\frac{V_i}{V_{o_i}} \right)^2 \right]$$

$$Q_{l_i}(V_i) = Q_{Lo_i} \left[k_{Q1_i} + k_{Q2_i} \left(\frac{V_i}{V_{o_i}} \right) + k_{Q3_i} \left(\frac{V_i}{V_{o_i}} \right)^2 \right]$$

In equations above, δ is the angular position of the rotor in electrical rad, ω is the rotor angle velocity in electrical rad/s, P_m is the mechanical input power in pu, D is the generator damping coefficient in pu, and H is the inertia constant in MWs/MVA. E'_d, E'_q, I'_d and I'_q are the d - and q -axes voltages and currents, P_{Lo_i} and Q_{Lo_i} represent the constants active and reactive power components at the nominal voltage, V_o ; $k_{p1_i} + k_{p2_i} + k_{p3_i} = k_{Q1_i} + k_{Q2_i} + k_{Q3_i} = 1$, for $i = n + 1, n + 2, \dots, m$ and k_{p1_i}, k_{Q1_i} represent the fraction of constant active and reactive power load, k_{p2_i}, k_{Q2_i} are the fraction of constant active and reactive current load, and k_{p3_i}, k_{Q3_i} are the fraction of constant active and reactive load constant impedance.

The other symbols have the usual meaning [8].

3.2.2 Structure-Preserving Power System Model

Let $\mathbf{x} = [\delta^T \quad \omega^T \quad \mathbf{E}_d^T \quad \mathbf{E}_q^T \quad \mathbf{E}_{fd} \quad \boldsymbol{\beta}_{svc}^T]^T$ be the vector of dynamic states, and $\mathbf{z} = [\mathbf{I}_d^T \quad \mathbf{I}_q^T \quad \mathbf{P}_g^T \quad \mathbf{Q}_g^T \quad \boldsymbol{\theta}^T \quad \mathbf{V}^T]^T$ be the vector of pseudo-state (algebraic) variables.

Combining the system equations (3.1) through (3.8) results in the nonlinear DAE system

$$\dot{\mathbf{x}} = \mathbf{f}(\mathbf{x}, \mathbf{z}) = [\mathbf{f}_\delta^T \quad \mathbf{f}_\omega^T \quad \mathbf{f}_{epd}^T \quad \mathbf{f}_{epq}^T \quad \mathbf{f}_{fd}^T \quad \mathbf{f}_{\beta svc}^T]^T \quad (3.12)$$

$$\mathbf{0} = \mathbf{g}(\mathbf{x}, \mathbf{z}) = [\mathbf{g}_d^T \quad \mathbf{g}_q^T \quad \mathbf{g}_p^T \quad \mathbf{g}_g^T \quad \mathbf{g}_{pg}^T \quad \mathbf{g}_{pl}^T \quad \mathbf{g}_{qg}^T \quad \mathbf{g}_{ql}^T \quad \mathbf{g}_{pr}^T \quad \mathbf{g}_{qr}^T]^T \quad (3.13)$$

Equations (3.12) and (13) represent a set of DAE equations of the form

$$\begin{aligned} \dot{\mathbf{x}}(t) &= \mathbf{f}(t, \mathbf{x}, \mathbf{z}) \quad , \quad \mathbf{x}(0) = \mathbf{x}_0 \\ \mathbf{0} &= \mathbf{g}(t, \mathbf{x}, \mathbf{z}) \end{aligned} \quad (3.14)$$

where $\mathbf{x} \in \mathcal{R}^n$ is the vector of system states, and $\mathbf{z} \in \mathcal{R}^m$ is the vector of algebraic states. Note that network characteristics are fully preserved by taking advantage of the sparse nature of the model.

In classical normal form analysis, the system (3.14) is reduced to an explicit state space representation $\dot{\mathbf{x}} = \bar{\mathbf{f}}(\mathbf{x})$ where \mathbf{x} is the vector of physical system states, and $\bar{\mathbf{f}}$ is a nonlinear vector that incorporates network (algebraic) effects [1]. However as the size and number of equations increases, this may become impractical. Further, important information regarding network structure is lost which might be of interest for the problem of designing or siting controllers.

A second approach consists of transforming the system of algebraic equations into a system of differential equations [9]. Taking the partial derivatives of the algebraic equations in (3.14) with respect to t and rearranging gives [10]

$$\dot{\mathbf{z}} = - \left(\frac{\partial \mathbf{g}}{\partial \mathbf{z}} \right)^{-1} \left(\frac{\partial \mathbf{g}}{\partial \mathbf{x}} \right) \mathbf{f}(\mathbf{x}, \mathbf{z}) - \left(\frac{\partial \mathbf{g}}{\partial \mathbf{z}} \right)^{-1} \frac{\partial \mathbf{g}}{\partial t} \quad (3.15)$$

where

$$\frac{\partial \mathbf{g}}{\partial \mathbf{z}} = \left[\begin{array}{cc|cc} \mathbf{A}_1 & & & \\ & \mathbf{A}_2 & & \\ \hline & & \mathbf{A}_3 & \\ & & & \mathbf{A}_4 \end{array} \right] = \left[\begin{array}{cccc|cccc} \frac{\partial \mathbf{g}_d}{\partial \mathbf{I}_d} & \frac{\partial \mathbf{g}_d}{\partial \mathbf{I}_q} & \mathbf{0} & \mathbf{0} & \frac{\partial \mathbf{g}_d}{\partial \theta} & \frac{\partial \mathbf{g}_d}{\partial \mathbf{V}} & \mathbf{0} & \mathbf{0} \\ \frac{\partial \mathbf{g}_q}{\partial \mathbf{I}_d} & \frac{\partial \mathbf{g}_q}{\partial \mathbf{I}_q} & \mathbf{0} & \mathbf{0} & \frac{\partial \mathbf{g}_q}{\partial \theta} & \frac{\partial \mathbf{g}_q}{\partial \mathbf{V}} & \mathbf{0} & \mathbf{0} \\ \frac{\partial \mathbf{g}_p}{\partial \mathbf{I}_d} & \frac{\partial \mathbf{g}_p}{\partial \mathbf{I}_q} & -\mathbf{I} & \mathbf{0} & \frac{\partial \mathbf{g}_p}{\partial \theta} & \frac{\partial \mathbf{g}_p}{\partial \mathbf{V}} & \mathbf{0} & \mathbf{0} \\ \frac{\partial \mathbf{g}_g}{\partial \mathbf{I}_d} & \frac{\partial \mathbf{g}_g}{\partial \mathbf{I}_q} & \mathbf{0} & -\mathbf{I} & \frac{\partial \mathbf{g}_g}{\partial \theta} & \frac{\partial \mathbf{g}_g}{\partial \mathbf{V}} & \mathbf{0} & \mathbf{0} \\ \hline \frac{\partial \mathbf{g}_{pg}}{\partial \mathbf{I}_d} & \frac{\partial \mathbf{g}_{pg}}{\partial \mathbf{I}_q} & -\mathbf{I} & \mathbf{0} & \frac{\partial \mathbf{g}_{pg}}{\partial \theta} & \frac{\partial \mathbf{g}_{pg}}{\partial \mathbf{V}} & \mathbf{0} & \mathbf{0} \\ \frac{\partial \mathbf{g}_{pl}}{\partial \mathbf{I}_d} & \frac{\partial \mathbf{g}_{pl}}{\partial \mathbf{I}_q} & \mathbf{0} & \mathbf{0} & \frac{\partial \mathbf{g}_{pl}}{\partial \theta} & \frac{\partial \mathbf{g}_{pl}}{\partial \mathbf{V}} & -\mathbf{I} & \mathbf{0} \\ \frac{\partial \mathbf{g}_{qg}}{\partial \mathbf{I}_d} & \frac{\partial \mathbf{g}_{qg}}{\partial \mathbf{I}_q} & \mathbf{0} & -\mathbf{I} & \frac{\partial \mathbf{g}_{qg}}{\partial \theta} & \frac{\partial \mathbf{g}_{qg}}{\partial \mathbf{V}} & \mathbf{0} & \mathbf{0} \\ \frac{\partial \mathbf{g}_{ql}}{\partial \mathbf{I}_d} & \frac{\partial \mathbf{g}_{ql}}{\partial \mathbf{I}_q} & \mathbf{0} & \mathbf{0} & \frac{\partial \mathbf{g}_{ql}}{\partial \theta} & \frac{\partial \mathbf{g}_{ql}}{\partial \mathbf{V}} & \mathbf{0} & -\mathbf{I} \\ \mathbf{0} & \mathbf{0} & \mathbf{0} & \mathbf{0} & \mathbf{0} & \frac{\partial \mathbf{g}_{pr}}{\partial \mathbf{V}} & -\mathbf{I} & \mathbf{0} \\ \mathbf{0} & \mathbf{0} & \mathbf{0} & \mathbf{0} & \mathbf{0} & \frac{\partial \mathbf{g}_{qr}}{\partial \mathbf{V}} & \mathbf{0} & -\mathbf{I} \end{array} \right]$$

If the Jacobian matrix $\partial \mathbf{g} / \partial \mathbf{z}$, is not singular, the system (3.15) can be transformed into a form that is amenable for normal form analysis. Denoting

$$(\partial \mathbf{g} / \partial \mathbf{z})^{-1} = \left[\begin{array}{cc} \mathbf{B}_1 & \mathbf{B}_2 \\ \mathbf{B}_3 & \mathbf{B}_4 \end{array} \right] \text{ it is straightforward to show that}$$

$$\mathbf{B}_1 = (\mathbf{A}_1 - \mathbf{A}_2 \mathbf{A}_4^{-1} \mathbf{A}_3)^{-1}$$

$$\mathbf{B}_2 = -\mathbf{B}_1 \mathbf{A}_2 \mathbf{A}_4^{-1}$$

$$\mathbf{B}_3 = -\mathbf{A}_4^{-1} \mathbf{A}_3 \mathbf{B}_1$$

$$\mathbf{B}_4 = \mathbf{A}_4^{-1} - \mathbf{A}_4^{-1} \mathbf{A}_3 \mathbf{B}_2$$

As observed, the singularity of the Jacobian matrix, $\partial \mathbf{g} / \partial \mathbf{z}$, is related to the network submatrix, \mathbf{A}_4 . Matrix $\partial \mathbf{g} / \partial \mathbf{z}$ also plays a role in the complexity and accuracy of the model; avoiding the inverse computation leads to less complex differential equations and Jacobian-related terms in the model.

There are two additional issues concerning representation (3.15) of the system. The first one is obtaining a dynamic representation of the algebraic constraints, such that the system (3.15) can be expressed in the framework of

singular perturbation theory. The other key issue in applying this formulation for modeling of algebraically constrained dynamic systems is finding representations of the system which allow one to apply existing results from normal forms theory. The basis of the selection of the singular perturbation representation is dealt with in the following sections.

3.3 Singular Perturbations Analysis Approach

3.3.1 Singularly Perturbed Dynamics

The primary goal is to convert the system (3.13) into the standard singularly perturbed form [11]

$$\begin{aligned}\dot{\mathbf{x}}(t) &= \hat{\mathbf{f}}(t, \mathbf{x}, \mathbf{z}, \varepsilon), \mathbf{x}(t_0) = \mathbf{x}_0, \mathbf{x} \in \mathcal{R}^n \\ \varepsilon \dot{\mathbf{z}} &= \hat{\mathbf{g}}(t, \mathbf{x}, \mathbf{z}, \varepsilon), \mathbf{z}(t_0) = \mathbf{z}_0, \mathbf{z} \in \mathcal{R}^m\end{aligned}\tag{3.16}$$

where ε is a small singular perturbation parameter. When ε approaches zero, the dynamics of \mathbf{z} becomes infinitely faster than that of \mathbf{x} , and under certain conditions, approaches that of the system $\dot{\mathbf{x}}(t) = \hat{\mathbf{f}}(t, \mathbf{x}, \mathbf{z}), \mathbf{0} = \hat{\mathbf{g}}(t, \mathbf{x}, \mathbf{z})$.

Following Gordon and Liu [9] a set of DAEs can be transformed into an explicit set of differential equations by adding an appropriate singularly perturbed dynamics.

More formally, let

$$\mathbf{w} = \hat{\mathbf{g}}(t, \mathbf{x}, \mathbf{z}), \quad \mathbf{w} \in \mathcal{R}^m\tag{3.17}$$

be a function that expresses the degree of violation of the algebraic (constraint) equation by the augmented system (3.15). The convergence of the model to the algebraic constraints of the DAEs can be examined through the dynamics of (3.16).¹

In order to guarantee that the constraint equation is met, a singular perturbation approach is used to introduce an asymptotically stable manifold $\dot{\mathbf{w}} = -(1/\varepsilon)\mathbf{w}$. From (3.16), this equation can be solved explicitly for $\dot{\mathbf{w}}$ in terms of $\dot{\mathbf{x}}$ as

$$\dot{\mathbf{w}} = -\frac{1}{\varepsilon}\mathbf{w} = \frac{\partial \mathbf{w}}{\partial t} + \frac{\partial \mathbf{w}}{\partial \mathbf{x}} \dot{\mathbf{x}} + \frac{\partial \mathbf{w}}{\partial \mathbf{z}} \dot{\mathbf{z}}\tag{3.18}$$

¹ Ideally the system converges to an invariant set $\mathbf{w} = \mathbf{0}$ in some neighborhood of the exact solution where the Jacobian is non-singular [9].

or, equivalently,

$$\varepsilon \dot{\mathbf{z}} = -\left(\frac{\partial \mathbf{w}}{\partial \mathbf{z}}\right)^{-1} \mathbf{w} - \varepsilon \left(\frac{\partial \mathbf{w}}{\partial \mathbf{z}}\right)^{-1} \left[\frac{\partial \mathbf{w}}{\partial t} + \frac{\partial \mathbf{w}}{\partial \mathbf{x}} \dot{\mathbf{x}} \right] \quad (3.19)$$

where, upon convergence $\mathbf{w} = \mathbf{0}$.

Equation (3.18) may now be interpreted in the singular perturbation framework (3.15). Using the expression for the algebraic constraints from (3.16) gives

$$\varepsilon \dot{\mathbf{z}} = -\left(\frac{\partial \mathbf{w}}{\partial \mathbf{z}}\right)^{-1} \hat{\mathbf{g}}(t, \mathbf{x}, \mathbf{z}) - \varepsilon \left(\frac{\partial \mathbf{w}}{\partial \mathbf{z}}\right)^{-1} \left[\frac{\partial \mathbf{w}}{\partial t} + \frac{\partial \mathbf{w}}{\partial \mathbf{x}} \hat{\mathbf{f}}(t, \mathbf{x}, \mathbf{z}, \varepsilon) \right] \quad (3.20)$$

Theoretical models to simplify (3.19) are given in [9] and [12,13] based on Lyapunov theory and are discussed below from the standpoint of the practical implementation of the method.

For small ε , the dynamics of the second term can be neglected, and the system behavior can be approximated by

$$\begin{aligned} \dot{\mathbf{x}} &= \hat{\mathbf{f}}(\mathbf{x}, \mathbf{z}, \varepsilon) \\ \varepsilon \dot{\mathbf{z}} &= -\left(\frac{\partial \mathbf{w}}{\partial \mathbf{z}}\right)^{-1} \hat{\mathbf{g}}(\mathbf{x}, \mathbf{z}) \approx -\left(\frac{\partial \mathbf{w}}{\partial \mathbf{z}}\right)^T \hat{\mathbf{g}}(\mathbf{x}, \mathbf{z}) \end{aligned} \quad (3.21)$$

where the simplification $(\partial \mathbf{w} / \partial \mathbf{z})^{-1} = (\partial \hat{\mathbf{g}} / \partial \mathbf{z})^{-1} \approx (\partial \mathbf{w} / \partial \mathbf{z})^T$ avoids the inversion of the extended power flow Jacobian. From a practical point of view, this allows the sparsity of the power system model to be maintained in some pattern that is consistent with other power system formulations while at the same time guarantees a degree of accuracy in the approximation and reduces modeling complexity. Our numerical simulations in Chapter 5 confirm these assertions.

The next theorem is of interest for the analysis of singularly perturbed systems.

Theorem 3.1. For a system² represented by (3.20) the system trajectories \mathbf{x} and \mathbf{z} can be expressed as [14]

$$\begin{aligned}\mathbf{x} &= \mathbf{x}(t) + O(\varepsilon) \\ \mathbf{z} &= \mathbf{z}(t) + O(\varepsilon)\end{aligned}$$

where $O(\varepsilon)$ is an error. This theorem holds provided that the following two assumptions are satisfied.

Assumption 3.1.1. For the equilibrium point in $t = 0$, $O(\varepsilon) = 0$ such that $O(\varepsilon)$ exists for $t > 0$.

Assumption 3.1.2. The eigenvalues for the augmented system given by (3.20) evaluated for ε have two sets of eigenvalues corresponding to the slow and fast dynamics, given by

$$\text{set}(\text{Re}(\lambda_z)) \leq \text{set}(\text{Re}(\lambda_x)) < 0$$

for $t = 0$, \mathbf{x}_0 and \mathbf{z}_0 in the domain of interest.

3.4 Normal Form Analysis of the Singularly Perturbed System

3.4.1 Second-Order Approximation

With ε small, but finite, the series expansion of (3.21) up to order 2, about the initial condition yields

$$\begin{bmatrix} \dot{\mathbf{x}} \\ \dot{\mathbf{z}} \end{bmatrix} = \frac{1}{\varepsilon} \begin{bmatrix} \varepsilon \frac{\partial \hat{\mathbf{f}}}{\partial \mathbf{x}} & \varepsilon \frac{\partial \hat{\mathbf{f}}}{\partial \mathbf{z}} \\ \frac{\partial \hat{\mathbf{g}}}{\partial \mathbf{x}} & \frac{\partial \hat{\mathbf{g}}}{\partial \mathbf{z}} \end{bmatrix} \begin{bmatrix} \mathbf{x} \\ \mathbf{z} \end{bmatrix} + \begin{bmatrix} \hat{\mathbf{f}}_2(\mathbf{x}, \mathbf{z}, \varepsilon) \\ \frac{1}{\varepsilon} \hat{\mathbf{g}}_2(\mathbf{x}, \mathbf{z}, \varepsilon) \end{bmatrix} \quad (3.22)$$

where the ε -dependent Jacobian matrix of the interconnected system is given by

$$\mathbf{J}(\varepsilon) = \begin{bmatrix} \mathbf{J}_{11} & \mathbf{J}_{12} \\ \mathbf{J}_{21} & \mathbf{J}_{22} \end{bmatrix} = \frac{1}{\varepsilon} \begin{bmatrix} \varepsilon \frac{\partial \hat{\mathbf{f}}}{\partial \mathbf{x}} & \varepsilon \frac{\partial \hat{\mathbf{f}}}{\partial \mathbf{z}} \\ \frac{\partial \hat{\mathbf{g}}}{\partial \mathbf{x}} & \frac{\partial \hat{\mathbf{g}}}{\partial \mathbf{z}} \end{bmatrix}$$

and the nonlinear vectors $\hat{\mathbf{f}}_2(\mathbf{x}, \mathbf{z}, \varepsilon)$ and $\hat{\mathbf{g}}_2(\mathbf{x}, \mathbf{z}, \varepsilon)$ are

² This theorem assumes the validity of the \mathbf{f} and \mathbf{g} models regardless the two different scales between \mathbf{x} and \mathbf{z} [15].

$$\begin{bmatrix} \hat{\mathbf{f}}_2(\mathbf{x}, \mathbf{z}, \varepsilon) \\ \hat{\mathbf{g}}_2(\mathbf{x}, \mathbf{z}, \varepsilon) \end{bmatrix} = \frac{1}{2\varepsilon} \begin{bmatrix} \varepsilon[\mathbf{x}^T \mathbf{z}^T] \mathbf{H}_2^1 \begin{bmatrix} \mathbf{x} \\ \mathbf{z} \end{bmatrix} \\ \vdots \\ \varepsilon[\mathbf{x}^T \mathbf{z}^T] \mathbf{H}_2^{n1} \begin{bmatrix} \mathbf{x} \\ \mathbf{z} \end{bmatrix} \\ \hline [\mathbf{x}^T \mathbf{z}^T] \mathbf{H}_2^{n+1} \begin{bmatrix} \mathbf{x} \\ \mathbf{z} \end{bmatrix} \\ \vdots \\ [\mathbf{x}^T \mathbf{z}^T] \mathbf{H}_2^{n+m} \begin{bmatrix} \mathbf{x} \\ \mathbf{z} \end{bmatrix} \end{bmatrix} \quad (3.23)$$

where the \mathbf{H}_2^j are the Hessian matrices of second order derivatives.

Setting ε to zero in the system (3.22) and neglecting second and higher order terms yields the reduced-order approximation $\dot{\mathbf{x}} = (\mathbf{J}_{11} - \mathbf{J}_{12} \mathbf{J}_{22}^{-1} \mathbf{J}_{21}) \mathbf{x}$. In the more general nonlinear case, however, an error is introduced which is a function of both, the size of ε and the nonlinear functions $\mathbf{g}_2(\mathbf{x}, \mathbf{z}, \varepsilon)$ as discussed below.

3.4.2 Jordan Form Representation

For systems of the form (3.22), standard normal form analyses can be conducted to analyze system behavior. Let $\Lambda = \mathbf{V} \mathbf{A} \mathbf{U} = \text{diag}(\lambda_1 \cdots \lambda_n \lambda_{n+1} \cdots \lambda_m)$ denote the diagonal matrix of eigenvalues and let $\mathbf{V} = \mathbf{U}^{-1}$ and \mathbf{U} be the matrices of left and right eigenvectors of the augmented system (3.22). These eigenvalues are given by the roots of the characteristic equation

$$\begin{aligned} \det \left[\mathbf{J} - \lambda \begin{bmatrix} \mathbf{I}_n & \\ & \mathbf{I}_m \end{bmatrix} \right] &= \det \left[\frac{1}{\varepsilon} \frac{\partial \hat{\mathbf{g}}}{\partial \mathbf{z}} - \lambda \mathbf{I}_m \right] \\ \det \left[\frac{\partial \hat{\mathbf{f}}}{\partial \mathbf{x}} - \lambda \mathbf{I}_n - \frac{\partial \hat{\mathbf{f}}}{\partial \mathbf{z}} \left(\frac{\partial \hat{\mathbf{g}}}{\partial \mathbf{z}} - \varepsilon \lambda \mathbf{I}_m \right)^{-1} \frac{\partial \hat{\mathbf{g}}}{\partial \mathbf{x}} \right] &= \\ P_1(\lambda, \varepsilon) P_2(\lambda, \varepsilon) &= 0 \end{aligned} \quad (3.24)$$

where $P_1(\lambda, \varepsilon)$ and $P_2(\lambda, \varepsilon)$ are polynomials in λ of degree m and n , respectively and whose coefficients are polynomials in ε . It is easy to verify that as $\varepsilon \rightarrow 0$, the n slow modes in $P_2(\lambda, \varepsilon)$ converge to the eigenvalues of the reduced model $\dot{\mathbf{x}} = (\mathbf{J}_{11} - \mathbf{J}_{11} \mathbf{J}_{22}^{-1} \mathbf{J}_{21}) \mathbf{x}$. Furthermore, it can be seen that in the limit, the fast scale eigenvalues of $P_1(\lambda, \varepsilon)$ go to infinity. An interesting discussion on the slow and fast dynamics of simple systems is given in [12].

The system in (3.22) is then transformed to the Jordan canonical form by using the ε -dependent structure-preserving coordinate change

$$\tilde{\mathbf{x}} = \begin{bmatrix} \mathbf{x} \\ \mathbf{z} \end{bmatrix} = \mathbf{U}(\varepsilon) \tilde{\mathbf{y}} \quad (3.25)$$

where $\mathbf{U}(\varepsilon)$ is the matrix of right eigenvectors from (3.22).

Substitution of (3.25) into (3.22) yields the complex Jordan canonical form

$$\dot{\tilde{\mathbf{y}}} = \Lambda \tilde{\mathbf{y}} + \mathbf{U}(\varepsilon)^{-1} \begin{bmatrix} \hat{\mathbf{f}}_2 \mathbf{U}(\varepsilon) \tilde{\mathbf{y}} \\ \hat{\mathbf{g}}_2 \mathbf{U}(\varepsilon) \tilde{\mathbf{y}} \end{bmatrix} = \Lambda \tilde{\mathbf{y}} + \mathbf{F}_2(\tilde{\mathbf{y}}) \quad (3.26)$$

where

$$\begin{aligned} \mathbf{F}_{2j}(\mathbf{y}) &= \sum_{k=1}^n v_{jk} \mathbf{f}_{2k}(\mathbf{U}\mathbf{y}, \varepsilon) + \sum_{l=1}^m v_{l+n} \mathbf{g}_{2l}(\mathbf{U}\mathbf{y}, \varepsilon) \\ &= \sum_{k=1}^{n+m} \sum_{l=1}^{n+m} C_{2kl}^j y_k y_l, \quad j = 1, 2, \dots, n, n+1, \dots, n+m. \end{aligned}$$

In its singularly perturbed model form, the system (3.26) is amenable for direct normal form analysis.

3.5 Reduction to Normal Form

The power system normal form representation studied here is the same as that introduced previously [1, 13], and is summarized next for completeness.

Let the system behavior be given by (3.26). A near identity change of coordinates of the form

$$\tilde{\mathbf{y}} = \tilde{\mathbf{z}} + \mathbf{h}_2(\tilde{\mathbf{z}}) \quad (3.27)$$

is sought that takes the system to the normal form

$$\dot{\tilde{\mathbf{z}}} = \Lambda \tilde{\mathbf{z}} + \mathbf{F}'_2(\tilde{\mathbf{z}}) \quad (3.28)$$

where the $\mathbf{h}_2(\tilde{\mathbf{z}})$ are undefined complex-valued polynomial vectors to be determined so that the terms of order are eliminated or simplified and the $\mathbf{F}'_2(\tilde{\mathbf{z}})$ are terms that can not be removed or simplified.

Substitution of (3.28) into (3.27) and use of the chain rule yields

$$[\mathbf{I} + D\mathbf{h}_2(\tilde{\mathbf{z}})] \{ \Lambda \tilde{\mathbf{z}} + \mathbf{F}'_2(\tilde{\mathbf{z}}) \} = \Lambda \tilde{\mathbf{z}} + \Lambda \mathbf{h}_2(\tilde{\mathbf{z}}) + \mathbf{F}_2(\tilde{\mathbf{z}} + \mathbf{h}_2(\tilde{\mathbf{z}})) \quad (3.29)$$

where $D\mathbf{h}_2(\tilde{\mathbf{z}}_2)$ is the Jacobian matrix of $\mathbf{h}_2(\mathbf{z}_2)$ with respect to \mathbf{z}_2 . Setting $\mathbf{F}_2'(\tilde{\mathbf{z}}) = 0$ and equating terms of like order yields the homological equation

$$D\mathbf{h}_2(\tilde{\mathbf{z}})\Lambda\tilde{\mathbf{z}} - \Lambda\mathbf{h}_2(\tilde{\mathbf{z}}) = \mathbf{F}_2(\tilde{\mathbf{z}}) \quad (3.30)$$

Explicit expressions for the second-order coefficients, $\mathbf{h}_2(\tilde{\mathbf{z}})$, used in the implementation of the method are given by Sanchez Gasca *et al.* [1] and are therefore not repeated here.

3.6 Numerical Implementation

Based on the above approach a computer algorithm was developed for nonlinear analysis of power system models described by DAEs.

Figure 3.2 illustrates the numerical approximation adopted in the studies. Note that, standard eigenvalues calculations for sparse linear systems are performed using commercial software. This allows the study of realistic power system representations.

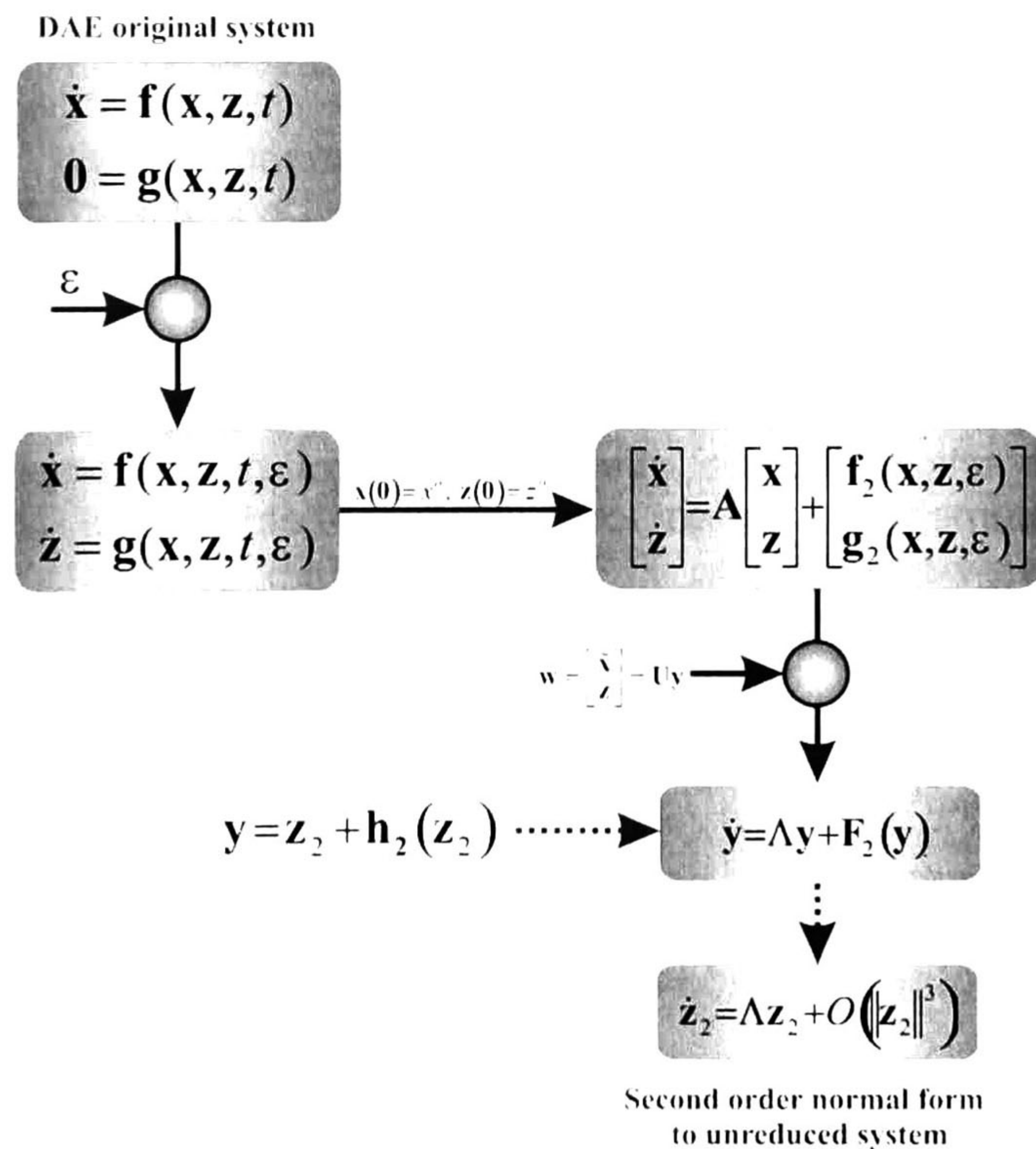


Figure 3.2. Flow chart of the structure-preserving normal form analysis procedure

3.7 Conclusions

A nonlinear analytical model of the power system is developed which preserves network structure. The method reduces the order and complexity of the dynamic model and allows the effect of network parameters and load characteristics to be explicitly identified. In particular, the effect of static voltage-dependent loads and SVC voltage support is represented.

This formulation can be used to estimate the effect of control action on the transmission network and to assess the effect of load characteristics on system behavior. In addition, the network variables contain potentially valuable information for monitoring system behavior and analyzing nonlinear interactions between system components that needs to be analyzed and exploited.

References

- [1] J. J. Sanchez-Gasca, V. Vittal, M. J. Gibbard, A. R. Messina, D. J. Vowles, S. Liu, and U. D. Annakkage, "Inclusion of higher order terms for small-signal (modal) analysis: committee report-task force on assessing the need to include higher order terms for small-signal (modal) analysis", *IEEE Power Systems*, vol. 20, pp. 1886-1904, Nov 2005
- [2] J. Gilsoo, V. Vittal and W. Kliemann, "Effect of nonlinear modal interaction on control performance: Use of normal forms technique in control design, Part I: General theory and procedure", *IEEE Trans. on Power Systems*, vol. 13, pp. 401-407, May 1998
- [3] C. M. Ling, V. Vittal, W. Kliemann, and A.A. Fouad, "Investigation of modal interaction and its effects on control performance in stressed power systems using normal forms of vector fields", *IEEE Transactions on Power Systems*, vol. 11, pp. 781-787, May. 1996
- [4] H. Amano, T. Kumano and T. Inoue, "Nonlinear stability indexes of power system oscillation using normal form analysis" *IEEE Trans. on Power Systems*, vol. 21, pp. 825-834, May 2006
- [5] I. Dobson and E. Barocio, "Scaling of normal form analysis coefficients under coordinate change", *IEEE Trans. on Power Systems*, vol. 19, pp. 1438-1444, Aug 2004
- [6] R. J. Betancourt, E. Barocio, J. Arroyo and A. R. Messina, "A real normal form approach to the study of resonant power systems", *IEEE Trans. on Power Systems*, vol. 21, pp. 431-432, Feb 2006

- [7] S. Liu, A. R. Messina and V. Vittal, "Assessing placement of controllers and nonlinear behavior using normal form analysis", *IEEE Trans. on Power Systems*, vol. 20, pp. 1486-1495, Aug 2005
- [8] P. W. Sauer and M. A. Pai, *Power System Dynamics and Stability*, Prentice Hall Upper Saddle River, NJ. 1998
- [9] W. Brandon, B. W. Gordon and S. Liu, "A singular perturbation approach for modeling differential-algebraic systems", *Journal of Dynamic Systems, Measurement and Control*, vol. 120, pp. 541-545, Dec 1998
- [10] Jean-Jacques E. Slotine and Weiping Li, *Applied Nonlinear Control*, New Jersey: Prentice-Hall, 1991
- [11] P. V. Kokotovic, K. K. Hassan and J. O'Reilly, *Singular Perturbation Methods in Control: Analysis and Design*. Academic Press Inc., 1986
- [12] G. M. Huang, K. Men and X. Song "A new remodeling technique for power system dynamic analysis", *Transmission and distribution conference and exhibitions: Asia and Pacific*, 2005
- [13] I. Martínez, A. R. Messina and E. Barocio, "Perturbation analysis of power system: Effects of second and third-order nonlinear terms on system dynamic behavior", *Electric Power Systems Research*, vol. 71, pp. 159-167, Oct 2004
- [14] M. Lli and J. Zaborszky, *Dynamics and Control of Large Electric Power Systems*, John Wiley and Sons. Inc., 2000

Chapter 4

A Structure-Preserving Approach to Power System Normal Form Analysis

Parametric sensitivity analysis is becoming a very important tool when studying dynamic system models. In this chapter, a structure-preserving approach to the approximate analysis of power system models described by DAE equations is explored that incorporates the operation of flexible ac transmission devices and load characteristics.

A general approach based on the extended normal form theory is proposed for the analysis of nonlinear response to parametric variations. The conceptual framework takes into account the nonlinear system structure and provides a rigorous base for the representation of network dynamic effects. First, analytical series solutions are obtained containing parameters of the system, thereby revealing the functional dependence on these parameters on the system behavior. Sensitivity analyzes of states to parameter variations are then used to approximate the effect of network and control characteristics on system dynamic behavior. The derived analysis methods may be used to infer the effect of network control and characteristics on wide-area system behavior and aid in the location and design of system controllers.

Several faithful research directions are identified including the location of FACTS controllers, the analysis of potential adverse interactions between controllers, the evaluation of load modulation, and the analysis of nonlinear mode propagation across the transmission system. The theory and analysis methods can be easily generalized to other types of network devices.

4.1 Background

Nonlinear mode interaction is known to contribute to different properties in physical processes. The nature of the interaction phenomenon is rather complex and depends on several interacting characteristics such as the control characteristics, the topology and operating condition of the system, and the characteristics of the transmission system.

In the previous chapters, a general framework for the analysis of nonlinear system behavior based on normal form theory and singular perturbation techniques was proposed. This framework permits consideration of general power system models described by sparse DAE systems and allows for the application of existing results from normal form theory to the analysis and characterization of system behavior.

In this chapter, we extend this approach by addressing the role of transmission network variables in system dynamic performance. A second-order representation of the power system is, to this end derived, that consider the explicit representation of load characteristics and multiple FACTS devices in the state representation. Based on this representation, closed form solutions are derived in which network characteristics are explicitly represented.

Parametric sensitivity analysis is used to obtain information concerning state variable variations with respect to infinitesimal perturbations in the values of model parameters.

The proposed formulation is general and can be used to address both, linear and nonlinear aspects of system dynamic performance.

4.2 Analytical Approach

4.2.1 Closed- Form Analytical Solutions

Having determined the normal form system and its associated transformations, approximate time-domain solutions are in this section developed using inverse nonlinear transformations between coordinate systems.

Let the system dynamic behavior in \mathbf{z}_2 coordinates be expressed as

$$\dot{\tilde{\mathbf{z}}}_2 = \begin{bmatrix} \dot{\mathbf{z}}_n \\ \dot{\mathbf{z}}_m \end{bmatrix} = \begin{bmatrix} \Lambda_n & \\ & \Lambda_m \end{bmatrix} \begin{bmatrix} \mathbf{z}_n \\ \mathbf{z}_m \end{bmatrix} + \begin{bmatrix} \mathbf{F}_{2_n}^r \\ \mathbf{F}_{2_m}^r \end{bmatrix} + O(3) \quad (4.1)$$

where $\Lambda_n = \text{diag}[\lambda_1 \ \lambda_2 \ \dots \ \lambda_n]$ and $\Lambda_m = \text{diag}[\lambda_{n+1} \ \lambda_{n+2} \ \dots \ \lambda_{n+m}]$. The functions $F_{2_n}^r$ and $F_{2_m}^r$ are called the resonant or secular parts of F and contain the essential part of the dynamical system.

Then, on neglecting the terms of order $O(3)$ and higher in (4.1), and assuming that no resonance conditions are met, we obtain

$$\dot{\tilde{\mathbf{z}}}_2 = \begin{bmatrix} \dot{\mathbf{z}}_n \\ \dot{\mathbf{z}}_m \end{bmatrix} = \begin{bmatrix} \Lambda_n & \\ & \Lambda_m \end{bmatrix} \begin{bmatrix} \mathbf{z}_n \\ \mathbf{z}_m \end{bmatrix} = \Lambda \tilde{\mathbf{z}}_2 \quad (4.2)$$

with initial conditions given by $\mathbf{z}_2^o = [\mathbf{z}_{n \times 1}^o \ \mathbf{z}_{m \times 1}^o]^T$. In the new coordinates, solution of this equation for $\mathbf{z}_2(t)$ gives

$$\mathbf{z}_{2_j}(t) = e^{\lambda_j t} z_{2_j}^o \quad \text{for } j = 1, 2, \dots, n, n+1, \dots, n+m \quad (4.3)$$

Approximate analytical solutions for second-order coordinates systems are then obtained by using the inverse transformations

$$\mathbf{y}(t) = \mathbf{z}_2(t) + \mathbf{h}_2(\mathbf{z}_2(t)) \quad (4.4)$$

and

$$\begin{bmatrix} \mathbf{x}(t) \\ \mathbf{y}(t) \end{bmatrix} = \mathbf{U} \mathbf{y}(t) \quad (4.5)$$

from which it follows that

$$x_p(t) = \sum_{j=1}^{n+m} u_{pj} y_j(t) = \sum_{j=1}^{n+m} u_{pj} e^{\lambda_j t} + \sum_{j=1}^{n+m} u_{pj} \left(\sum_{k=1}^{n+m} \sum_{l=k}^{n+m} h_{2_{pkl}}^o z_{2_k}^o(t) z_{2_l}^o(t) e^{(\lambda_k + \lambda_l)t} \right) \quad \text{for } p=1, 2, \dots, n \quad (4.6)$$

and

$$y_q(t) = \sum_{j=1}^{n+m} u_{qj} y_j(t) = \sum_{j=1}^{n+m} u_{qj} e^{\lambda_j t} + \sum_{j=1}^{n+m} u_{qj} \left(\sum_{k=1}^{n+m} \sum_{l=k}^{n+m} h_{2_{qkl}}^o z_{2_k}^o(t) z_{2_l}^o(t) e^{(\lambda_k + \lambda_l)t} \right) \quad \text{for } q=n+1, n+2, \dots, n+m \quad (4.7)$$

Given a particular operating condition, Eqs. (4.6) and (4.7) enable analytical solutions to be readily obtained.

Figure 4.1 shows a graphical interpretation of the closed form analytical solutions.

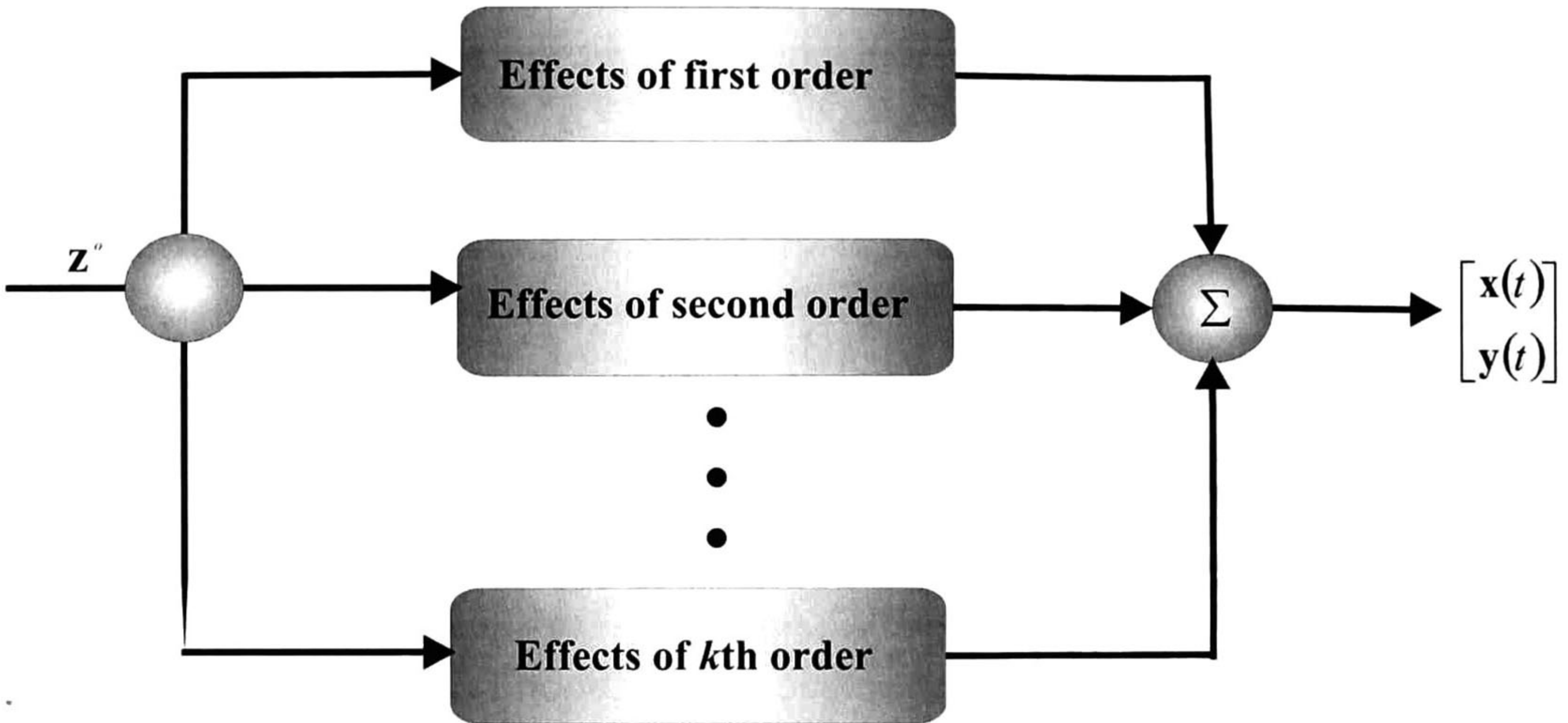


Figure 4.1. Schematic diagram illustrating the derivation of closed-form analytical solutions in physical space.

Equations (4.6) and (4.7) have many interesting characteristics which allow a number of important conclusions to be reached. The analysis of these expressions shows that normal form solutions can be expressed as a linear combination of modal components in z_2 coordinates. These modal contributions add up to produce a real solution in the original coordinates, x .

It should be emphasized that, each of these components can be seen as the contribution of the individual mode combinations to the overall system solution; this is a unique feature of nonlinear analysis that can not be studied using conventional techniques.

4.2.2 Time Evolution of Network Variables

Based on the above formulation, an efficient technique to assess the influence on network characteristics on system dynamic behavior is proposed.

From (4.7), closed-form time-domain solutions for the fast, network variables can be obtained up to the desired order of approximation, as

$$\beta_{SFC_w}(t) = \sum_{j=1}^m u_{wj} z_{j_0} e^{\lambda_j t} + \sum_{j=1}^m u_{wj} \left[\sum_{k=1}^m \sum_{l=k}^m h_{2_wkl} z_{k_0} z_{l_0} e^{(\lambda_k + \lambda_l)t} \right] \quad \text{for } w=n-ng+1, n-ng+2, \dots, n \quad (4.8)$$

$$\theta_p(t) = \sum_{j=1}^m u_{pj} z_{j_o} e^{\lambda_j t} + \sum_{j=1}^m u_{pj} \left[\sum_{k=1}^m \sum_{l=k}^m h_{2, pkl} z_{k_o} z_{l_o} e^{(\lambda_k + \lambda_l) t} \right] \quad p=n+1, \dots, m \quad (4.9)$$

$$V_q(t) = \sum_{j=1}^m u_{qj} z_{j_o} e^{\lambda_j t} + \sum_{j=1}^m u_{qj} \left[\sum_{k=1}^m \sum_{l=k}^m h_{2, qkl} z_{k_o} z_{l_o} e^{(\lambda_k + \lambda_l) t} \right] \quad q=m+1, \dots, 2m \quad (4.10)$$

$$P_{Lr}(t) = \sum_{j=1}^m u_{rj} z_{j_o} e^{\lambda_j t} + \sum_{j=1}^m u_{rj} \left[\sum_{k=1}^m \sum_{l=k}^m h_{2, rkl} z_{k_o} z_{l_o} e^{(\lambda_k + \lambda_l) t} \right] \quad r=2m+1, \dots, 2m+1+nl \quad (4.11)$$

$$Q_{Ls}(t) = \sum_{j=1}^m u_{sj} z_{j_o} e^{\lambda_j t} + \sum_{j=1}^m u_{sj} \left[\sum_{k=1}^m \sum_{l=k}^m h_{2, skl} z_{k_o} z_{l_o} e^{(\lambda_k + \lambda_l) t} \right] \quad r=2m+1+nl, \dots, 2m+1+2nl \quad (4.12)$$

where nl is the number of load buses with active or reactive power.

Equations (4.8) through (4.7) provide approximate solutions to system behaviour in which first –and higher order terms are isolated. The associated eigenvalues λ_j and the structural parameters, h_{jk} , play a crucial role in the observed system response.

More specifically, given the initial conditions, z_j^o, z_l^o , $j, l = 2m+1, \dots, 2m+1+nl$ and structural parameters, h'_{jk} , it is then possible to obtain the specific effect of parameters of interest on system behaviour. This model is general and can be used to estimate the influence of any network variable on the (physical) states of interest.

From this general result a procedure has been derived for parametric sensitivity analysis.

4.2.3 Sensitivity to Parameter Variations

Assuming that both, the initial conditions and structural parameters are known, the above information can be used to compute sensitivity relations between modes and states that explicitly capture control and network effects.

In this section, a general model to infer the network characteristics on global system behaviour is proposed. Figure 4.2 provides a conceptual representation of the proposed framework.

Two main loops are identified:

1. The internal loop associated with the structural $h_{2, jkl}$ parameters obtained from the normal form representation, and
2. The loop associated with the perturbation of initial conditions, \mathbf{x}^o

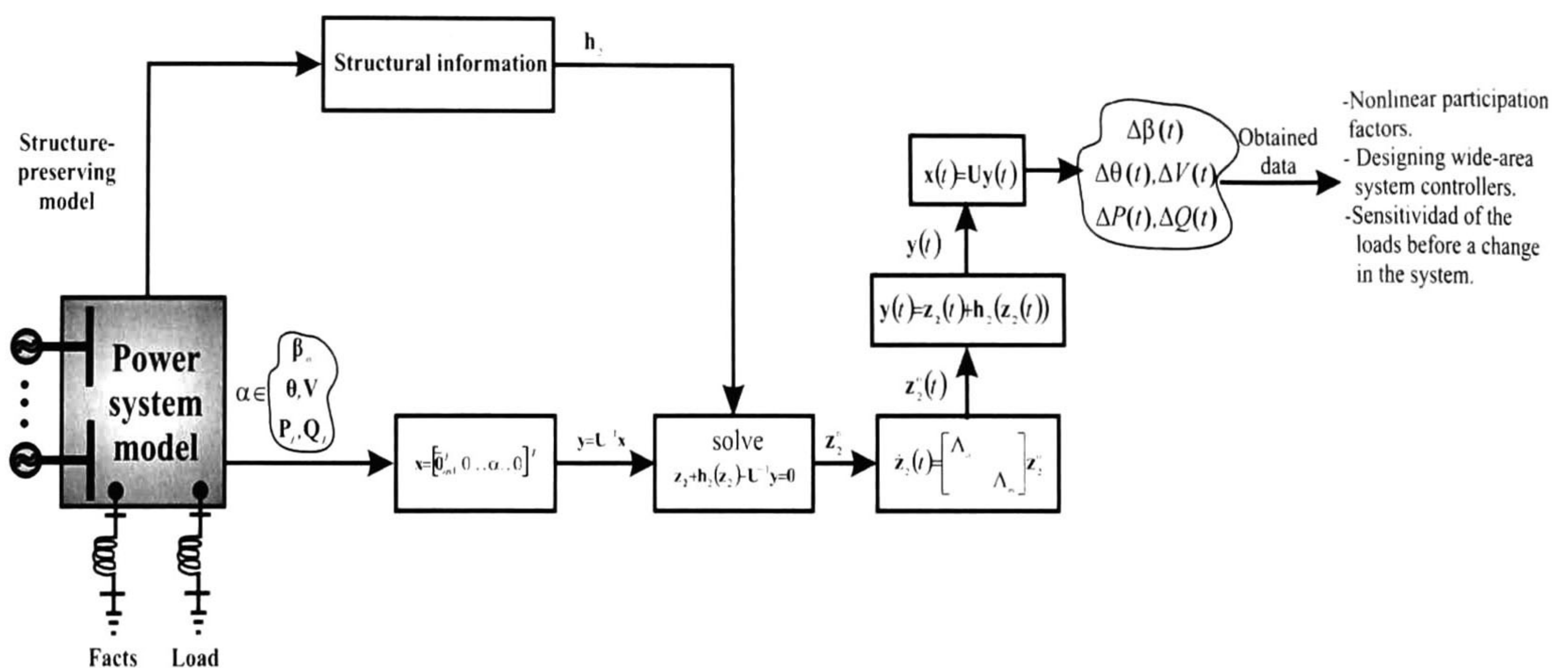


Figure 4.2. Overview of the proposed algorithm for modal analysis.

Computation of closed-form analytical solutions to arbitrary excitation can be carried out as follows:

1. For a given disturbance, \mathbf{x}^o determine initial conditions in the Jordan and normal form spaces using the inverse relationships

$$\begin{aligned} \mathbf{y}^o &= \mathbf{U}^{-1} \mathbf{x}^o, \\ \mathbf{z}^o + \mathbf{h}_2(\mathbf{z}^o) - \mathbf{y}^o &= \mathbf{0} \end{aligned} \quad (4.13)$$

2. Determine the time evolution of selected (states) and pseudo states using Eqs. (4.8) through (4.12)
3. Compute analytical measures of the interaction between modes and states. Determine the specific influence of network and control characteristics on wide-area system behaviour.

The core of this analysis is the determination of initial conditions for normal form analysis. The analysis below focuses on fairly simple system controllers and network characteristics, but the theory is sufficiently general as to include a variety of system controllers.

Before proceeding to a detailed discussion of the system modal response, let us review the nature of load and network characteristics. Subsequent sections discuss other network devices.

4.2.4 Effect of Load Characteristics

Load characteristics are known to significantly influence system dynamic behavior.

Following the development outlined above, we assume that load characteristics can be appropriately represented by a ZIP model of the form [1]

$$P_{L_i}(V_i) = P_{L_{o_i}} \left[k_{p_{1_i}} + k_{p_{2_i}} \left(\frac{V_i}{V_{o_i}} \right) + k_{p_{3_i}} \left(\frac{V_i}{V_{o_i}} \right)^2 \right]$$

$$Q_{L_i}(V_i) = Q_{L_{o_i}} \left[k_{Q_{1_i}} + k_{Q_{2_i}} \left(\frac{V_i}{V_{o_i}} \right) + k_{Q_{3_i}} \left(\frac{V_i}{V_{o_i}} \right)^2 \right]$$

where $k_{p_{1_i}} + k_{p_{2_i}} + k_{p_{3_i}} = k_{Q_{1_i}} + k_{Q_{2_i}} + k_{Q_{3_i}} = 1$, $i = n+1, n+2, \dots, m$, $k_{p_{1_i}}, k_{Q_{1_i}}$ are the fractions of constant active and reactive power load, $k_{p_{2_i}}, k_{Q_{2_i}}$ are the fractions of constant active and reactive current load, and $k_{p_{3_i}}, k_{Q_{3_i}}$ are the fractions of constant active and reactive load constant impedance.

By properly choosing the value of these parameters the effect of various typical load characteristics can be simulated, i.e. constant power, constant current and constant impedance [2].

Formally, one may write

$$P_{L_i}(V_i) = P_{L_{o_i}} \left[k_{p_{1_i}} + k_{p_{2_i}} \left(\frac{V_i}{V_{o_i}} \right) + k_{p_{3_i}} \left(\frac{V_i}{V_{o_i}} \right)^2 \right] \quad (4.14)$$

$$Q_{L_i}(V_i) = Q_{L_{o_i}} \left[k_{Q_{1_i}} + k_{Q_{2_i}} \left(\frac{V_i}{V_{o_i}} \right) + k_{Q_{3_i}} \left(\frac{V_i}{V_{o_i}} \right)^2 \right] \quad (4.15)$$

To a first approximation, the sensitivity of the j th bus load to changes in the terminal voltage, ΔV_i in Eqs. (4.14) and (4.15) can be expressed in terms of the bus voltage deviations, as

$$\Delta P_{L_j}(t) \approx \frac{\partial P_{L_j}(V_j)}{\partial V_j} \Delta V_j(t) + \frac{\partial P_{L_j}(V_j)}{\partial P_{L_j}} \Delta P_{L_j}^o \quad (4.16)$$

$$\Delta Q_{L_j}(t) \approx \frac{\partial Q_{L_j}(V_j)}{\partial V_j} \Delta V_j(t) + \frac{\partial Q_{L_j}(V_j)}{\partial P_{L_j}} \Delta P_{L_j}^o \quad (4.17)$$

where

$$\frac{\partial P_{L_i}}{\partial V_j} = \begin{cases} P_{L_{o_i}} \left[k_{p_{2i}} \left(\frac{1}{V_{o_i}} \right) + k_{p_{3i}} \left(\frac{2V_i}{V_{o_i}} \right) \right] , & i = j \\ 0 , & i \neq j \end{cases} .$$

and

$$\frac{\partial P_{L_i}}{\partial V_j} = \begin{cases} P_{L_{o_i}} \left[k_{p_{2i}} \left(\frac{1}{V_{o_i}} \right) + k_{p_{3i}} \left(\frac{2V_i}{V_{o_i}} \right) \right] , & i = j \\ 0 , & i \neq j \end{cases}$$

Physically, Eqs. (4.16) and (4.17) give the contribution of both, changes in the load magnitude and load characteristics to changes in the bus voltage deviations. It should be emphasized that these two effects are not necessarily related. Thus, for instance, the system response may be associated with other system perturbations at other system locations.

Figure 4.3 provides a conceptual illustration of the physical phenomena suggesting the presence of multiple feedback loops. Two main effects are identified: the effect of changes in the load level, and an indirect effect associated with the network response to the load variations.

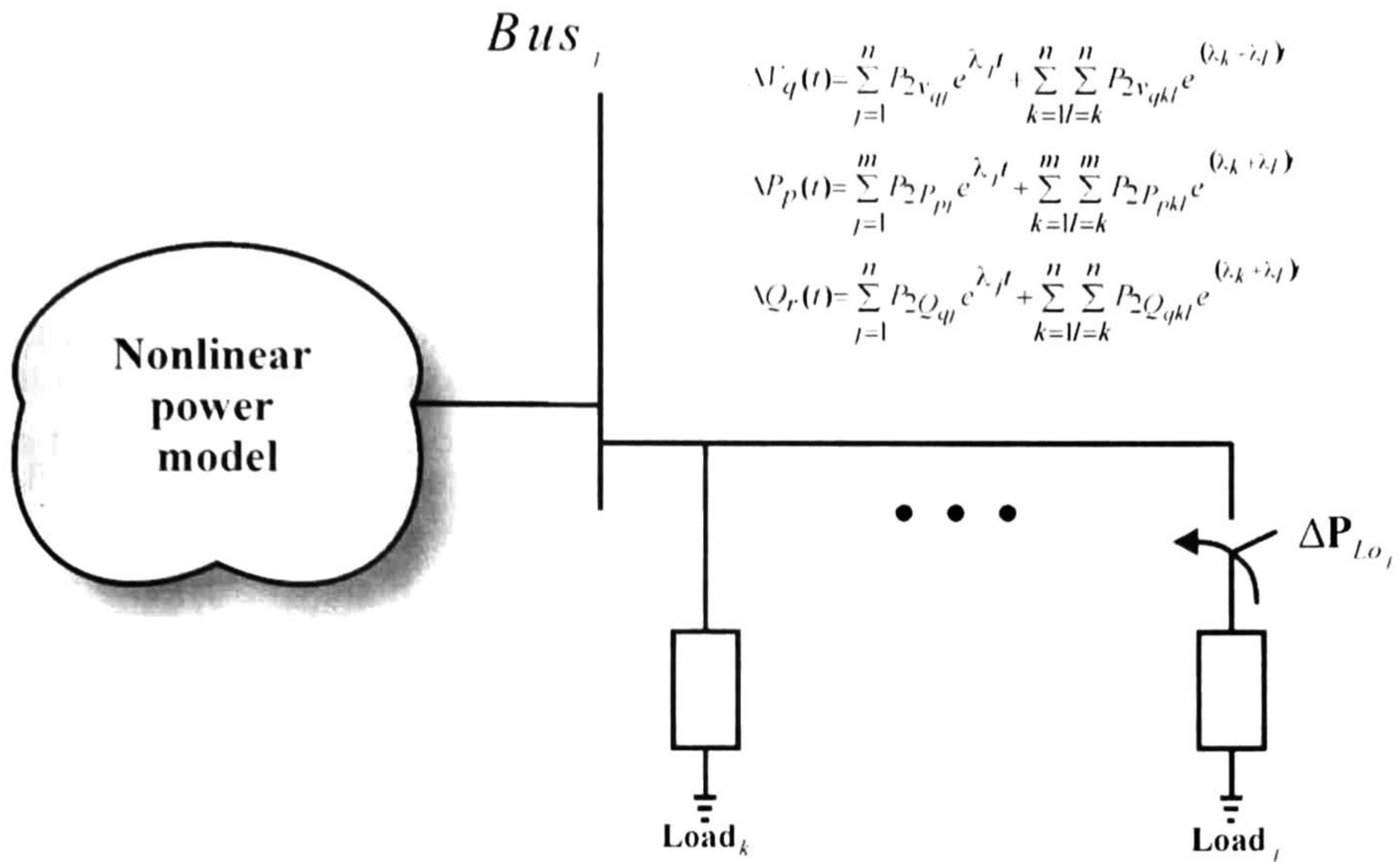


Figure 4.3. Schematic of the adopted power modulation concept.

The analysis suggests that by proper perturbation of the system model, the participation of each individual load to the specific mode of concern can be determined.

Following Shu *et al.* [3], let the initial conditions in physical coordinates \mathbf{x}^o , be expressed as

$$\mathbf{x}^o = [0, \dots, 0, \alpha \Delta P_{L_o}, 0, \dots, 0]^T \quad (4.18)$$

where α is an appropriate scaling factor (normally unit) chosen to provided the desired degree of excitation of a given state, and ΔP_{L_o} represents a given perturbation. Then the initial conditions in the Jordan and normal form spaces are computed from (4.13).

Having computed the initial conditions in NF space, the influence of each load on the mode of concern can be readily determined.

The procedure can be summarized as follows:

- (i). Perturb each system load by using (4.18)
- (ii). Compute initial conditions in the Jordan form space by using (4.13). Compute the time evolution of the load by using

$$\Delta P_{L_r}(t) = \sum_{j=1}^m P_{2L_{rj}} e^{\lambda_j t} + \sum_{k=1}^m \sum_{l=k}^m P_{2L_{rkl}} e^{(\lambda_k + \lambda_l)t} \quad (4.19)$$

- (iii). Compute the first –and second-order participations of the load to the l th mode or mode combination $\lambda_k + \lambda_l$
- (iv). Identify nodes having large participation in the mode(s) of concern and determine geographical boundaries for these contributions. These modes represent suitable locations in which load modulation might be used to enhance damping of critical modes. They also represent potential locations of shunt controllers aimed at enhancing wide-area system damping.

By grouping nodes (loads) having a large participation in a given mode, the influence of load in the global (local) dynamics can be readily determined.

As is apparent from (4.19), $P_{2L,l}$ represents the second-order participation of the l th single-eigenvalue mode in the l th load. Similarly, $P_{2L,kl}$ represents the second-order participation of the l th load bus in the mode formed by the combination of the eigenvalues λ_k and λ_l [4].

With appropriate modifications, the above approach can be used to determine more general nonlinear relationships. This approach generalizes existing approaches to nonlinear sensitivity analysis that incorporate control actions [5].

4.2.5 Transmission Line Participations

For each transmission line, the tie-line power can be approximated by

$$P_{t_{ij}} \approx \frac{V_i V_j}{X_{ij}} \sin(\theta_i - \theta_j) \quad (4.20)$$

Using the same procedure as before, we can write the tie-line sensitivity to changes in the terminal voltage as

$$\Delta P_{t_{ij}}(t) \approx \frac{\partial P_{t_{ij}}}{\partial V_i} \Delta V_i + \frac{\partial P_{t_{ij}}}{\partial V_j} \Delta V_j + \frac{\partial P_{t_{ij}}}{\partial \theta_i} \Delta \theta_i + \frac{\partial P_{t_{ij}}}{\partial \theta_j} \Delta \theta_j \quad (4.21)$$

Substitution of the bus voltage magnitude and phase deviations from Eqs. (4.9) and (4.10) provides the extent of distribution of modal components along the transmission network.

The results of the preceding analysis can be extended to the case of other network parameters.

4.2.6 SVC Voltage Support

Flexible ac transmission system (FACTS) devices are being increasingly utilized in many electric power systems to enhance voltage control and system dynamic performances. Among the existing devices, static VAR compensators (SVCs) are selected to assess the ability of the method to include the effects of network control actions on system nonlinear behavior. The incorporation of other FACTS technologies follows along similar lines.

FACTS devices are introduced in the basic model as linearized relationships between the small changes in real and reactive injections and the corresponding changes in terminal voltage at the connecting nodes. Figure 4.4 depicts the general nature of the adopted model to represents SVCs.

Let the reactive power supplied by the i th SVC be given by $Q_{svc_i}(\beta_{svc_i}, V_i) = \beta_{svc_i} V_i^2$. Neglecting higher order terms, the contribution of each SVC to the power oscillation flow is given by

$$\Delta Q_{svc_i}(t) = \frac{\partial Q_{svc_i}}{\partial \beta_{svc_i}} \Delta \beta_{svc_i} + \frac{\partial Q_{svc_i}}{\partial V_i} \Delta V_i \quad (4.22)$$

in which the derivatives,

$$\frac{\partial Q_{svc_i}}{\partial \beta_{svc_i}} = \begin{cases} V_i^2 \\ 0 \end{cases}$$

$$\frac{\partial Q_{svc_i}}{\partial V_i} = \begin{cases} 2V_i \beta_{svc_i} \\ 0 \end{cases}$$

represent the sensitivity of the reactive power drawn by the devices to changes in the susceptance and terminal voltage. Here, $\Delta Q_{svc_i}(t)$ is the incremental change in the device reactive power, $\Delta \beta_{svc_i}$ is the incremental change in the device susceptance, and ΔV_i is the incremental change in the device voltage magnitude.

Following a similar line of analysis to that used in the study of load modulation, assume now that each SVC is given an initial perturbation, $\Delta \beta_{svc_i}$,

$$\mathbf{x}^0 = [0, \dots, 0, \alpha \Delta \beta_{svc_i}, 0, \dots, 0]^T \quad (4.23)$$

From (4.8), the resulting susceptance variations of SVC i , becomes

$$\Delta \beta_{svc_i}(t) = \sum_{j=1}^m \beta_{2svc_i} e^{\lambda_j t} + \sum_{k=1}^m \sum_{l=k}^m \beta_{2svc_{kl}} e^{(\lambda_k + \lambda_l) t}$$

The influence of SVC to the modal oscillation flow can then be estimated using the algorithm outline above. Note that, in this case, several interacting loops should be incorporated in the analysis, namely (see Fig. 4.4)

- (i). An internal SVC loop
- (ii). Interaction loops involving two or more SVCs or other control devices
- (iii). Interaction loops with load perturbation
- (iv). Other network-state loops

The information provided by these expressions is useful for modal interaction analysis, sensitivity studies, and placement of controllers. An interesting by-product of the above analysis within the small-signal analysis framework, is the ability to assess control-control interactions involving multiple controllers. Reasoning along the same lines yields similar expressions for other system controllers.

Although this method of the first approximation of nonlinear equations holds only for small changes about the initial conditions, it is of considerable practical importance.

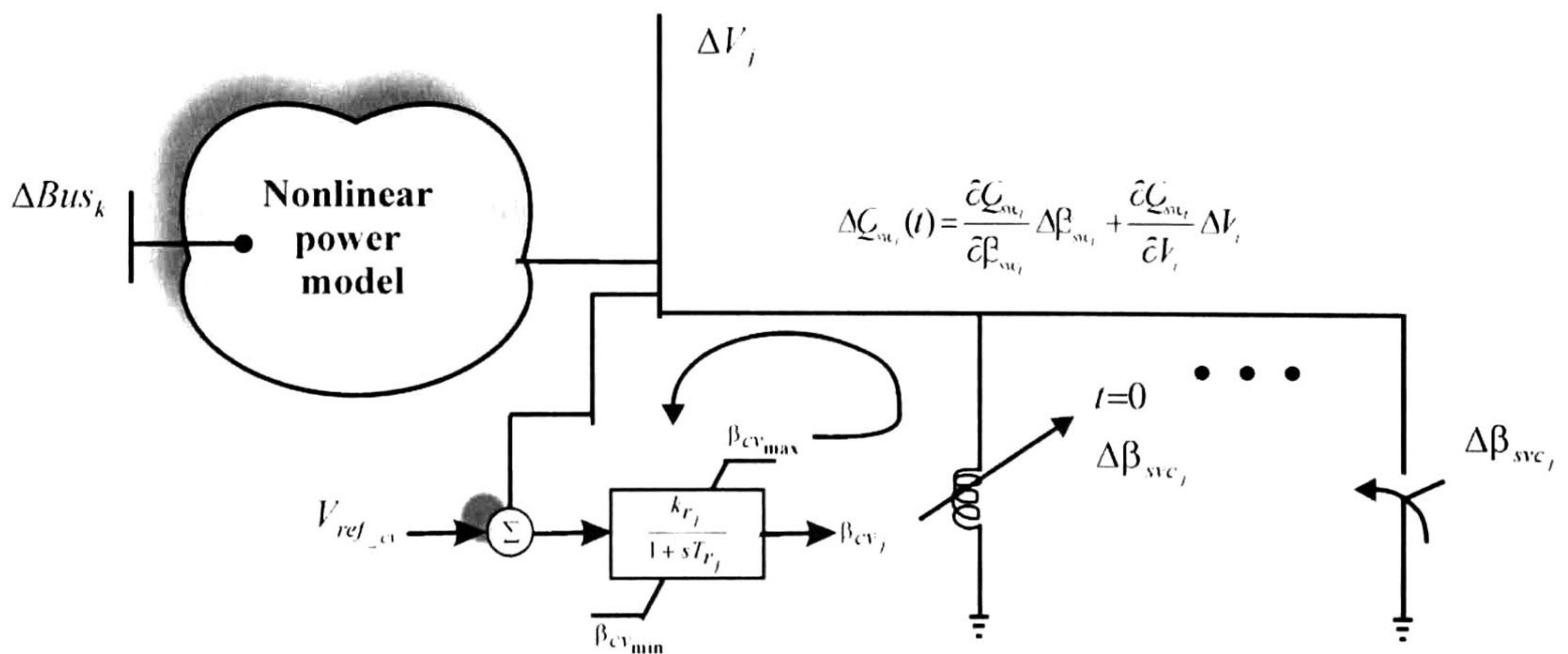


Figure 4.4. Conceptual representation of SVCs for sensitivity analysis

Numerical results illustrating the application of the developed procedure are presented in Chapter 6.

4.3 Network-Based Participation Factors

4.3.1 Nonlinear Participation Factors

The developed algorithms have an interesting interpretation in terms of nonlinear participation factors. From the system model in Eq. (4.1), closed-form time-domain solutions for the fast, network variables can be obtained as

$$x_p(t) = \sum_{j=1}^{n+m} u_{pj} e^{\lambda_j t} + \sum_{j=1}^{n+m} u_{pj} \left(\sum_{k=1}^{n+m} \sum_{l=k}^{n+m} h_{2_{pkl}}^o z_{2_k}^o(t) z_{2_l}^o(t) e^{(\lambda_k + \lambda_l)t} \right) \text{ for } p=n-ng+1, n-ng+2, \dots, n \quad (4.24)$$

and

$$y_q(t) = \sum_{j=1}^{n+m} u_{qj} e^{\lambda_j t} + \sum_{j=1}^{n+m} u_{qj} \left(\sum_{k=1}^{n+m} \sum_{l=k}^{n+m} h_{2_{qkl}}^o z_{2_k}^o(t) z_{2_l}^o(t) e^{(\lambda_k + \lambda_l)t} \right) \text{ for } q=n+1, n+2, \dots, n+m \quad (4.25)$$

The following approach is used to obtain the nonlinear participations of the parameters of the network.

In order to define nonlinear participation factors assume now that a network variable is perturbed by a small quantity α , where $\alpha \in [\Delta\beta_{svc} \quad \Delta\theta \quad \Delta V \quad \Delta P_L \quad \Delta Q_L]$. Then the initial condition in Jordan and normal form spaces become

$$\mathbf{y}^o = \mathbf{U}^{-1} \mathbf{x}^o, \quad \mathbf{z}^o + \mathbf{h}_2(\mathbf{z}^o) - \mathbf{y}^o = \mathbf{0}$$

Substitution of the initial condition \mathbf{z}^o into (18),(19) results in

$$y_q(t) = \sum_{j=1}^{n+m} p_{2_{qj}} e^{\lambda_j t} + \sum_{k=1}^{n+m} \sum_{l=k}^{n+m} p_{2_{qkl}} e^{(\lambda_k + \lambda_l)t} \quad (4.25)$$

In particular, for the model considered

$$\beta_{SVC_w}(t) = \sum_{j=1}^{n+m} p_{2_{\beta_{svc} wj}} e^{\lambda_j t} + \sum_{k=1}^{n+m} \sum_{l=k}^{n+m} p_{2_{\beta_{svc} wkl}} e^{(\lambda_k + \lambda_l)t} \quad w = n - ng + 1, n - ng + 2, \dots, n \quad (4.26)$$

$$\theta_p(t) = \sum_{j=1}^{n+m} p_{2_{\theta pj}} e^{\lambda_j t} + \sum_{k=1}^{n+m} \sum_{l=k}^{n+m} p_{2_{\theta pkl}} e^{(\lambda_k + \lambda_l)t} \quad \text{for } p = n + 1, \dots, m \quad (4.27)$$

$$V_q(t) = \sum_{j=1}^{n+m} p_{2_{Vqj}} e^{\lambda_j t} + \sum_{k=1}^{n+m} \sum_{l=k}^{n+m} p_{2_{Vqkl}} e^{(\lambda_k + \lambda_l)t} \quad \text{for } q = m + 1, \dots, 2m \quad (4.28)$$

$$P_{Lr}(t) = \sum_{j=1}^{n+m} p_{2P_{L,rj}} e^{\lambda_j t} + \sum_{k=1}^{n+m} \sum_{l=k}^{n+m} p_{2P_{L,rkl}} e^{(\lambda_k + \lambda_l)t} \quad \text{for } r = 2m + 1, \dots, 2m + 1 + nl \quad (4.29)$$

$$Q_{Ls}(t) = \sum_{j=1}^{n+m} p_{2Q_{L,sj}} e^{\lambda_j t} + \sum_{k=1}^{n+m} \sum_{l=k}^{n+m} p_{2Q_{L,skl}} e^{(\lambda_k + \lambda_l)t} \quad \text{for } r = 2m + 1 + nl, \dots, 2m + 1 + 2nl \quad (4.30)$$

By analogy with the definition of speed-based nonlinear participation factors in [6], p_{2qj} ($p_{2\beta_{vc,wj}}, p_{2\theta_{pj}}, p_{2V_{qj}}, p_{2P_{L,rj}}, p_{2Q_{L,sj}}$) represent the second-order participation of the i th bus parameters in the j th single-eigenvalue mode and p_{2qkl} ($p_{2\beta_{vc,wkl}}, p_{2\theta_{pkl}}, p_{2V_{qkl}}, p_{2P_{L,rkl}}, p_{2Q_{L,skl}}$) represents the second-order participation of the i th bus parameters in the mode formed by the combination of the eigenvalues λ_k and λ_l .

Once incremental network parameters deviations are determined it is possible to assess the specific contribution of transmission elements to the inter-area oscillations. The details are omitted.

4.4 Discussion

Approximate closed-form solutions were utilized to investigate the effect of network characteristics on system behavior. The method is of particular interest for the preliminary evaluation of the role of the transmission network in the stability phenomena and the study of interactions among existing controllers. Potential specific applications of the method are in identifying and extraction of modal sensitivities, placement of controllers and assessing control-network interactions.

The analytical framework provides greater insight into the issue of which physical parameters have the greater impacts on system dynamic response. The general framework for deriving modal information discussed in this chapter, is easily particularized to accommodate specific system characteristics.

It seems possible that the analysis method considered above could also be adapted to the analysis of higher order representations. It appears, however, that this would result in a considerable increase in system complexity. We further examine this important subject in Chapter 6 in the light of our numerical results.

References

- [1] T. V. Cutsem and C. Vournas, *Voltage Stability of Electric Power Systems*, Publisher by Springer-Verlag New York Inc, 01 Oct 2007
- [2] U. Eminoglu and M. H. Hocaoglu, "A New Power Flow Method for Radial Distributions Systems Including voltage Dependent load Models", *Electric Power Research*, vol. 76, pp. 106-114, Sep 2005
- [3] S. Liu, A. R. Messina and V. Vittal, "A Normal Form Analysis Approach to Siting Power System Stabilizers (PSSs) and Assessing Power System Nonlinear Behavior", *IEEE Transactions on Power Systems*, vol. 21, pp. 1755-1762., Nov 2006
- [4] I. Dobson, "Strong resonance effects in NF analysis and subsynchronous resonance", in *Proc.. Bulk Power Systems Dynamics and Control V*, Onomichi, Japan, Aug. 2001.
- [5] S. Liu, A. R. Messina and V. Vittal, "Assessing placement of controllers and nonlinear behavior using normal form analysis", *IEEE Trans. on Power Systems*, vol. 20, pp. 1486-1495, Aug 2005
- [6] S.K. Starrett and A. A. Fouad, "Nonlinear measures of mode-machine participation", *Power Systems, IEEE Transactions*, vol. 13, pp. 389-394, May 1998

Chapter 5

Normal Form Analysis of DAE Systems: Application to a Small Test System

Systems that are composed of coupled differential and algebraic equations pose an important problem in the simulation of power system dynamic behavior. This chapter discusses the application of structure-preserving models to the analysis of system dynamic behavior of nonlinear power system models described by differential algebraic equations. Effort is also directed towards the incorporation of load models and network control devices in the normal form method.

Results obtained using a two-machine test power system are presented illustrating the application of nonlinear modal analysis to assess power system dynamic behavior. Normal form theory is In particular, results of the second-order normal form study are presented. Detailed numerical simulations using transient stability simulations are conducted to check the validity of the analysis and to establish the accuracy of numerical solutions. The study focuses on the ability of structure-preserving power system models to characterize nonlinear phenomena in realistic power system representations. Numerical issues associated with the application of the method are discussed. The results obtained from the proposed approach were also compared with other reported methods.

It is shown that practical power system models exhibit a multi-time scale behavior that can be exploited for detailed nonlinear investigation analysis.

5.1 Test Results

The study system is based on the two-area, 4-machine system shown in Fig. 5.1 [1]. The test system comprises four generators representing two electric areas, 6 buses and two loads. Each area includes two generators with equal power outputs. Detailed steady state and transient data are provided in the Appendix B.

System structure is longitudinal and symmetrical with local load and unevenly distributed generating sources. Dynamic characteristics are heavily dependent on network characteristics and the amount of power transfer over the inertia. In addition, the lack of voltage support at critical system locations can also have a detrimental effect on system dynamic behavior. As discussed in Ref. [1], voltage support in this system is essentially provided by conventional fixed shunt compensation.

The next subsection reviews some specific characteristics of the adopted model which are relevant to understanding the nature of system oscillations in the system.

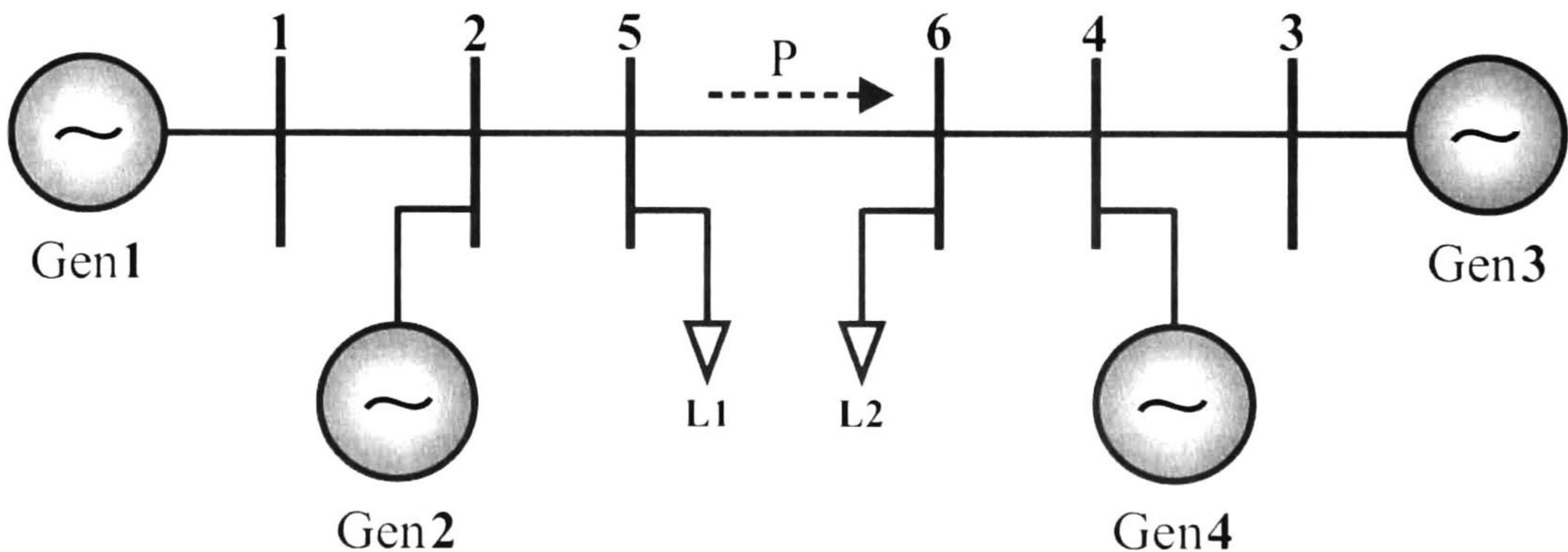


Figure 5.1. Two-area, four-machine test system

5.1.1 Modeling Assumptions

We briefly describe the system model used for this study. For the case under investigation, each generator is represented by a two-axis model that represents the swing dynamics and flux decay dynamics.

Fast static excitation models are included on all generators [2]. For simplicity, loads are represented as constant impedances ($\alpha_p = \alpha_q = 2$).

The state-space model of the augmented nonlinear DAE system has 40 states; 20 physical states and 20 pseudo-states associated with the network representation. The states of the system are $\delta, \omega, E'_d, E'_q, E'_{fd}$ for each machine:

the 28 network pseudo-states are $\mathbf{I}_d, \mathbf{I}_q, \mathbf{P}_g, \mathbf{Q}_g$ for the generator buses, and \mathbf{V} and θ for load buses. The overall system has 48 eigenvalues.

Two operating scenarios representing heavy and light loading conditions are presented to examine the ability of the developed technique to accurately capture system dynamic behavior.

The operating cases are summarized below.

Case 1 – A moderate stress system condition with a 300 MW power transfer between the interconnected areas, and

Case 2 - A stressed system condition obtained by increasing the level of power transfer to about 400 MW.

In both cases, the disturbance for transient stability assessment is a three phase stub fault at bus 5 cleared in 0.04s.

5.1.2 Modal Characteristics

Tables 5.1 through 5.4 provide the dynamic (slow) system eigenvalues obtained from the linear part of (5.21) evaluated at the initial time¹

$$\mathbf{A}(t_o) = -\mathbf{J}_o^T(t_o) \quad (5.1)$$

as a function of the singular perturbation parameter ε .

For comparison, the eigenvalues obtained using commercial software are also shown; these eigenvalues correspond with those of the reduced system $\dot{\mathbf{x}} = (\mathbf{J}_{11} - \mathbf{J}_{12}\mathbf{J}_{22}^{-1}\mathbf{J}_{21})\mathbf{x}$ in standard studies.

Comparison with the conventional eigenvalue solution, as shown in Table 5.1 and 5.3, indicates that there is a very good agreement between both formulations suggesting that the method can provide both, local and global information on system behavior.

¹ Note that the Jacobian matrix needs to be evaluated only once in the developed model.

Table 5.1. Slow eigenvalues of the system for the case study 1 for different values of ε

Mode #	$\varepsilon = 1e-1$	$\varepsilon = 1e-4$	$\varepsilon = 1e-6$	Full solutions
1	0.658±j7.541	-77.006	-77.091	-77.091
2	-5.925±j5.981	-85.798	-85.820	-85.820
3	1.238±j7.416	-96.399	-96.451	-96.451
4	-3.608±j2.545	-95.353	-95.405	-95.405
5	-4.147	-21.219	-21.211	-21.211
6	-3.171±j2.027	-13.075	-13.079	-13.079
7, 8	-3.295±j0.180	-1.332±j8.160	-1.335±j8.157	-1.335±j8.157
9, 10	-2.759	-2.254±j7.689	-2.256±j7.686	-2.257±j7.686
11	0.451±j2.685	-10.215	-10.206	-10.206
12	-6.260	-10.476	-10.467	-10.467
13, 14	-6.870	-0.344±j3.075	-0.345±j3.075	-0.346±j3.075
15, 16	-0.552	-5.160±j0.065	-5.157±j0.065	-5.157±j0.065
17	-0.000	0.000	-0.0001	-0.0001
18	---	-0.506	-0.506	-0.506
19	---	-2.423	-2.423	-2.423
20	---	-2.364	-2.364	-2.364

Table 5.2. Fast pseudo-eigenvalues of the system for the case study 1 for different values of ε

Mode #	$\varepsilon = 1e-1$	$\varepsilon = 1e-4$	$\varepsilon = 1e-6$
1	-5.880±6.265	-2498.265	-2.498e+005
2	-15.112±6.795	-3236.716	-3.2373e+005
3	-18.677±7.228	-3759.664	-3.7601e+005
4	-22.345	-4698.320	-4.6986e+005
5	-22.766	-6507.708	-6.508e+005
6	-22.997	-6628.318	-6.6285e+005
7	-24.583	-7194.431	-7.2004e+005
8	-26.485	-7317.363	-7.3232e+005
9	-26.613	-17928.199	-1.7928e+006
10	-81.742	-19257.381	-1.9258e+006
11	-89.241	-21941.475	-2.1942e+006
12	-97.862	-22312.984	-2.2312e+006
13	-98.455	-24580.996	-2.4582e+006
14	-6068.809	-24960.938	-2.4963e+006
15	-6609.101	-27306.533	-2.7307e+006
16	-6788.533	-27957.273	-2.7958e+006
17	-7249.635	-6.0687e+006	-6.0687e+008
18	-32255.149	-6.609e+006	-6.609e+008
19	-34946.373	-6.7885e+006	-6.7885e+008
20	-41267.218	-7.2495e+006	-7.2495e+008
21	-44111.432	-3.2255e+007	-3.2255e+009
22	-522092.951	-3.4946e+007	-3.4946e+009
23	-537850.335	-4.1267e+007	-4.1267e+009
24	-555781.240	-4.4111e+007	-4.4111e+009
25	-570092.049	-5.2209e+008	-5.2209e+010
26	---	-5.3785e+008	-5.3785e+010
27	---	-5.5578e+008	-5.5578e+010
28	---	-5.7009e+008	-5.7009e+010

Table 5.3. Slow eigenvalues of the system for the case study 2 for different values of ε

Mode #	$\varepsilon = 1e-1$	$\varepsilon = 1e-4$	$\varepsilon = 1e-6$	Full solutions
1	0.018±j1.905	-77.050	-77.137	-77.138
2	-2.687±j1.736	-85.273	-85.286	-85.286
3	-3.619±j2.519	-96.212	-96.266	-96.266
4	-4.266±j1.642	-95.351	-95.404	-95.404
5	-5.992	-20.831	-20.822	-20.822
6	-6.656	-13.684	-13.688	-13.689
7, 8	1.223±j7.460	-1.386±j 8.124	-1.389±j8.121	-1.389±j8.121
9, 10	0.756± j7.554	-2.131±j 7.759	-2.133±j7.756	-2.133±j7.757
11	-5.812±j5.750	-10.206	-10.196	-10.196
12	-2.847	-10.649	-10.638	-10.639
13, 14	-3.647	-0.230±j 1.996	-0.231±j1.996	-0.231±j1.997
15, 16	-0.000	-5.336±j 0.235	-5.334±j0.235	-5.334±j0.235
17	-0.496	-0.000	-0.004	-0.0001
18	---	-0.434	-0.434	-0.434
19	---	-2.820	-2.819	-2.820
20	---	-2.552	-2.552	-2.553

Table 5.4. Fast pseudo-eigenvalues of the system for the case study 2 for different values of ε

Mode #	$\varepsilon=1e-1$	$\varepsilon=1e-4$	$\varepsilon=1e-6$
1	-5.805±j 6.156	-2536.276	-2.5362e+005
2	-15.244±j 7.211	-2871.967	-2.8723e+005
3	-18.270±j 7.355	-4176.254	-4.1768e+005
4	-22.627	-4534.604	-4.5349e+005
5	-22.755±j0.197	-6447.877	-6.4484e+005
6	-24.154	-6614.245	-6.6146e+005
7	-26.474±j0.010	-7237.344	-7.2429e+005
8	-81.973	-7321.590	-7.327e+005
9	-88.661	-17756.678	-1.7757e+006
10	-97.929	-18527.774	-1.8528e+006
11	-98.329	-21643.544	-2.1644e+006
12	-6056.202	-22003.962	-2.2004e+006
13	-6326.674	-24879.111	-2.4881e+006
14	-7113.966	-25013.723	-2.5016e+006
15	-7315.756	-27455.246	-2.7456e+006
16	-32029.450	-27920.866	-2.7922e+006
17	-33424.475	-6.0561e+006	-6.0561e+008
18	-41546.335	-6.3266e+006	-6.3266e+008
19	-42550.954	-7.1139e+006	-7.1139e+008
20	-497574.670	-7.3156e+006	-7.3156e+008
21	-503753.253	-3.2029e+007	-3.2029e+009
22	-544164.686	-3.3424e+007	-3.3424e+009
23	-548803.406	-4.1546e+007	-4.1546e+009
24	---	-4.2551e+007	-4.2551e+009
25	---	-4.9757e+008	-4.9757e+010
26	---	-5.0375e+008	-5.0375e+010
27	---	-5.4416e+008	-5.4416e+010
28	---	-5.488e+008	-5.488e+010

In the succeeding sections, results will be presented that compare the modified normal analysis results with those obtained from conventional step-by-step solutions (SBSS) for a broad set of selected signals.

5.2 Numerical Issues

The theory in Chapter 4 was used to determine closed-form analytical approximations to system behavior. Following the approach outlined in section 4.2.1, the time evolution of the k th state can be expressed as

$$x_p(t) = \sum_{j=1}^{n+m} u_{pj} e^{\lambda_j t} + \sum_{j=1}^{n+m} u_{pj} \left(\sum_{k=1}^{n+m} \sum_{l=k}^{n+m} h_{2_{pkl}}^o z_{2_k}^o(t) z_{2_l}^o(t) e^{(\lambda_k + \lambda_l)t} \right) \text{ for } p = 1, 2, \dots, n \quad (5.2)$$

and the network states as

$$y_q(t) = \sum_{j=1}^{n+m} u_{qj} e^{\lambda_j t} + \sum_{j=1}^{n+m} u_{qj} \left(\sum_{k=1}^{n+m} \sum_{l=k}^{n+m} h_{2_{qkl}}^o z_{2_k}^o(t) z_{2_l}^o(t) e^{(\lambda_k + \lambda_l)t} \right) \text{ for } q = n+1, n+2, \dots, n+m \quad (5.3)$$

Equations (5.2) and (5.3) allow the contribution of each network parameter to be singled out and quantified. It also provided an estimate of the network parameters of nonlinear mode interactions.

In the following series of simulations we assume that the system is subject to a perturbation in the initial conditions. The perturbation considered is a change in the initial conditions $\Delta \mathbf{x}^o = \left[\Delta \delta^T \quad \Delta \mathbf{w}^T \quad \Delta \mathbf{E}_d'^T \quad \Delta \mathbf{E}_q'^T \quad \Delta \mathbf{E}_{fd}'^T \right]^T$ and $\Delta \mathbf{z}^o = \left[\Delta \mathbf{I}_d^T \quad \Delta \mathbf{I}_q^T \quad \Delta \mathbf{P}_g^T \quad \Delta \mathbf{Q}_g^T \quad \Delta \theta^T \quad \Delta \mathbf{V}^T \right]^T$. The basic data and operating condition of this system are given in Appendix.

5.3 Model Validation

5.3.1 Time Domain Simulations and Results

This section describes results of simulation studies performed to validate and demonstrate the accuracy of the developed procedures. Normal form analysis was tested by comparison with full numerical solution of the system model using a transient stability program. For each case above, approximate closed form solutions were obtained using the procedures in [3]. For direct comparison to SBSS, the normal form solutions are computed in the physical domain. Figures 5.2 through 5.12 provide a comparison of selected full system solution with the solution from the second-order normal form approach. In these studies a value of $\varepsilon = 1e^{-6}$ was used in all calculations.

The solid lines represent the detailed system response calculated with a commercial transient stability program. The dashed lines are the results obtained using normal form analysis.

For the low stress case in Figures 5.13 through 5.23, normal form theory and SBSS agree very well over the entire simulation window. Our experience for this case shows that, numerical results are not greatly sensitive to the choice of ϵ . For the highly stressed condition, normal form results provide a fair estimate of system behavior, although some discrepancies are found, especially as time increases. This is a highly stressed condition for which the normal form modeling assumptions may not be entirely valid, pointing to the importance of incorporating higher order effects in the normal form representation. This aspect is currently under investigation.

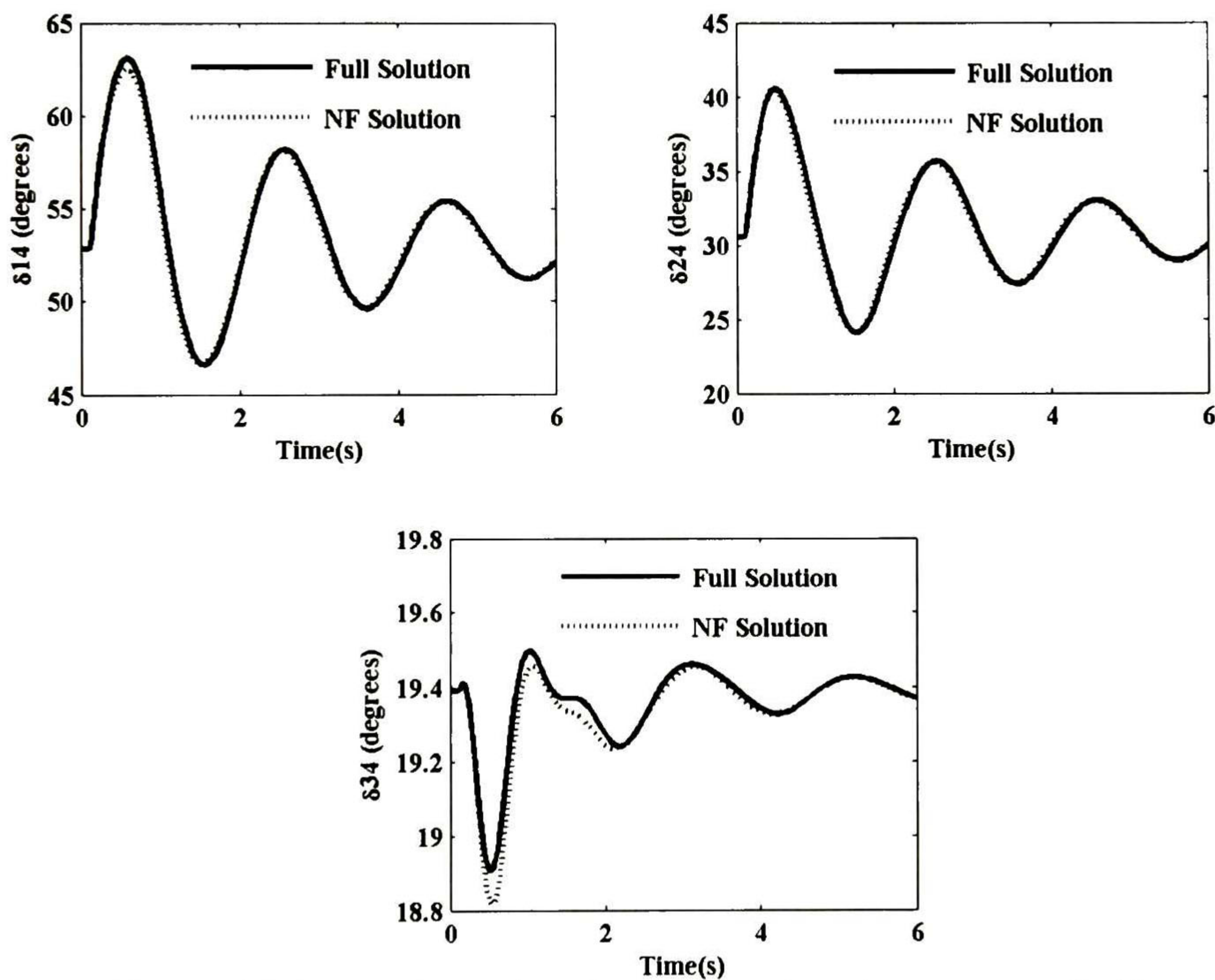


Figure 5.2. Comparison of relative rotor angle swings computed with conventional, and the structure preserving model. Case study 1.

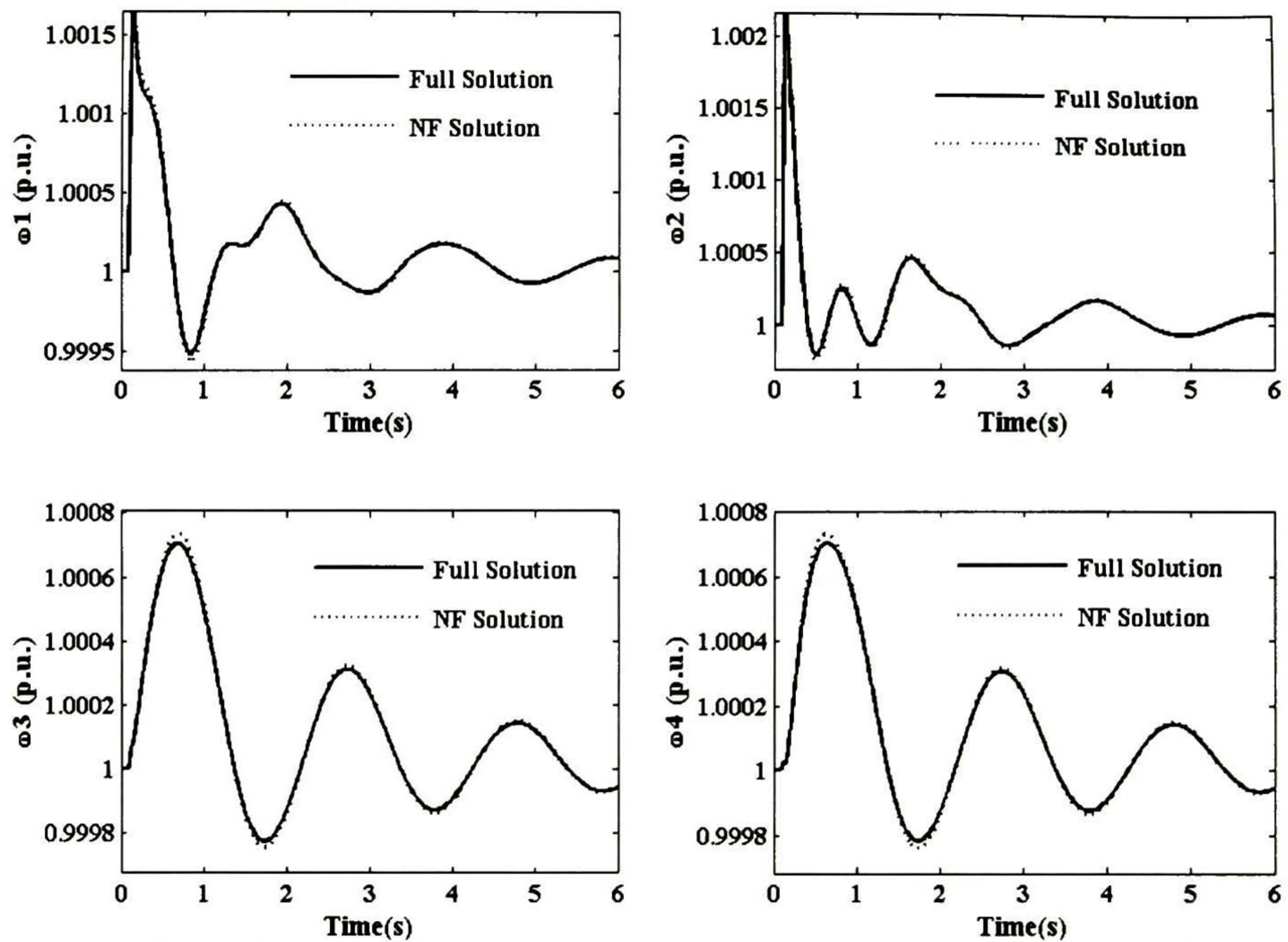


Figure 5.3. Comparison of relative rotor speed swings computed with conventional, and the structure preserving model. Case study 1.

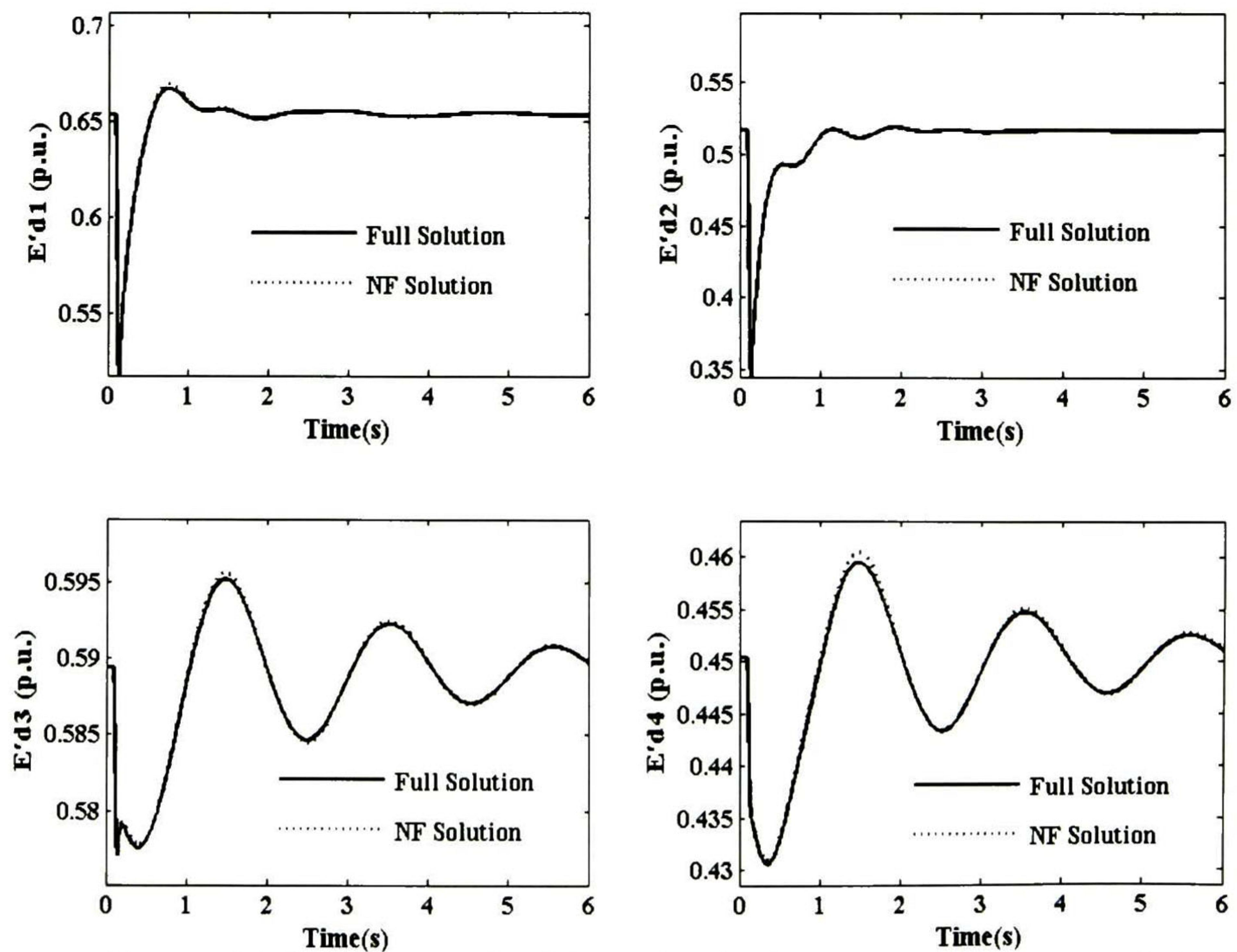


Figure 5.4. Comparison of relative rotor d -axis voltage swings computed with conventional, and the structure preserving model. Case study 1.

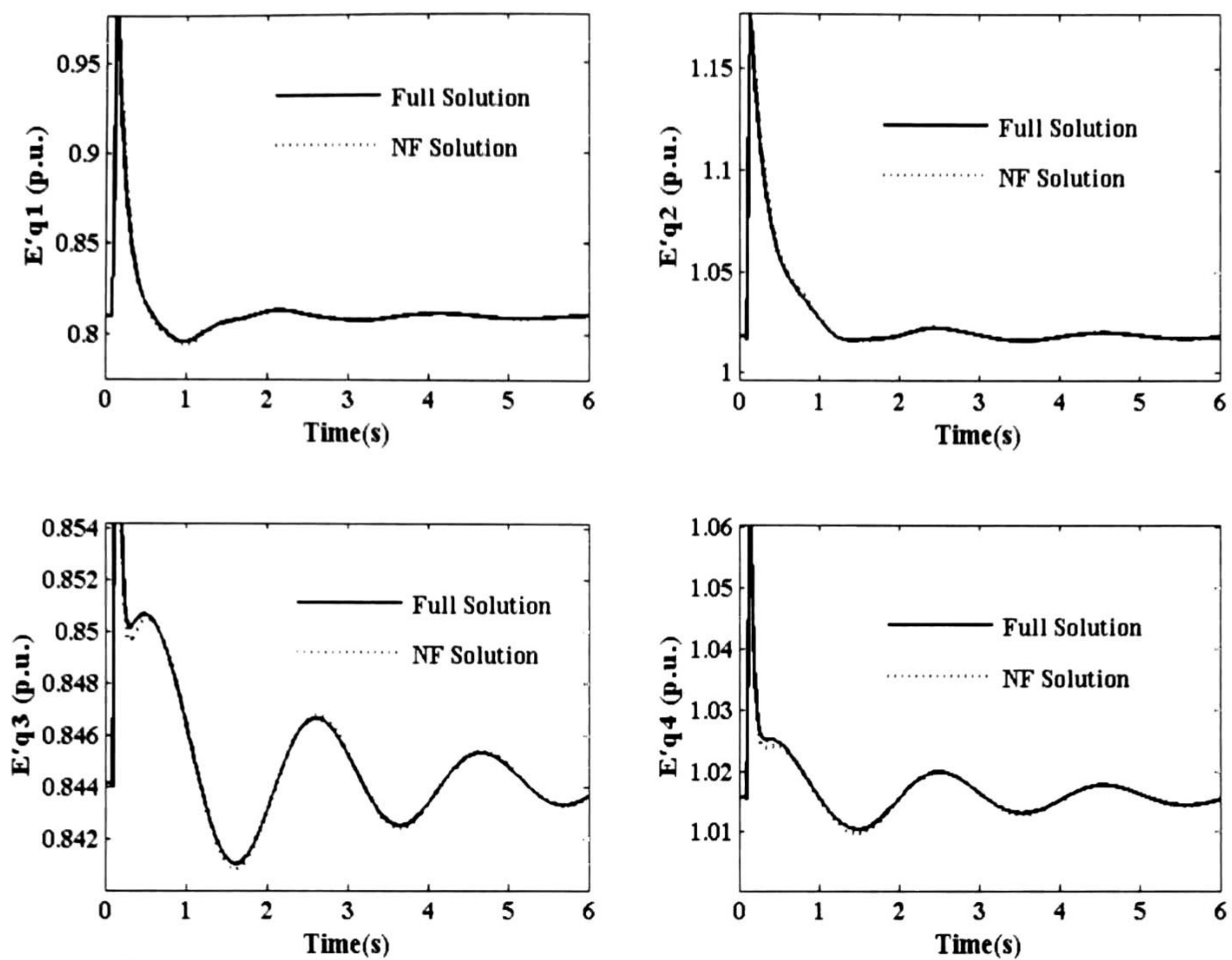


Figure 5.5. Comparison of relative rotor q -axis voltage swings computed with conventional, and the structure preserving model. Case study 1.

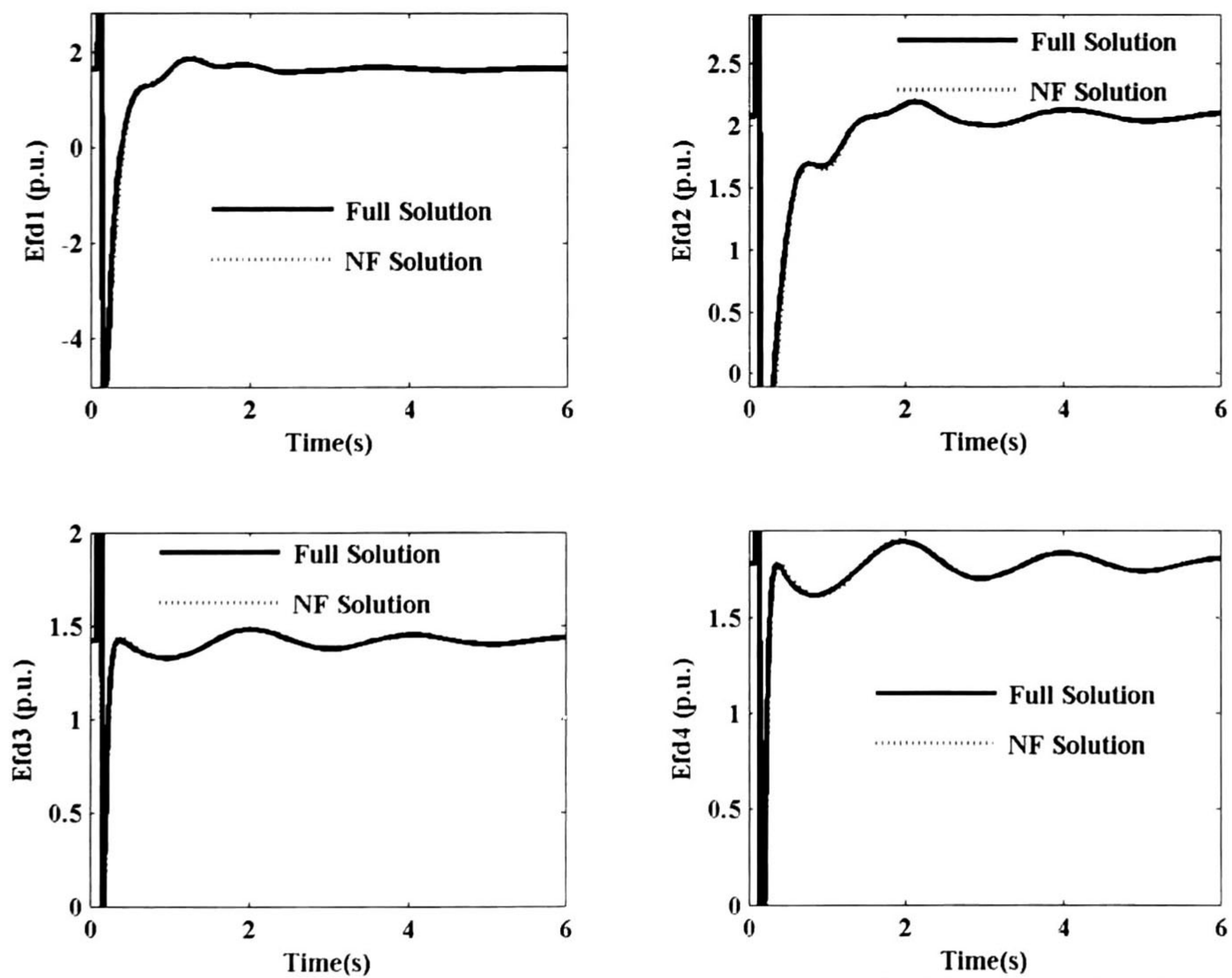


Figure 5.6. Comparison of field voltage computed with conventional, and structure preserving model. Case study 1.

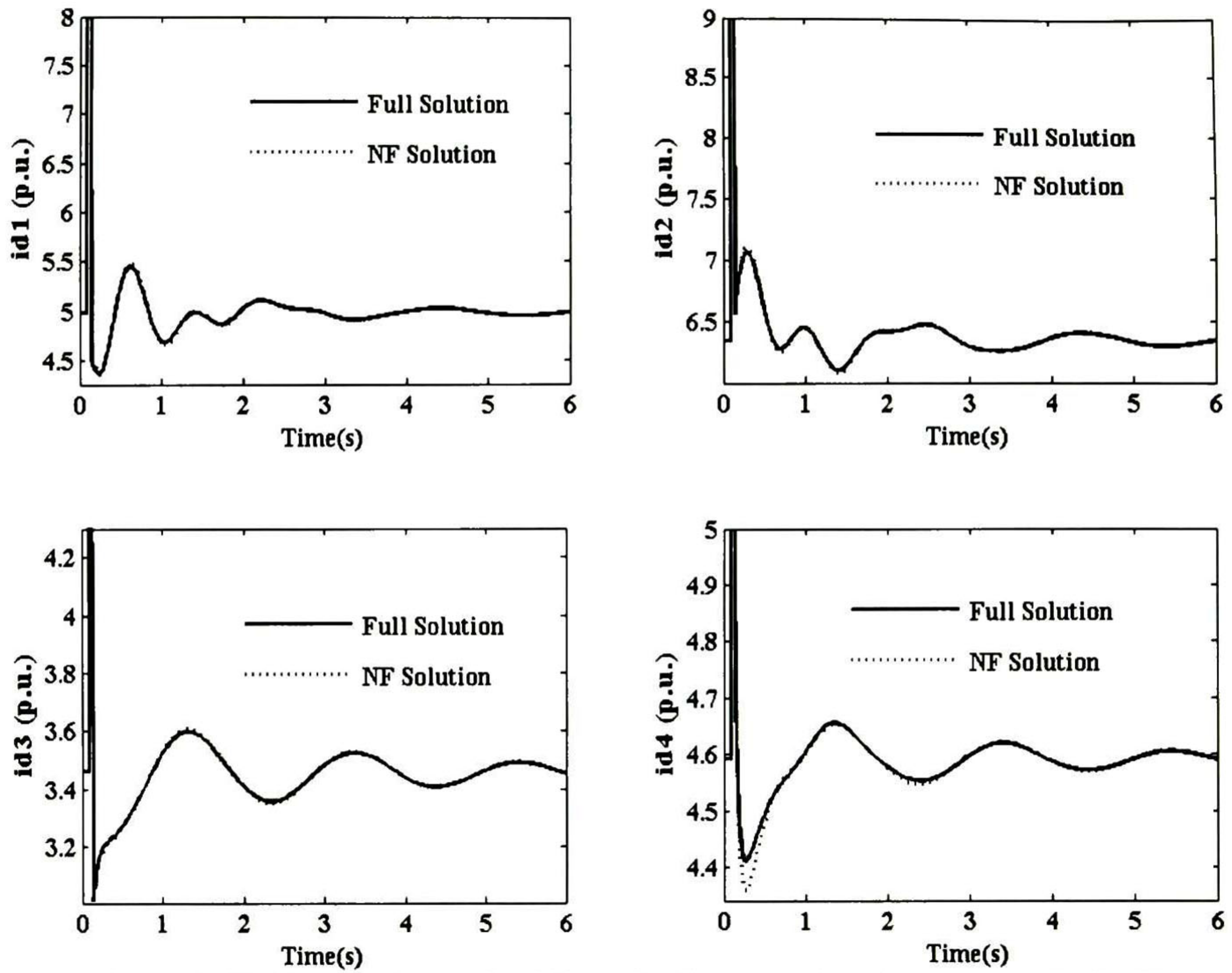


Figure 5.7. Comparison of relative d -axis current swings computed with conventional, and the structure preserving model. Case study 1.

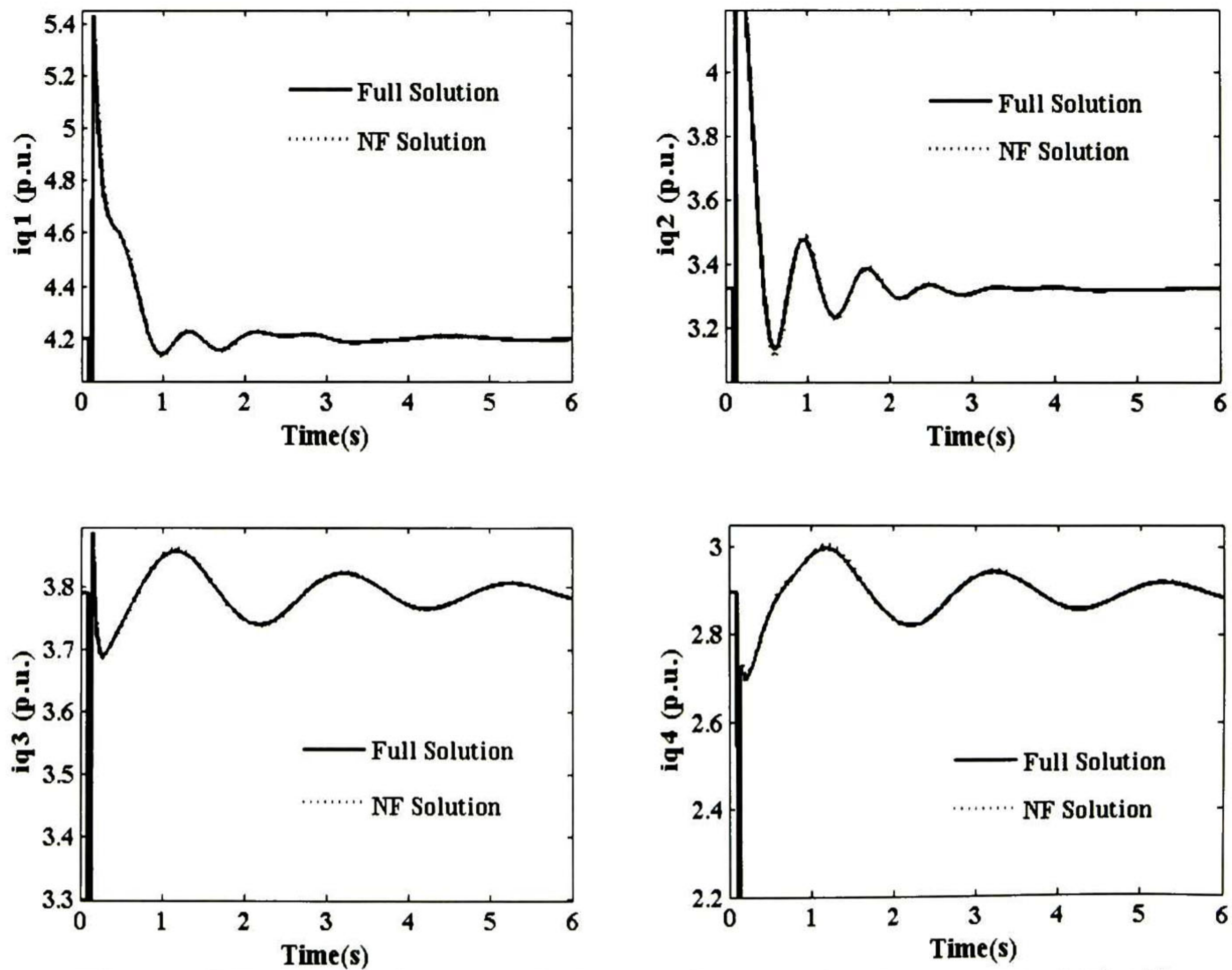


Figure 5.8. Comparison of relative q -axis current swings computed with conventional, and the structure preserving model. Case study 1.

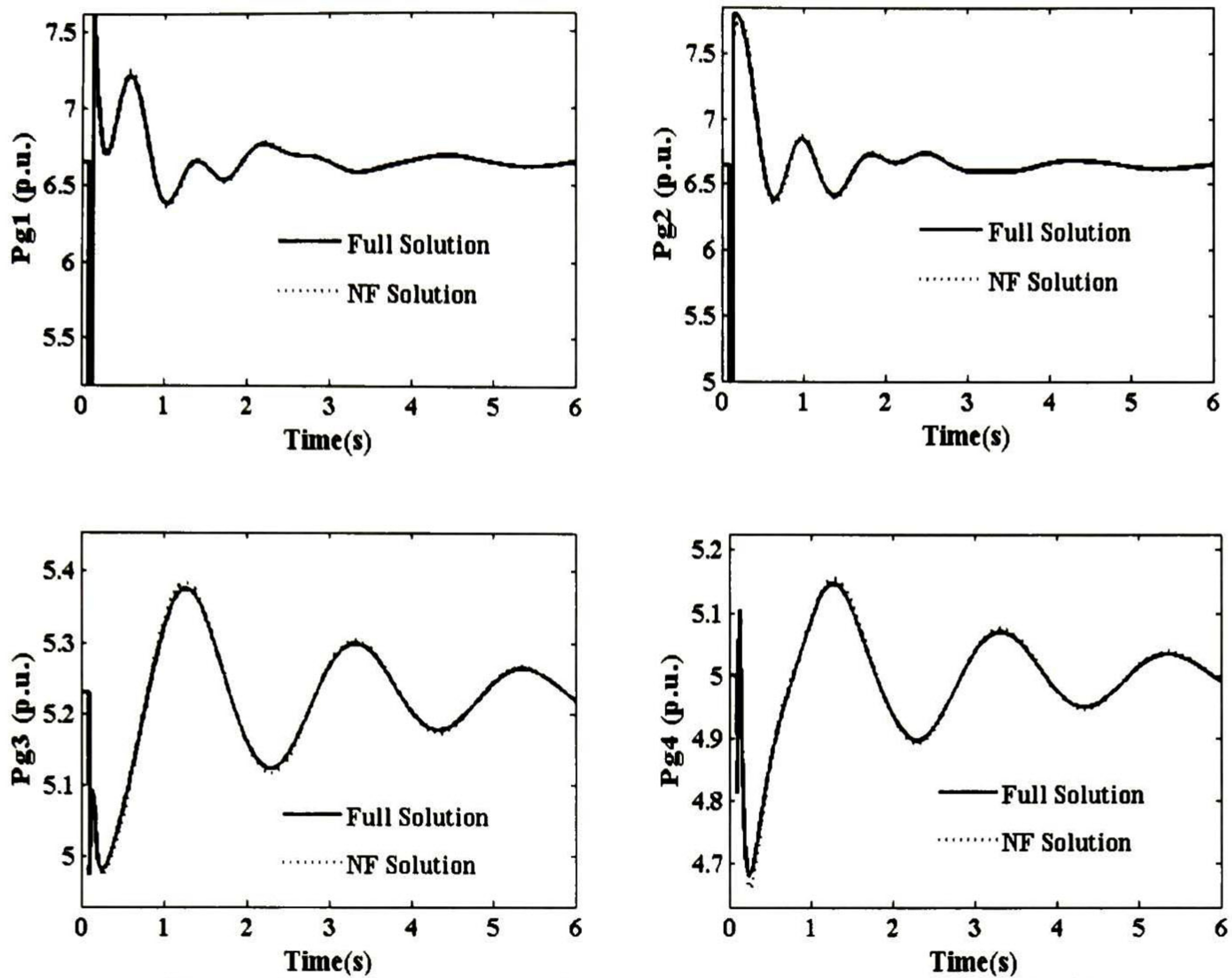


Figure 5.9. Comparison of active output power computed with conventional, and the structure preserving model. Case study 1.

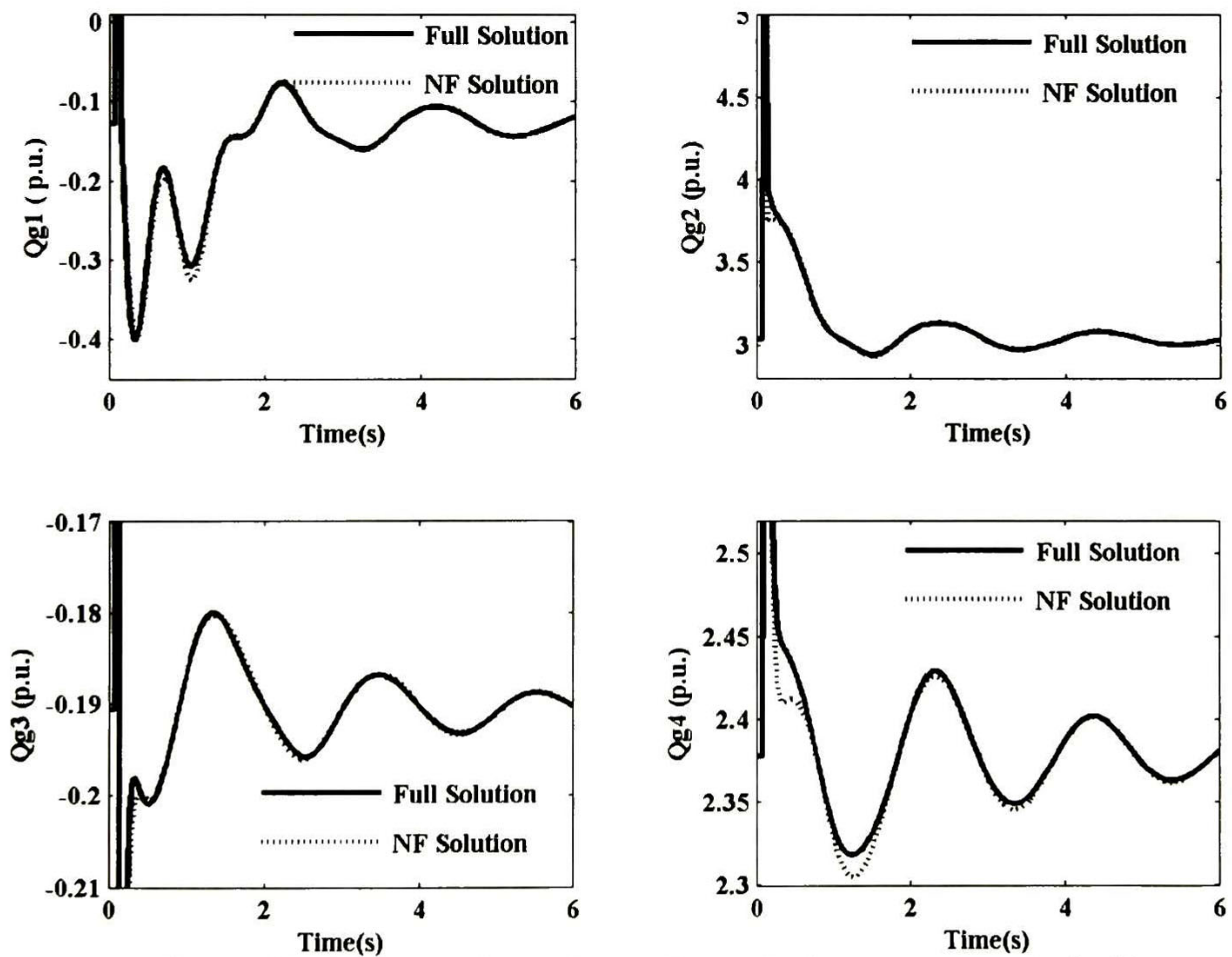


Figure 5.10. Comparison of reactive output power computed with conventional, and the structure preserving model. Case study 1.

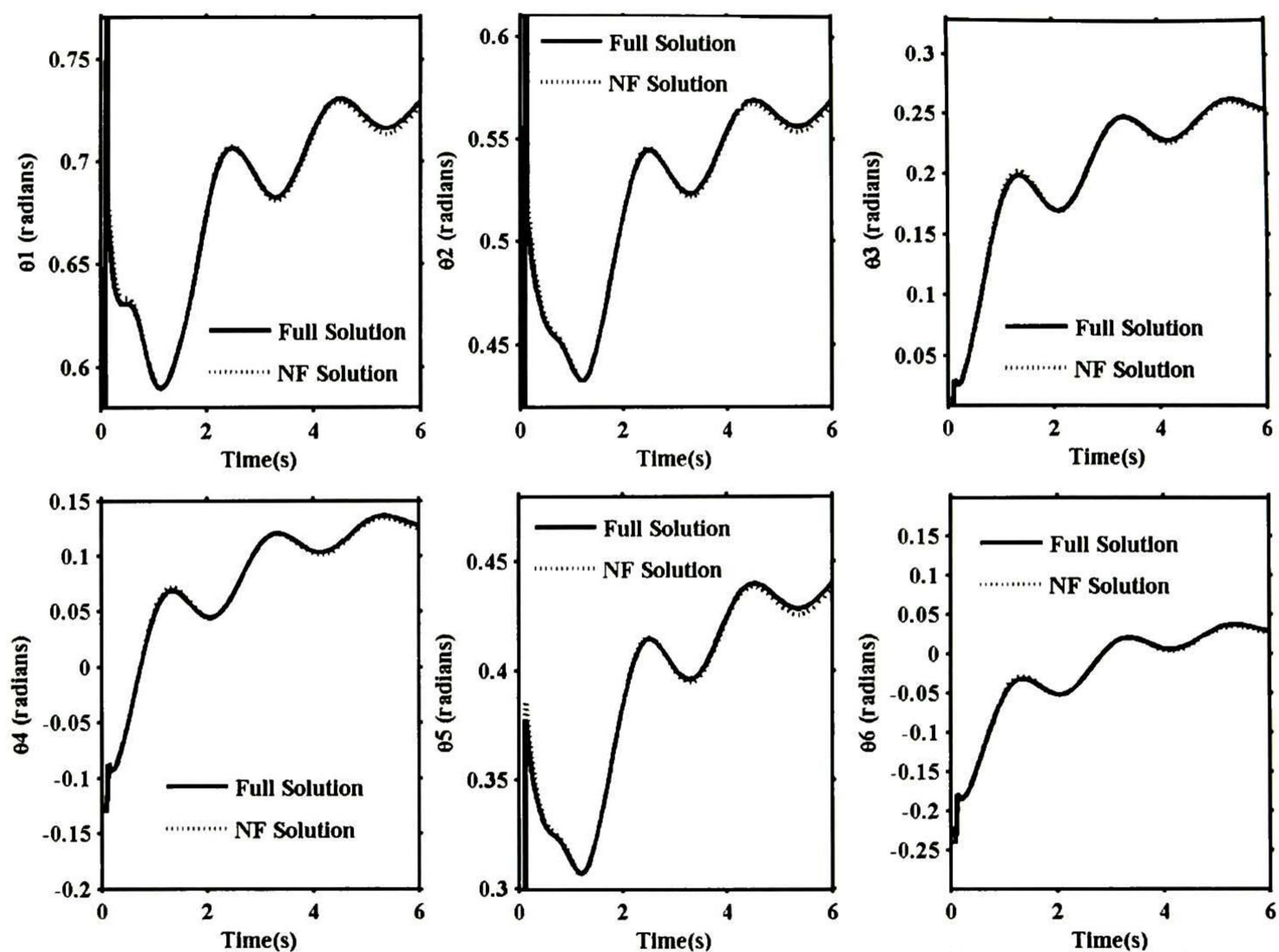


Figure 5.11. Comparison of phase angles computed with conventional, and structure preserving model. Case study 1.

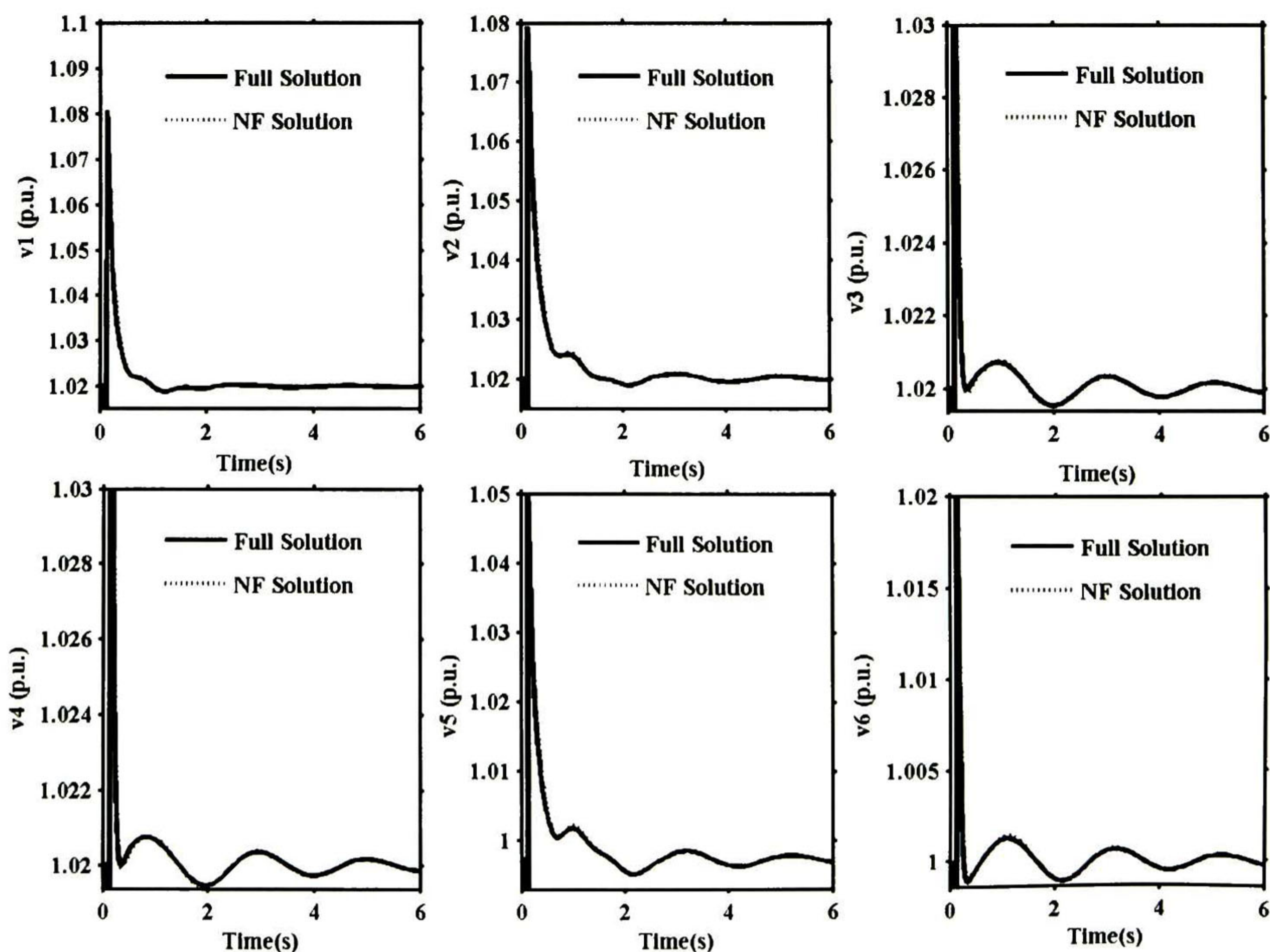


Figure 5.12. Comparison of bus voltage magnitude computed with conventional, and structure preserving model. Case study 1.

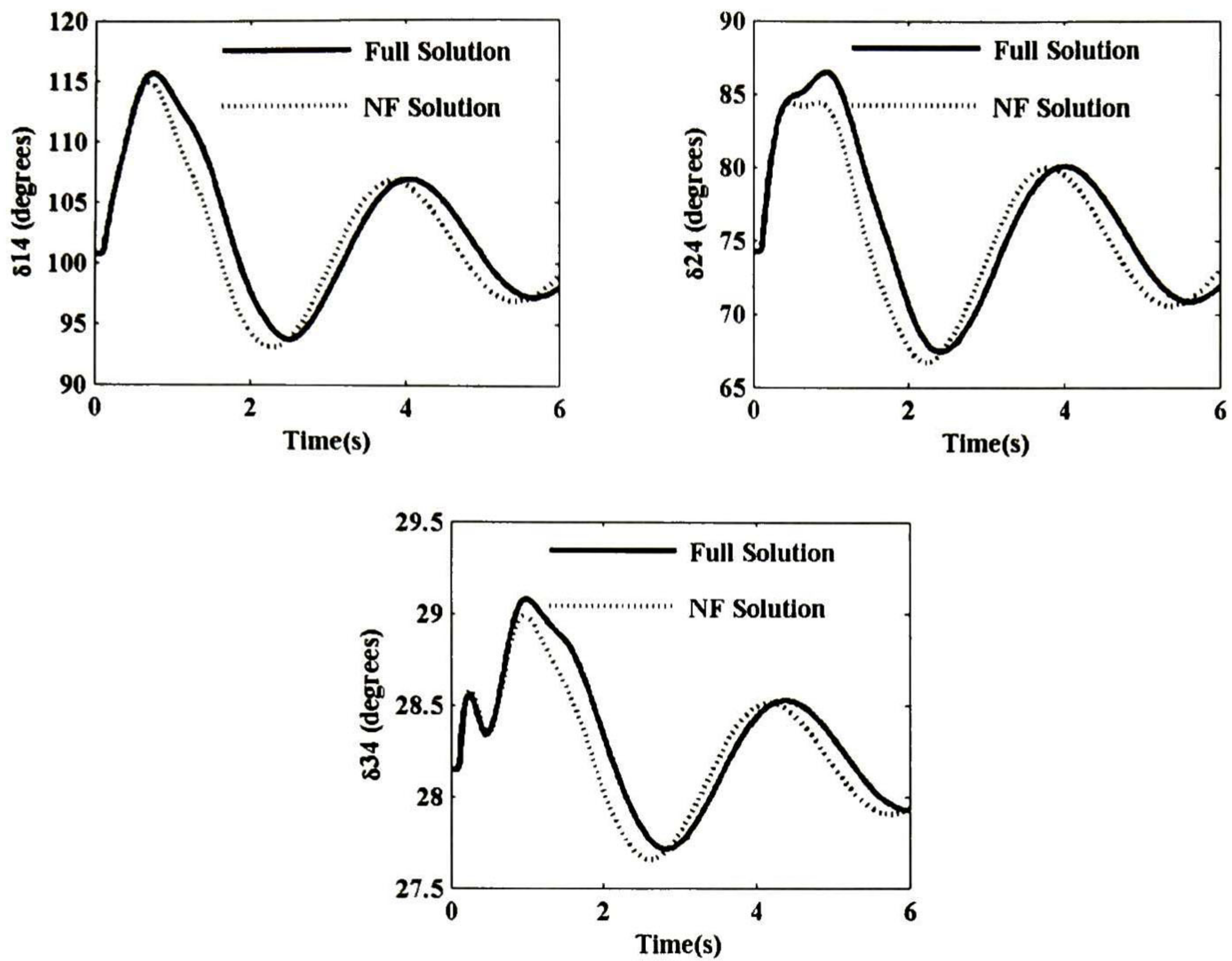


Figure 5.13. Comparison of relative rotor angle swings computed with conventional, and structure preserving model. Case study 2.

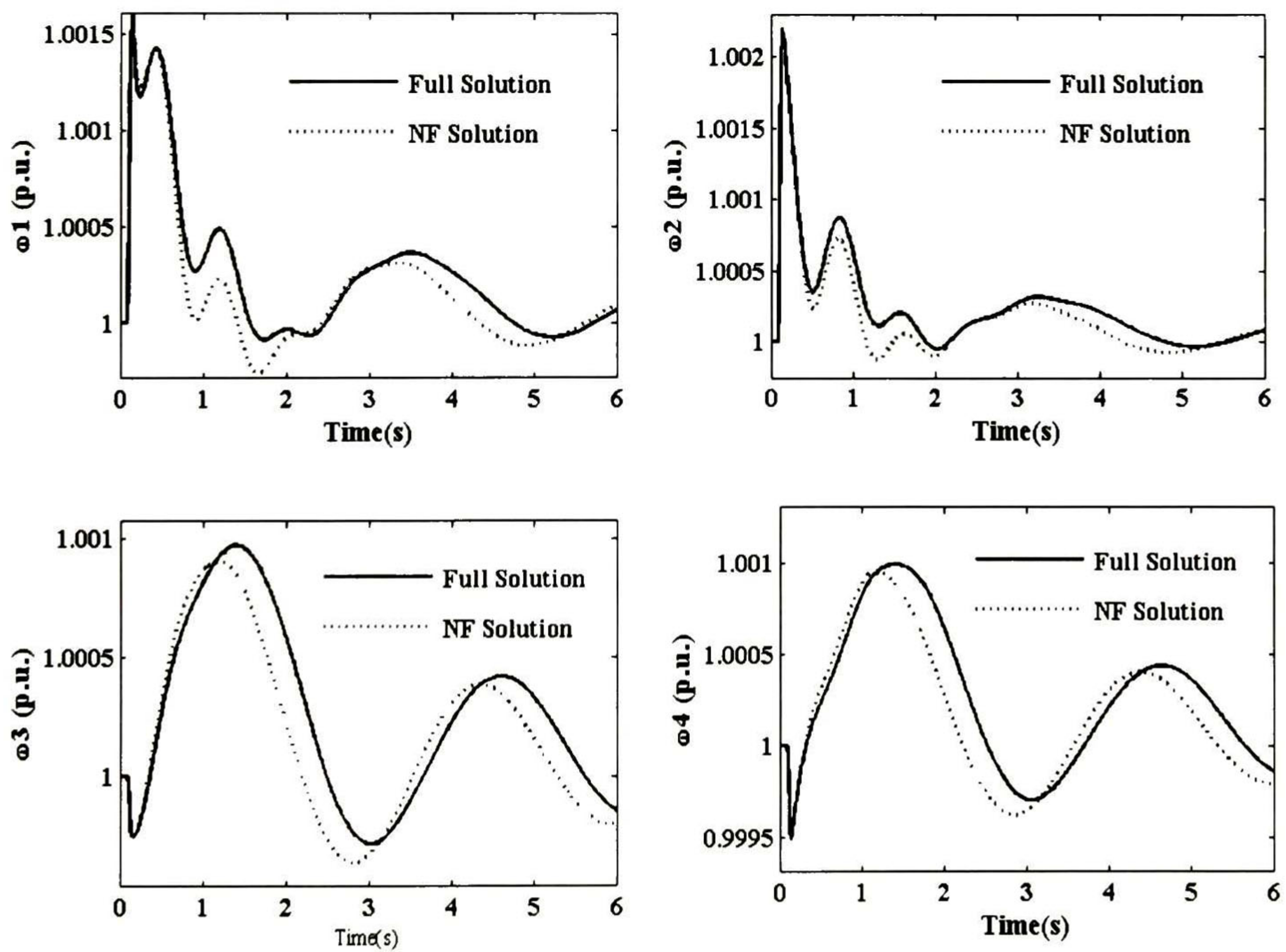


Figure 5.14. Comparison of relative rotor speed swings computed with conventional, and the structure preserving model. Case study 2.

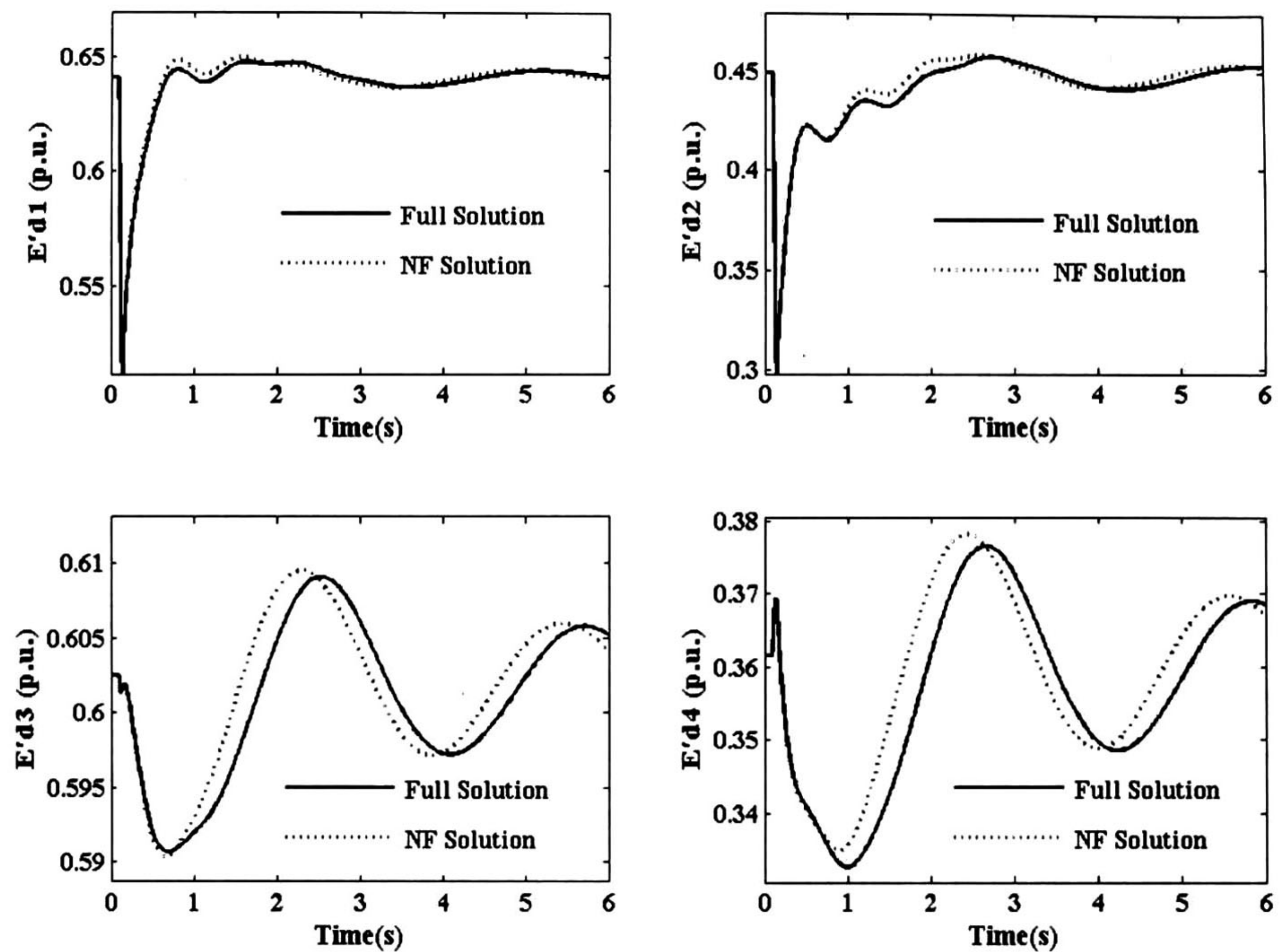


Figure 5.15. Comparison of relative rotor d -axis voltage swings computed with conventional, and the structure preserving model. Case study 2.

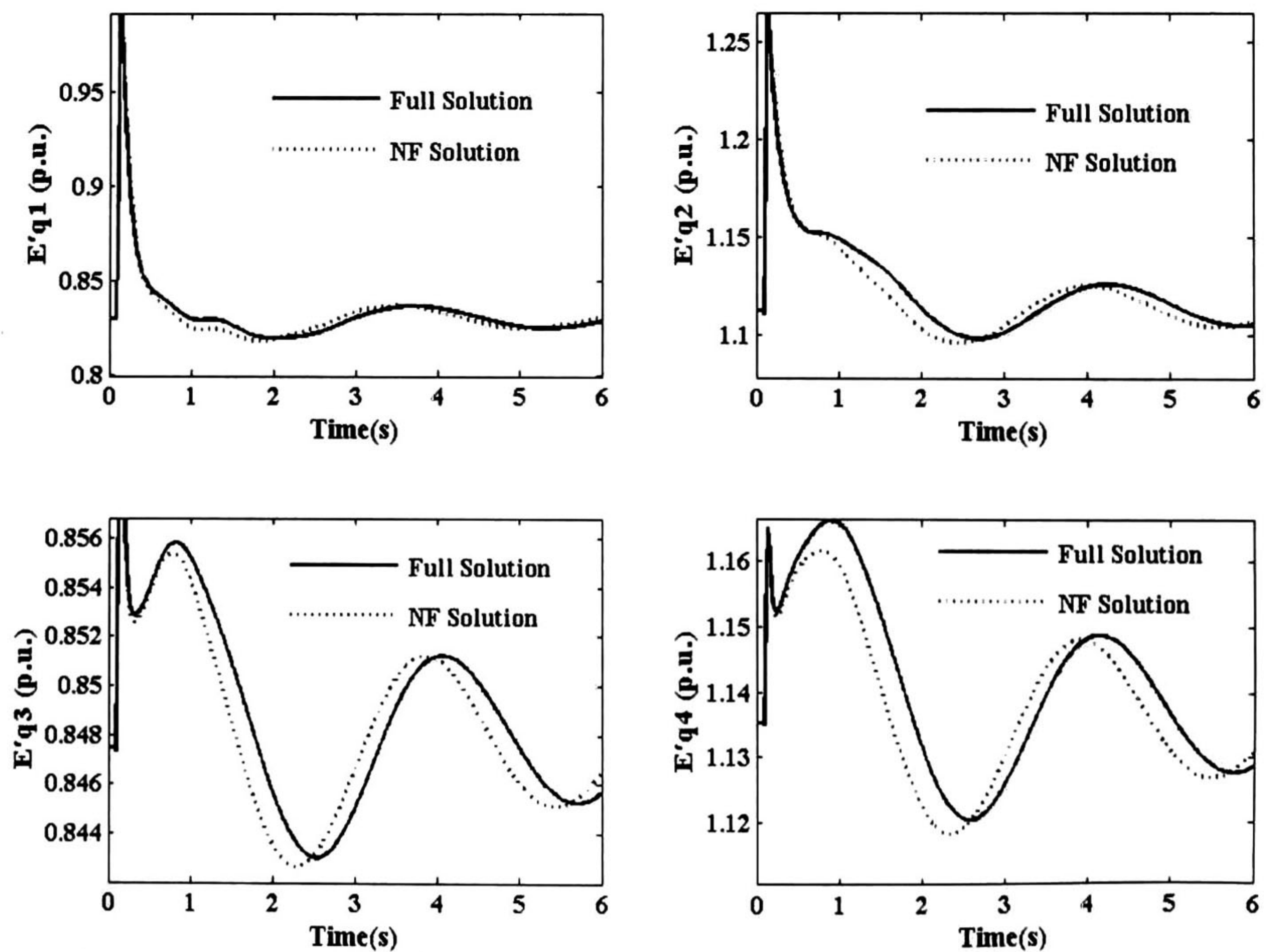


Figure 5.16. Comparison of relative rotor q -axis voltage swings computed with conventional, and the structure preserving model. Case study 2.

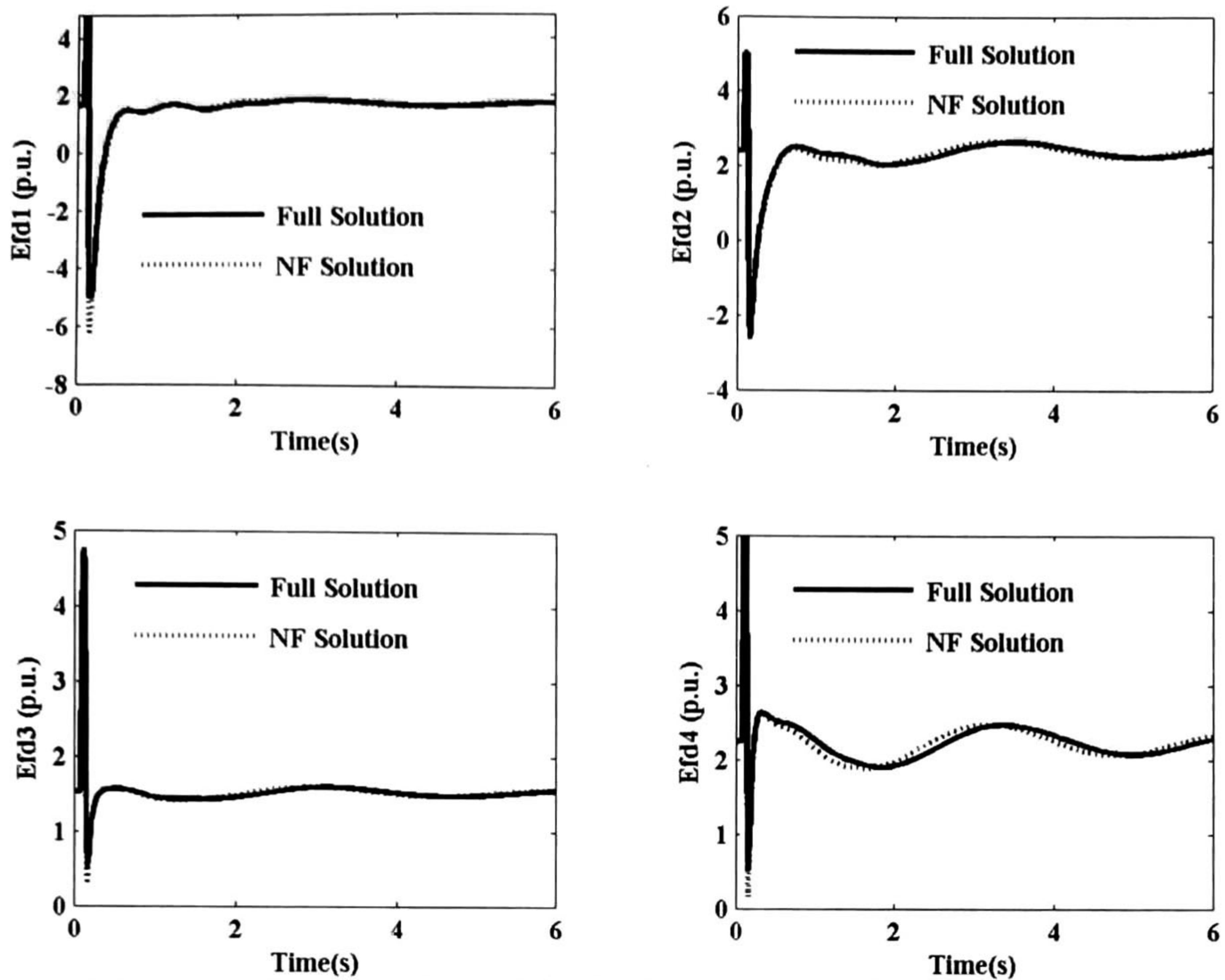


Figure 5.17. Comparison of field voltage computed with conventional, and structure preserving model. Case study 2.

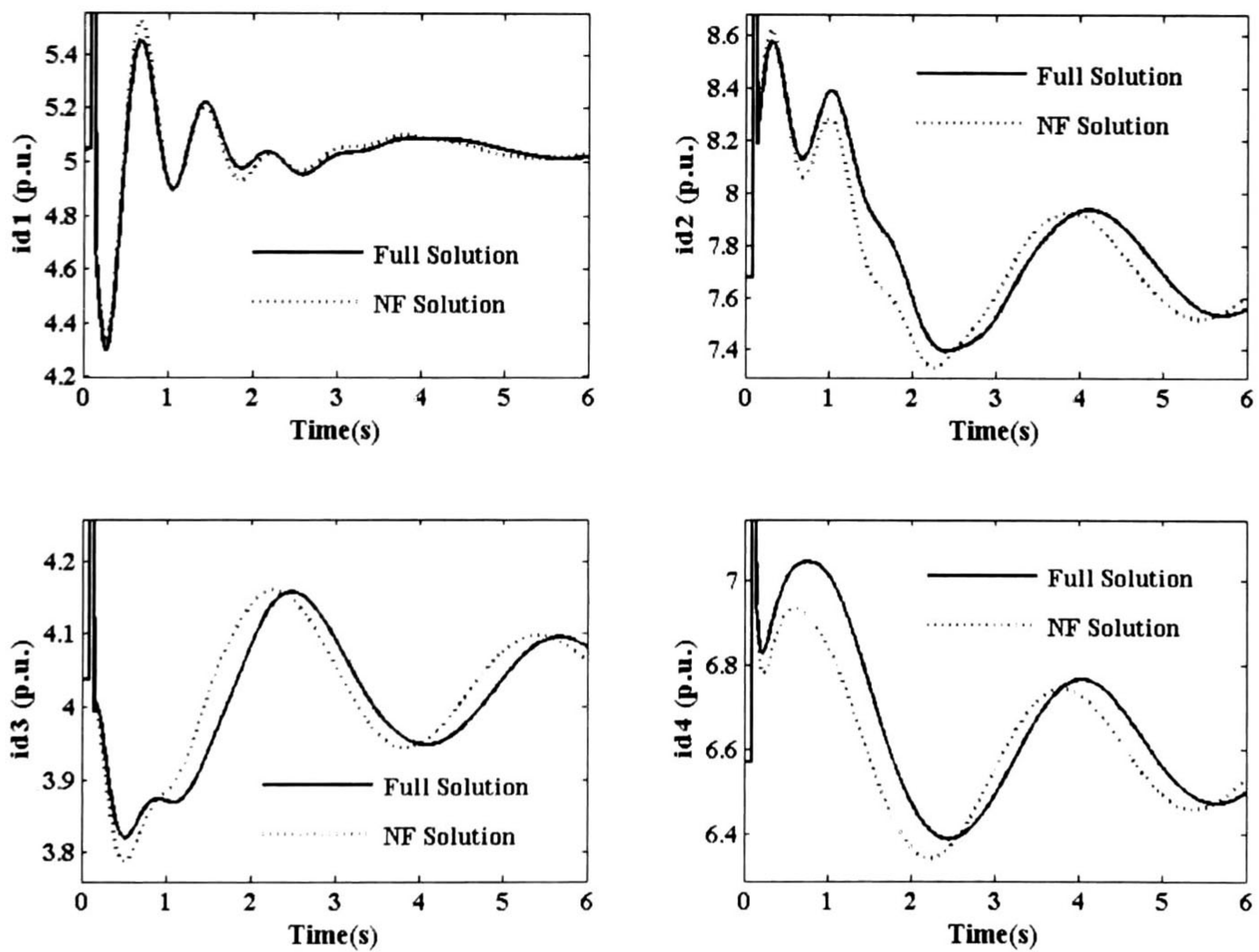


Figure 5.18. Comparison of relative rotor d -axis current swings computed with conventional, and the structure preserving model. Case study 2.

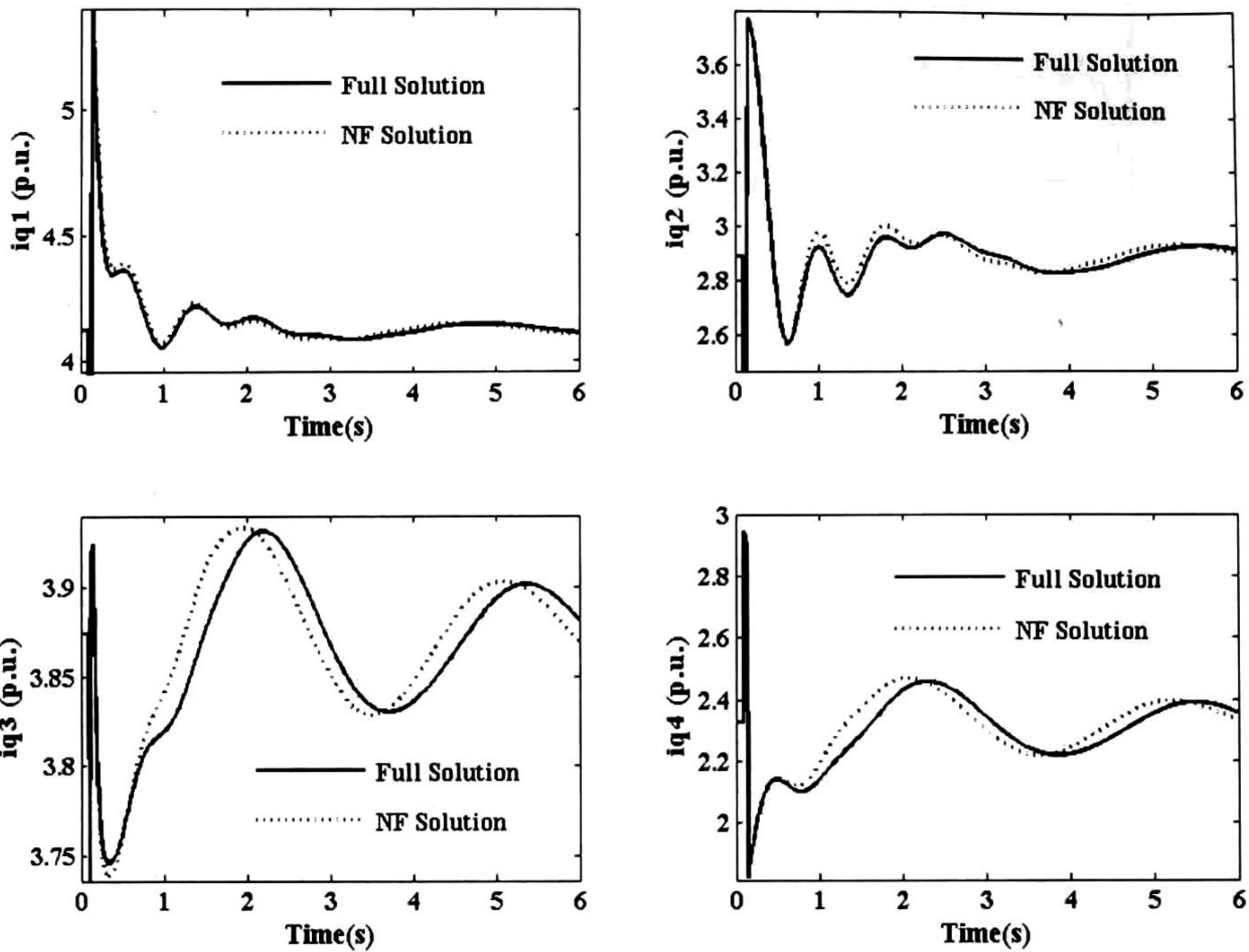


Figure 5.19. Comparison of relative rotor q -axis current swings computed with conventional, and the structure preserving model. Case study 2.

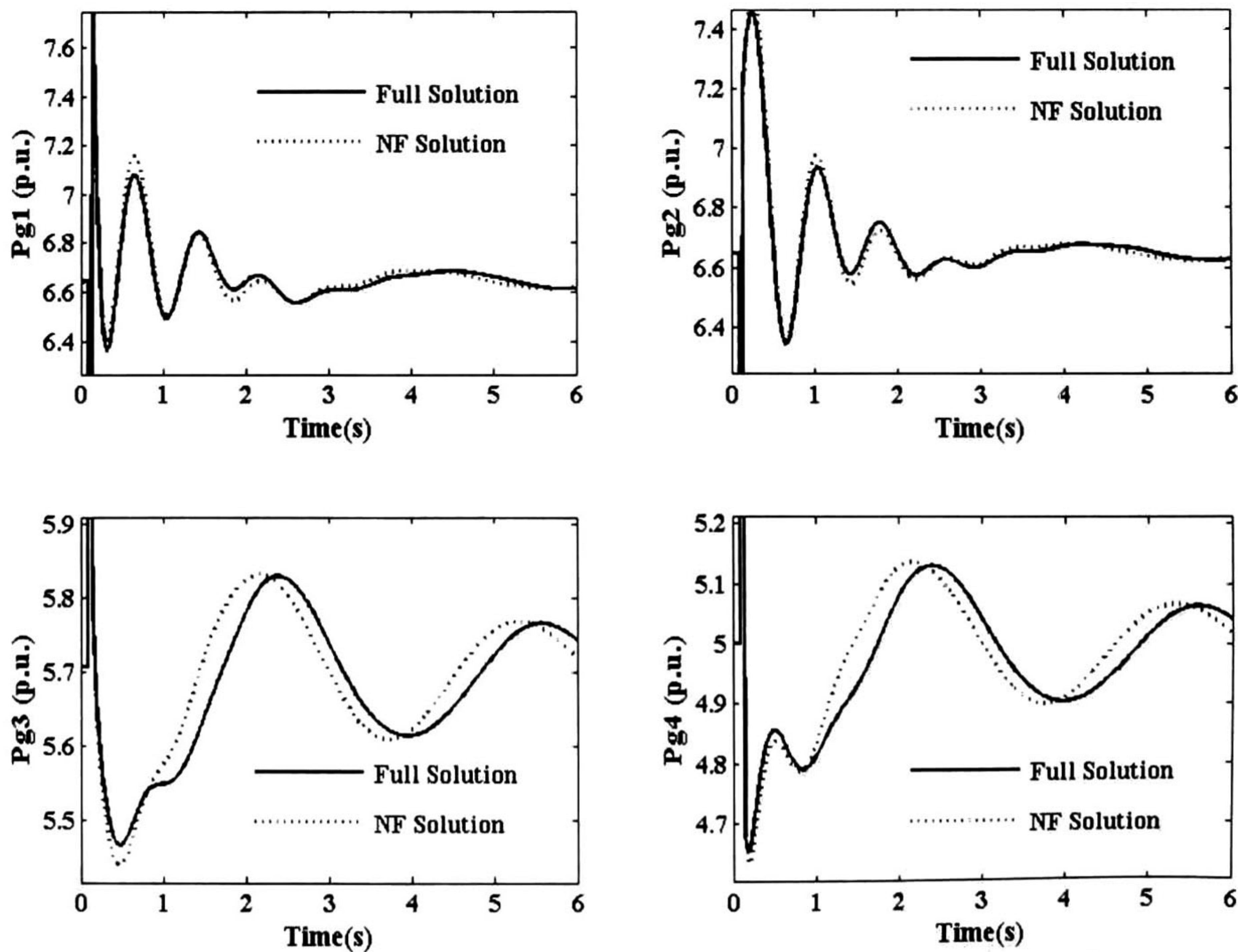


Figure 5.20. Comparison of active output power computed with conventional, and structure preserving model. Case study 2.

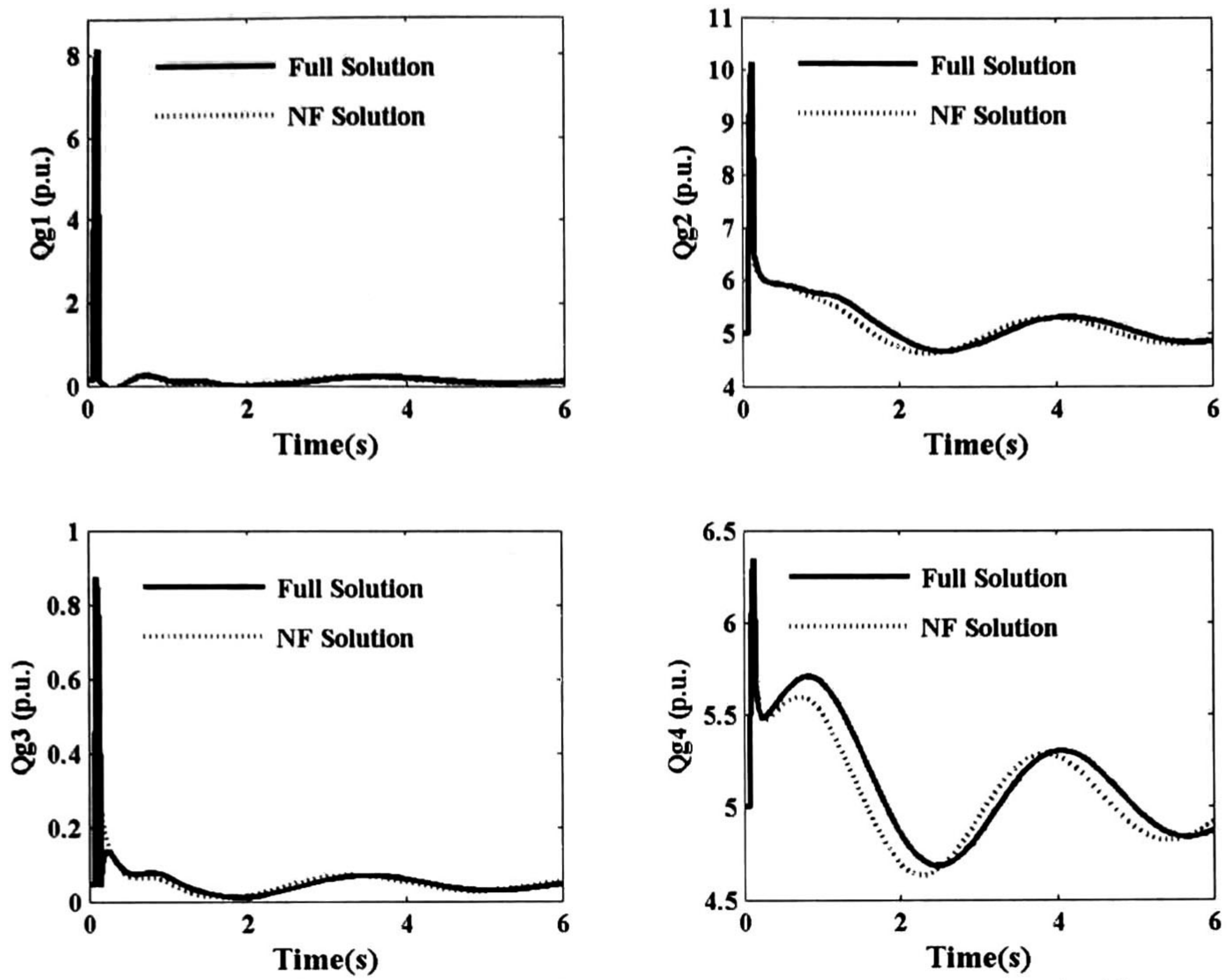


Figure 5.21. Comparison of reactive output power computed with conventional, and structure preserving model. Case study 2.

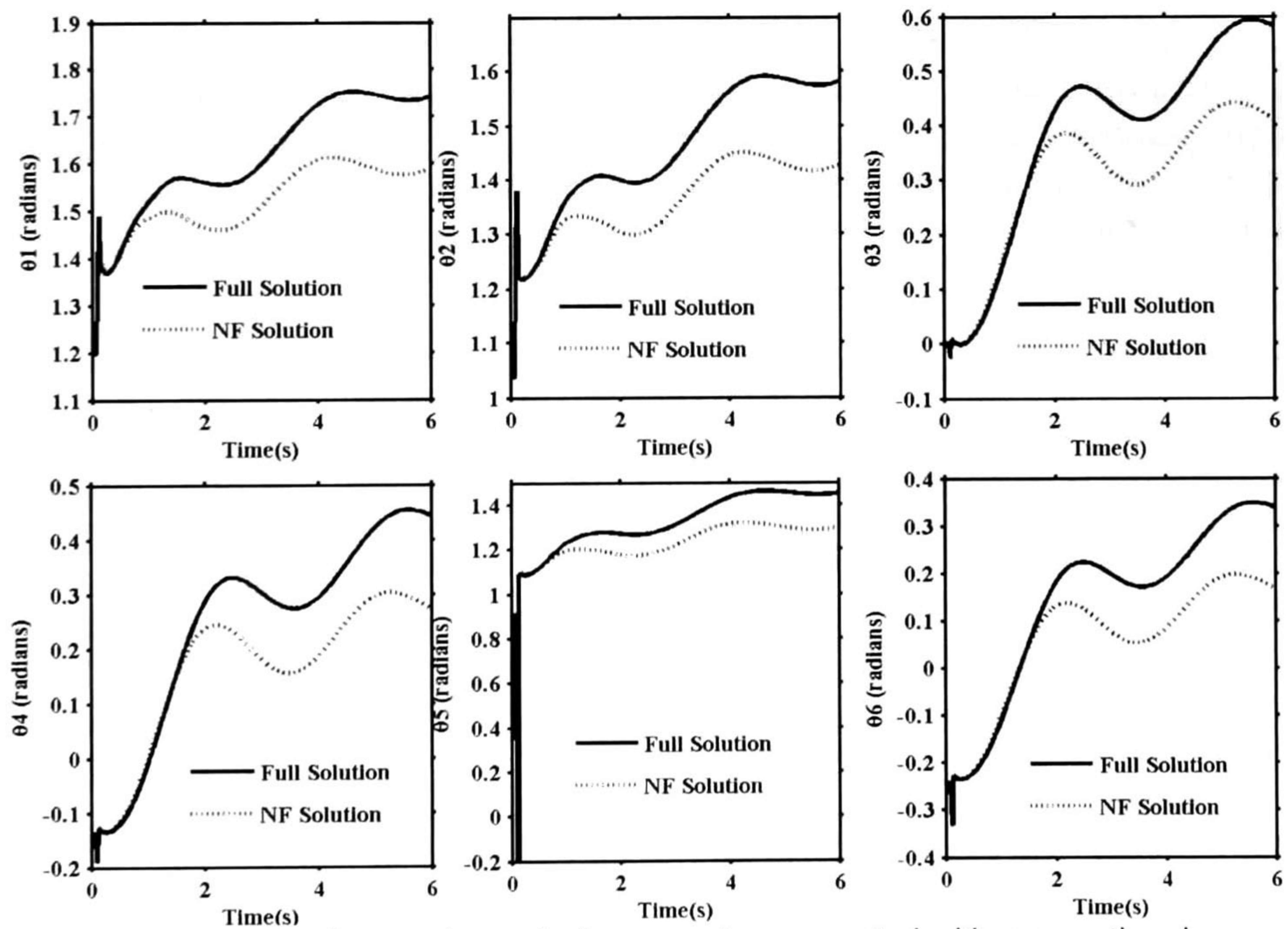


Figure 5.22. Comparison of phase angles computed with conventional, and structure preserving model. Case study 2.

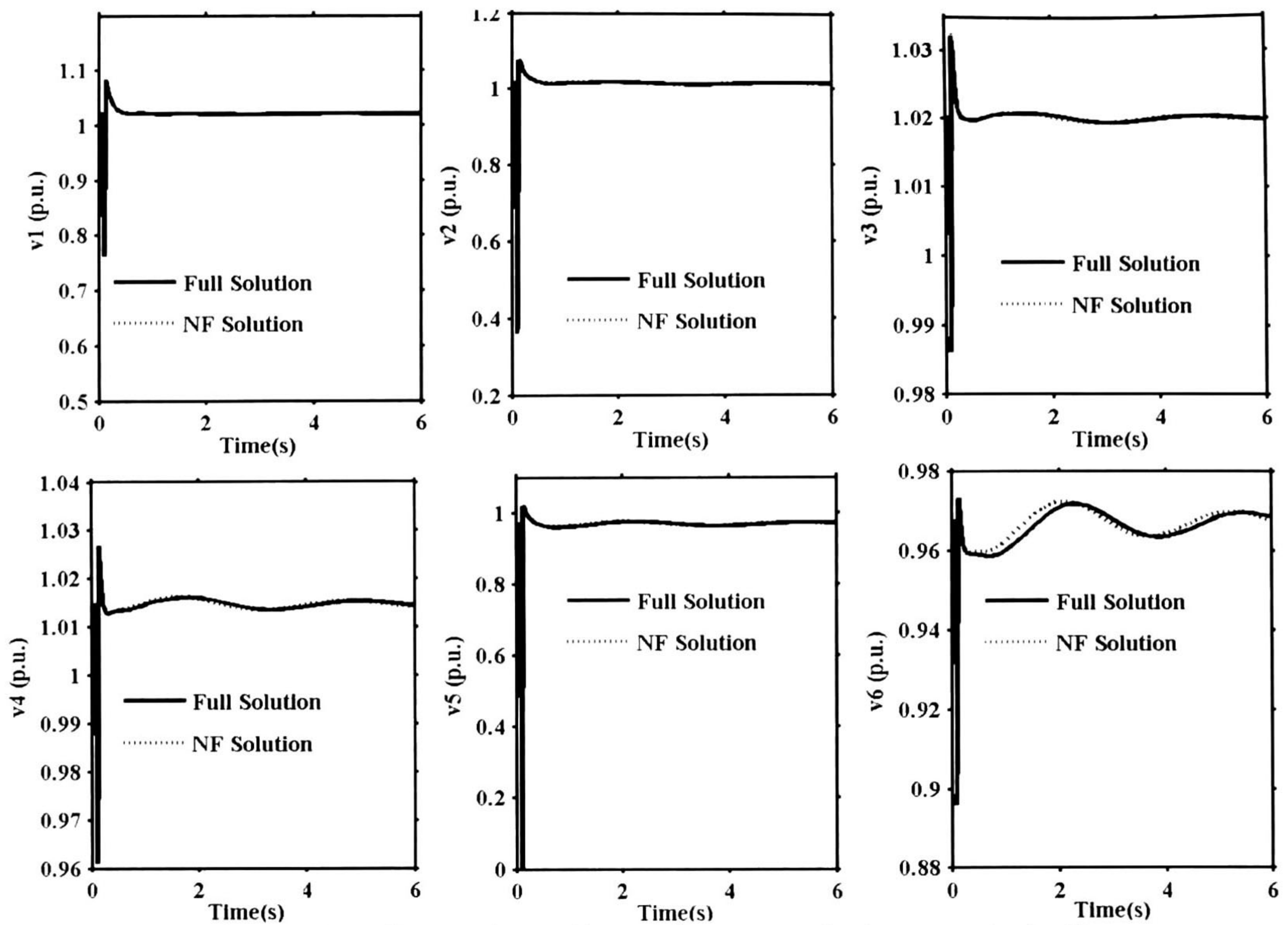


Figure 5.23. Comparison of bus voltage magnitude computed with conventional, and structure preserving model. Case study 2.

The analysis of theoretical aspects influencing the time period over which system solutions are accurate deserves further investigation. Extensions to the proposed formulation are also being investigated to improve the accuracy of the method, particularly for highly stressed conditions.

5.4 Discussion

In this chapter we examined the application of the developed theory to the study of system nonlinear dynamic behavior. The accuracy of the model is quantified by comparing normal form simulations with those from commercial stability software. The approximations work well even for systems where nonlinearity is very strong. These solutions provide physical insight into the primary effects of nonlinearity. An appealing aspect of the new approximate method is that it increases the range of applicability of normal form analysis for use in both, voltage stability and angle stability analysis. Also, because of the formal nature of this procedure, it is possible to extend the approximate solution to higher order, although the advantage of doing so should be justified.

The results of this study suggest that power system models exhibit a two-time-scale property that can be exploited for effective system modeling. No other previous or current research about that exploits this information is known.

Analysis of a simplified test system illustrates that this technique may accurately represent nonlinear system behavior. The agreement between theory and detailed system simulations is in good agreement. The encouraging results presented here, however, have been obtained through numerical investigations based on semi-simplified system representations. They also indicate the need for future investigations which more completely treat the role of control devices on the transmission system on system behavior.

We emphasize that the proposed approach is of particular interest for studying the potential for control stability enhancement by FACTS controllers and the study of the impact of load characteristics on system nonlinear behavior. Studies are being conducted to address the above issues.

References

- [1] M. Klein, G. J. Rogers and P. Kundur, "A fundamental study of inter-area oscillations in power systems", *IEEE Trans. Power Systems*, vol. 6, pp. 914-921, Aug 1991
- [2] P. W. Sauer and M. A. Pai, *Power System Dynamics and Stability*, Prentice Hall Upper Saddle River, NJ. 1998
- [3] J. J. Sanchez-Gasca, V. Vittal, M. J. Gibbard, A. R. Messina, D. J. Vowles, S. Liu, and U. D. Annakkage, "Inclusion of higher order terms for small-signal (modal) analysis: committee report-task force on assessing the need to include higher order terms for small-signal (modal) analysis", *IEEE Power Systems*, vol. 20, pp. 1886-1904, Nov 2005

Chapter 6

Evaluation of Network Contribution to Global Behavior

Network characteristics are known to significantly influence power system dynamic performance. In particular, load characteristics and the use of flexible ac system controllers may have a profound impact on the nature and extent of inter-area oscillations, depending on their location, setting or characteristics. This is an aspect of the application of normal form analysis that has not been addressed in previous research.

In this chapter, a comprehensive evaluation of the effects of parametric changes in network characteristics in affecting system response is presented. The influence is discussed of load location and characteristics and the control actions on system-wide dynamic behavior; the method can be applied to DAE systems of various structures and arbitrary size.

Linear analysis is first used to identify the dominant interacting modes of oscillation, and network parameters that have a greater influence than others in each mode are determined through the use of nonlinear participation factors. Using the loads and devices that have larger participation in the critical modes, relevant disturbed areas are identified. These clusters are then used in the proposed method for large signal stability assessment. Examples of applications of the developed approaches on a 16-machine, 68-bus test power systems are presented to estimate load and controllers' effect on system dynamic performance.

6.1 The Test System

The EPRI RP764 hypothetical 68-bus test system was selected for use in testing the ability of the method to identify critical transmission parameters [1]. This system consists of 68 buses, 16 machines and 86 transmission lines.

The system model used in these studies contains sixteen fully represented system generators. This representation includes detailed AVR representations and subtransient d-q models for most generators. Loads are modeled as being generally dependent on voltage.

Figure 6.1 shows a simplified single-line diagram of the study system illustrating major transmission and generating facilities.

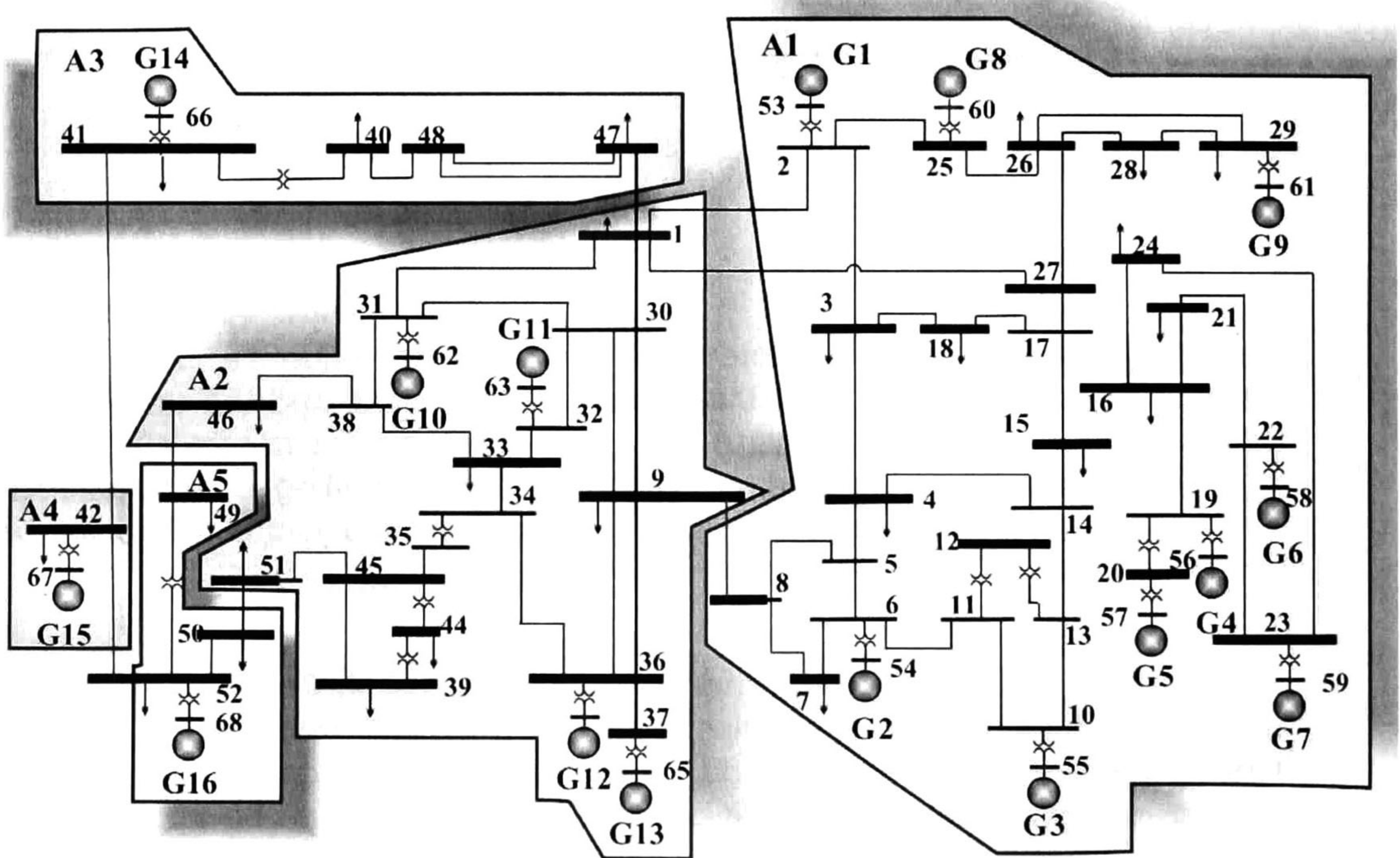


Figure 6.1. Sixteen-machine, five-area study system

6.1.1 Modeling Considerations

In the present study, two operating scenarios are adopted to evaluate the ability of the method to identify relevant disturbed system areas following major contingencies.

These cases are summarized below.

Case 1 – A structure-preserving model case in which all generators are represented by a fourth-order d - q axis model with constant voltage control and loads are represented as voltage dependent functions. In this model, loads are represented by a ZIP model as 70% constant current and 30% constant impedance characteristics ($k_{p1}, k_{Q1} = 0, k_{p2}, k_{Q2} = 0.7, k_{p3}, k_{Q3} = 0.3$ in Eq. (4.14)). This representation results in 80 states and 206 pseudo (algebraic) states.

Case 2 – A structure-preserving model case in which all generators are represented by a fourth-order d - q axis model and loads are represented as constant impedances ($k_{p1}, k_{Q1} = 0, k_{p2}, k_{Q2} = 0, k_{p3}, k_{Q3} = 1$ in the ZIP model). In addition, voltage support by means of static VAR compensators is added at selected major load buses. This representation results in 81 states and 136 pseudo-states

A value of $\varepsilon = 1e-5$ was used in all studies.

Because of the complexity of the nonlinear model a refinement procedure was used to obtain a more tractable solution that preserves network structure. Following our previous results [2,3], the network dynamic can be described as [2,3].

$$\varepsilon \dot{\mathbf{z}} = -\mathbf{A}(\mathbf{x}, \mathbf{z})\mathbf{w} \quad (6.1)$$

where \mathbf{A} is the $m \times m$ power-flow Jacobian matrix obtained from a power flow solution, modified to include the voltage-dependent static load characteristics. The advantage of this method is that analytical expressions can be derived while retaining a desired order of accuracy.

Modal analysis of the extended singularly perturbed system is used below to identify the dominant modes and system states that have a dominant contribution to system behavior.

6.2 Modal analysis

6.2.1 Dominant Modes

The 16-machine test system has four inter-area electromechanical modes of oscillation; the associated eigenvalues and the areas participating in these modes are identified in Tables 6.1 and 6.2.

The system exhibits four groups of slow coherent areas involved in the exchange of swing energy associated with these modes:

Area 1. Machines G1-G9

Area 2. Machines G10-G13

Area 3. Machine G14

Area 4. Machine G15

Area 5. Machine G16

The geographical location for the coherent areas determined from coherency techniques [4,5] is shown in Fig. 6.1.

Table 6.1. Case 1. Inter-area modes of oscillation

Mode #	Eigenvalue	Freq. (Hz)	Damp. %	Area	Dominant Machines
31,32	-0.022±2.430	0.386	0.871	Areas 1 and 2 vs. Areas 3,4,5	G5 and G9
34,35	-0.094±3.778	0.601	2.484	Areas 2 and 5 vs. Areas 1,3	G16 and G14
36,37	-0.108±4.338	0.690	2.486	Areas 2,3 vs. Areas 4,5	G13 and G12
38,39	-0.220±5.198	0.827	4.228	Areas 2 and 4 vs. Areas 3 and 5	G15 and G16

Table 6.2. Case 2. Inter-area modes of oscillation

Mode #	Eigenvalue	Freq. (Hz)	Damp. %	Area	Dominant Machines
31,32	-0.068 ± j2.666	0.424	2.54	Areas 1 and 2 vs. Areas 3,4,5	G5 and G6
34,35	-0.123 ± j3.476	0.553	3.53	Areas 2 and 5 vs. Area 3	G16 and G14
36,37	-0.081 ± j4.620	0.735	1.75	Area 2 vs. Area 4	G12 and G13
38,39	-0.236 ± j5.043	0.802	4.67	Areas 2 and 4 vs. Areas 3 and 5	G15 and G14

Attention in the following analysis is restricted to the analysis of nonlinear behavior associated with inter-area mode 31. This mode represents an oscillation in which machines in Areas 1 (machines G1-G9) and 2 (machines G10-G13) oscillate mainly against machines in the rest of the system (machines G15, G14, and G16).

On the basis of this model, normal form analyzes were carried out to investigate the participation of system variables in dominant intersystem oscillations as well as to validate the developed procedures.

Two complementary approaches to identify the parameters having the most influence on system-wide behavior as well as to analyze the potential for adverse interactions among controllers have been developed in this research. The first method is based on the analysis of linear participation factors. The second method of analysis is based on the study of perturbation-based nonlinear participation factors in this research.

The following is a brief discussion of the cases giving the most important results.

6.2.2 Perturbation-Based Nonlinear Participations

Singular perturbation analysis provides a method for finding a structure-preserving approach to the DAE model. In order to obtain the desired contribution of the network variables, each bus voltage variables was perturbed separately using the procedure in Chapter 4 and the nonlinear participation factors corresponding to the mode of concern were calculated.

In the light of this analysis, the contribution of the k th mode to the time evolution of the i th bus voltage magnitude and the j th load can be obtained as

$$\Delta\beta_{SVC_w}(t) = p_{2\beta_{svc}w_i} e^{\lambda_j t} + \sum_{k=1}^r \sum_{l=k}^r p_{2\beta_{svc}w_{kl}} e^{(\lambda_k + \lambda_l)t} \quad (6.2a)$$

$$\Delta\theta_p(t) = p_{2\theta_{pl}} e^{\lambda_j t} + \sum_{k=1}^r \sum_{l=k}^r p_{2\theta_{pkl}} e^{(\lambda_k + \lambda_l)t} \quad (6.2b)$$

$$\Delta V_q(t) = p_{2V_{qj}} e^{\lambda_j t} + \sum_{k=1}^r \sum_{l=k}^r p_{2V_{qkl}} e^{(\lambda_k + \lambda_l)t} \quad (6.2c)$$

$$\Delta P_{Lr}(t) = p_{2P_{Lrj}} e^{\lambda_j t} + \sum_{k=1}^r \sum_{l=k}^r p_{2P_{Lrkl}} e^{(\lambda_k + \lambda_l)t} \quad (6.2d)$$

$$\Delta Q_{Ls}(t) = p_{2Q_{Lsj}} e^{\lambda_j t} + \sum_{k=1}^r \sum_{l=k}^r p_{2Q_{Lskl}} e^{(\lambda_k + \lambda_l)t} \quad (6.2e)$$

By identifying the largest participations associated with the mode combination $(\lambda_k + \lambda_l)$, geographical areas having a participation in a given mode can be readily determined.

Here, a large participation factor indicates a high involvement of the bus (load) in the swing dynamics.

6.3 Test Results: Effect of Load Characteristics on System Behavior

Equations (6.2d) and (6.2e) are used in this analysis to infer the effect of load characteristics on system-wide behavior. The analysis consists of two parts. In the first part, modal analysis of the dominant mode(s) is conducted by determining the dominant loads involved in the oscillation. Using this information, relevant load zones are identified. These load zones are then used in the proposed formulation for identifying critical load and transmission corridors.

In the second part, the nonlinear modal based nonlinear participation factors are used to estimate critical loading conditions.

6.3.1 Ranking of Load Participations: A Linear Analysis Approach

Load participation factors provide a measure of the sensitivity of the change in the load reactive power output in response to changes in modal bus voltage deviations. This identifies the loads that play an important role in a particular mode.

The 20 highest participating buses as determined from conventional linear participation factors are given in Table 6.3. From the in Table 6.4, it follows that buses 52 and 20 located in the extremes of the oscillation (machines G16 and machines G5, G9), have the largest contribution to the swing dynamics.

Table 6.3. Dominant load-based linear participation factors $p_k = u_{ki} v_{ki}$

Order of importance	Perturbed bus	Relative Participation
1	52	1.000
2	20	0.368
3	18	0.364
4	4	0.348
5	37	0.229
6	15	0.226
7	16	0.223
8	24	0.208
9	3	0.200
10	29	0.189
11	27	0.183
12	21	0.182
13	51	0.180
14	7	0.165
15	23	0.148
...
20	25	0.100

Figure 6.2 shows the corresponding mode shapes of machines G5 and G9, and the load shapes computed from the left eigenvector for the inter-area mode 31. As suggested in Table 6.3, the load at bus 52 appears to have a large participation relative to the participation of the dominant machine (machine G5). In turn the load at bus 20 is seen to have a smaller and out of phase participation.

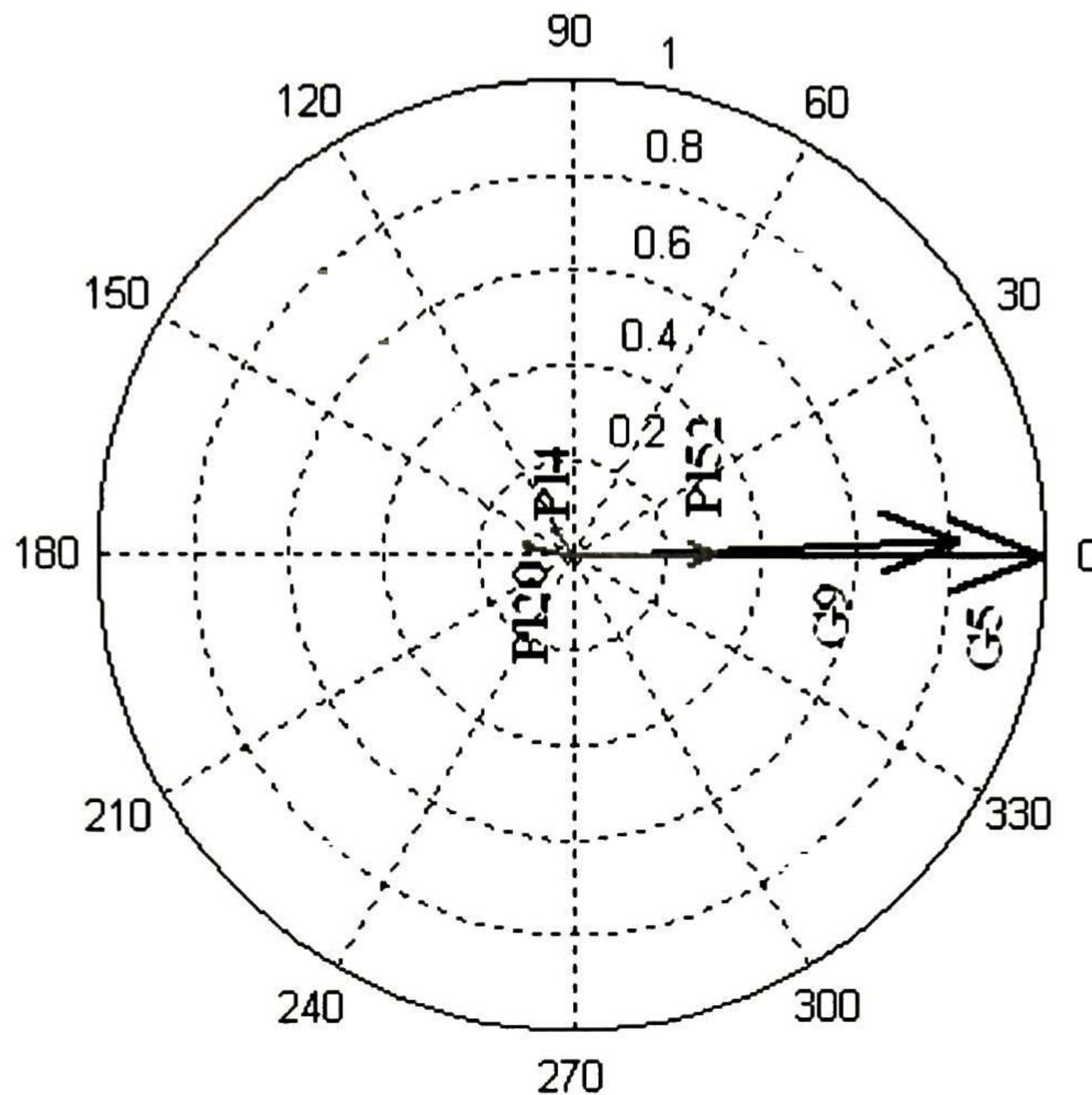


Figure 6.2 Linear participations to generators and dominant active load.

6.3.2 Nonlinear Analysis Approach

Based on this analysis, non-linear based participation factors were used to identify the critical loads. In the simulations, each load was perturbed separately and the corresponding time evolution was computed. In this procedure a perturbation α of unit magnitude was used.

The time-evolution of each load was then expressed in the form

$$\Delta P_{L_r}(t) = \sum_{j=1}^m P_{2L_{rj}} e^{\lambda_j t} + \sum_{k=1}^m \sum_{l=k}^m P_{2L_{rkl}} e^{(\lambda_k + \lambda_l)t} \quad (6.3)$$

Tables 6.4 and 6.5 list the ranking of critical loads provided by the analysis of nonlinear participation factors for the inter-area mode. Second-order nonlinear participation factors identify bus 20, in the neighborhood of the most dominant machine (G5), as the bus having the largest participation in the inter-area mode. Of particular interest, the nonlinearly interacting modes $\lambda_{31} + \lambda_j$, $j=1, \dots, n$ identify clusters of critical loads. This is a unique feature of nonlinear analysis that is not available in conventional formulations.

Thus for instance, bus 20 is shown to strongly interact with buses 16, 20, 4 and to a lesser extent with buses 26, 15, 9 and 37 in Area 1.

Table 6.4 . Dominant first -order nonlinear participation factor, P_{2Lrj}

Order of importance	bus	Relative Participation
1	37	1.000
2	20	0.430
3	4	0.362
4	8	0.351
5	15	0.172
6	24	0.171
7	21	0.155
8	3	0.132
9	29	0.131
10	27	0.119
11	23	0.114
12	52	0.108
13	7	0.106
14	28	0.079
15	25	0.071
...
20	18	0.043

Table 6.5. Dominant load bus-based nonlinear participation factors , P_{2Lrkl}

Order of importance	Perturbed load-bus	Relative Participation	Nonlinearly interacting buses
1	20	1.000	16, 20, 4, 26, 15, 9, 37
2	4	0.196	4, 52, 26, 41, 51, 39, 40
3	37	0.182	37, 49, 9, 28, 46, 45, 52
4	12	0.151	26, 51, 52, 54, 24, 25, 9
5	24	0.111	24, 26, 52, 16, 4, 47, 46
6	25	0.109	26, 25, 39, 16, 4
7	23	0.080	16, 23, 26, 15, 4
8	8	0.075	8, 52, 37, 41, 4
9	28	0.073	51, 28, 9, 50, 16
10	21	0.070	16, 21, 37, 52, 15
11	16	0.049	16, 26, 52, 4, 16
12	50	0.030	28, 40, 45, 42, 27
13	46	0.028	49, 47, 52, 51, 21
14	52	0.020	49, 52, 45, 28, 44
15	47	0.018	49, 47, 51, 42, 52

Figure 6.3 shows the corresponding critical areas involved in the oscillation.

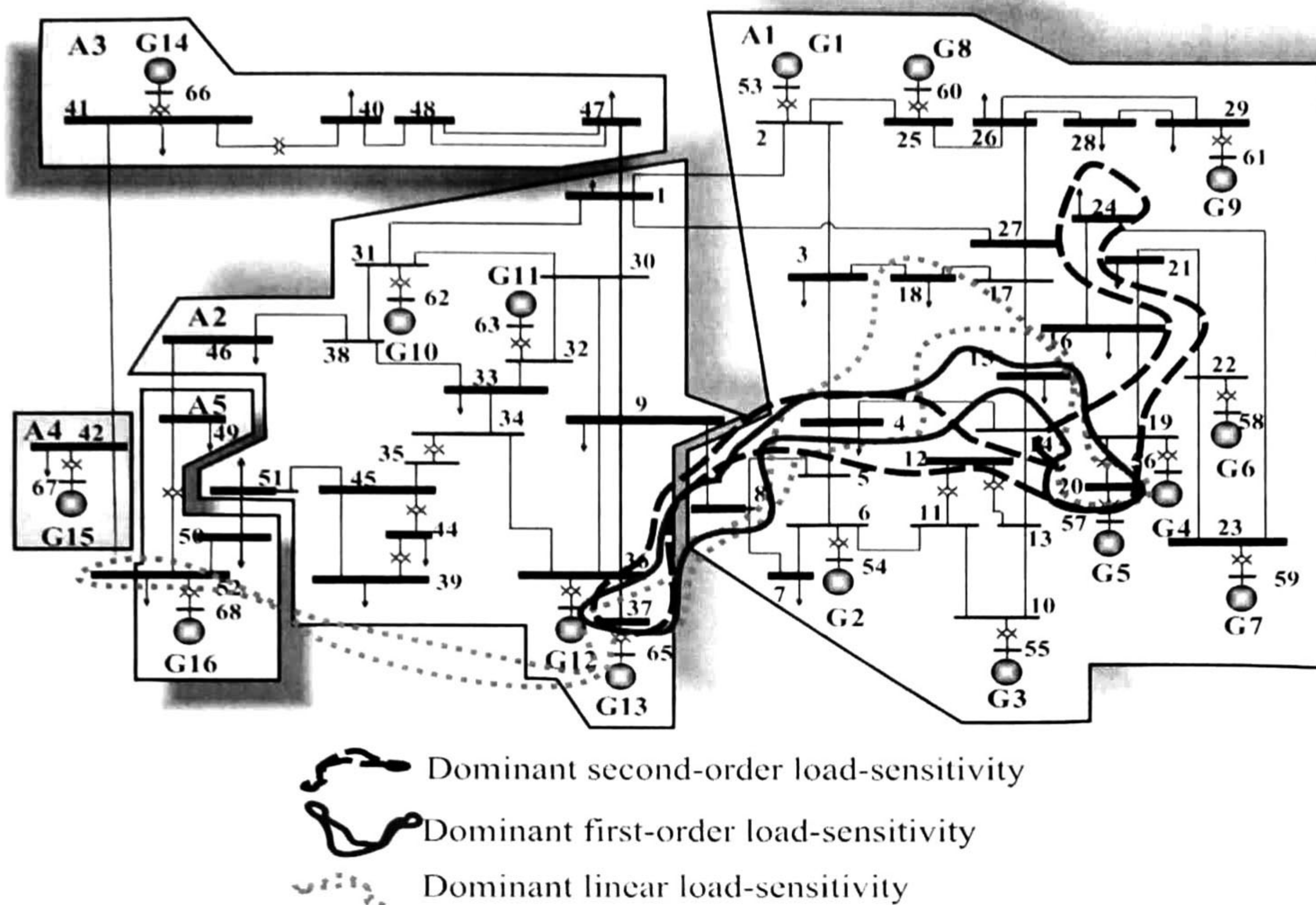


Figure 6.3. Location of sensitivity on load buses

Also of interest, Fig. 6.4. shows the point to point connection of the critical buses in the fourth column of Table 6.5. Figure 6.5 compares the time evolution of the network variables for the adopted system representations. For completeness the full SBSS is also plotted.

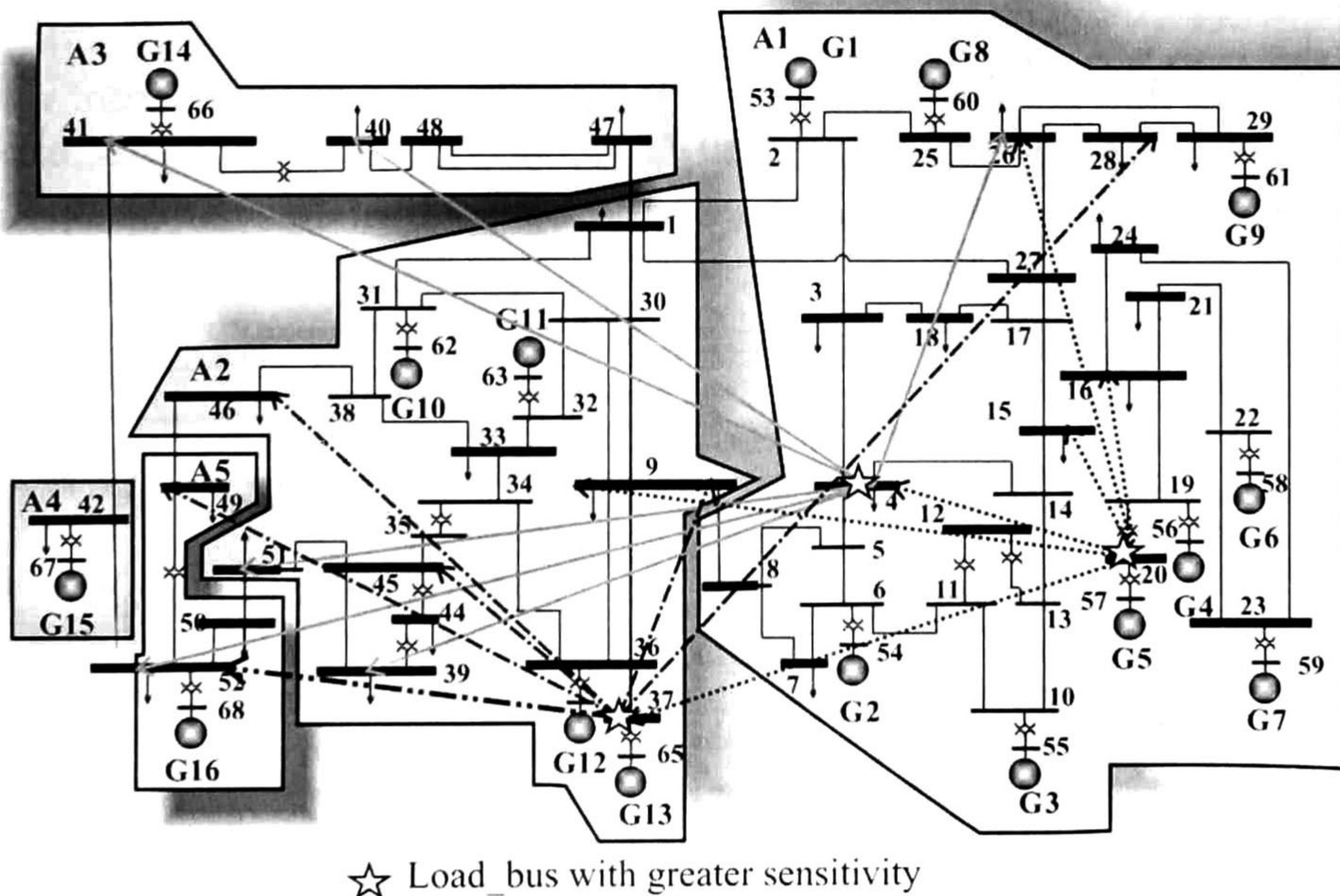


Figure 6.4. Interactions of nonlinear sensitivity of load buses

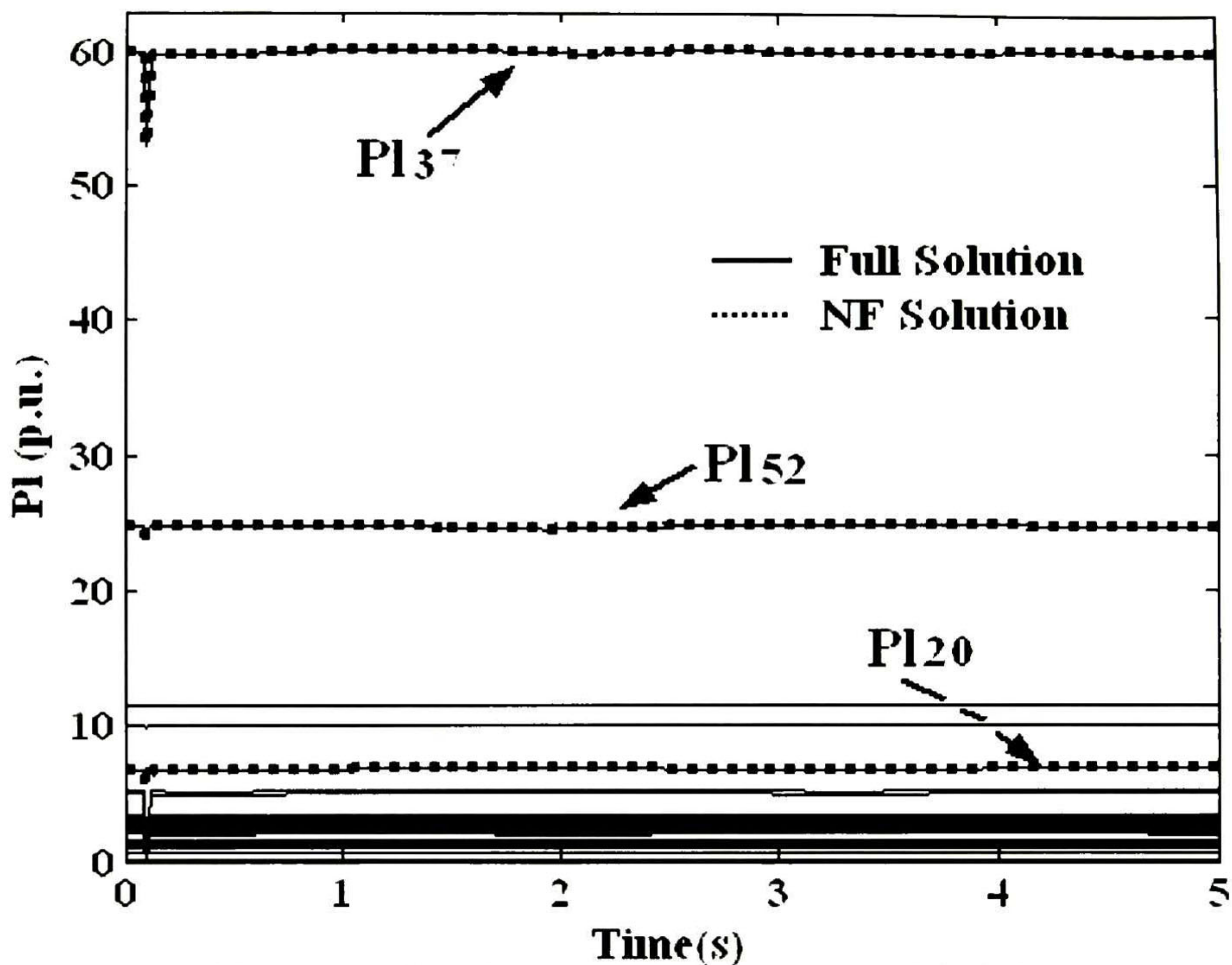


Figure 6.5. Closed-form solutions of active load deviations

6.3.3 Evaluation of Critical Operating Conditions

Having identified the critical buses using nonlinear information, detailed studies were conducted to verify the soundness of the results. From Table 6.5, the bus load was selected for analysis.

Tables 6.6 and 6.7 show the linear eigenvalues for two different values of load at bus 20, namely $P_{L20} = 5.50 pu$, and $P_{L20} = -1.10 pu$. As expected, eigenvalue analyses show that decreasing the load at bus 20 decreases the stability of inter-area mode 31.

Table 6.6. Evolutions of inter-area modes to $P_{Lo20} = 5.500 p.u.$

Mode #	Eigenvalue
31,32	$0.006 \pm j2.349$
34,35	$-0.089 \pm j3.750$
36,37	$-0.109 \pm j4.293$
38,39	$-0.220 \pm j5.194$

Table 6.7. Evolutions of inter-area modes to $P_{L,020} = -1.100$ p.u.

Mode #	Eigenvalue
31,32	$0.272 \pm j1.797$
34,35	$-0.072 \pm j3.545$
36,37	$-0.122 \pm j4.102$
38,39	$-0.223 \pm j5.176$

Figures 6.6 through 6.9 show the system response to a step change in the active load power at bus 20. Examination of these results, shows that the system becomes unstable, thus illustrating the usefulness of the method to identify critical network parameters.

In all cases, normal form solutions provide an accurate representation of system behavior even for the most stringent (unstable conditions) which are not normally considered in normal form studies.

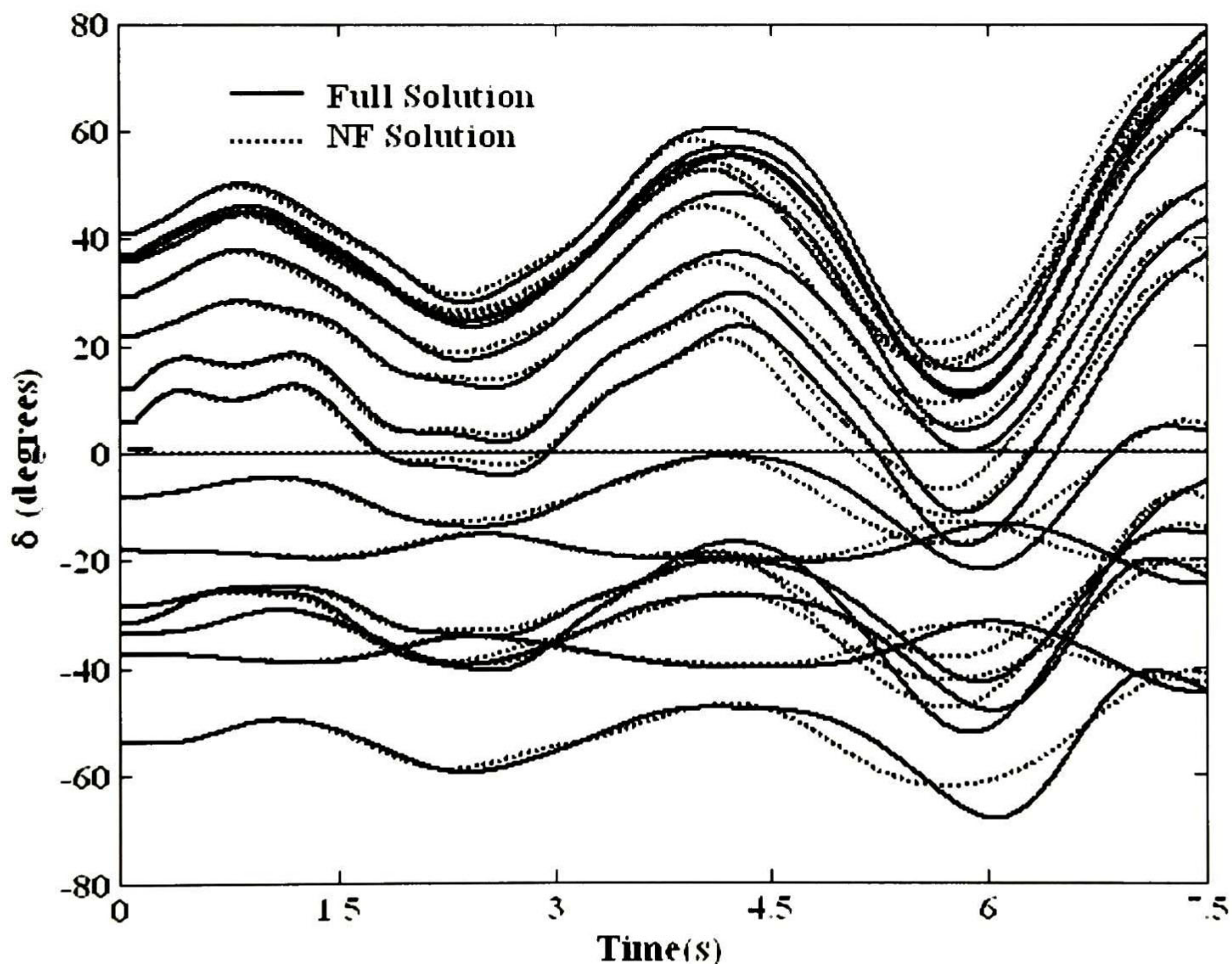


Figure 6.6. Comparison of relative rotor speed swings computed with conventional, and the structure preserving model with δ_{16} as reference

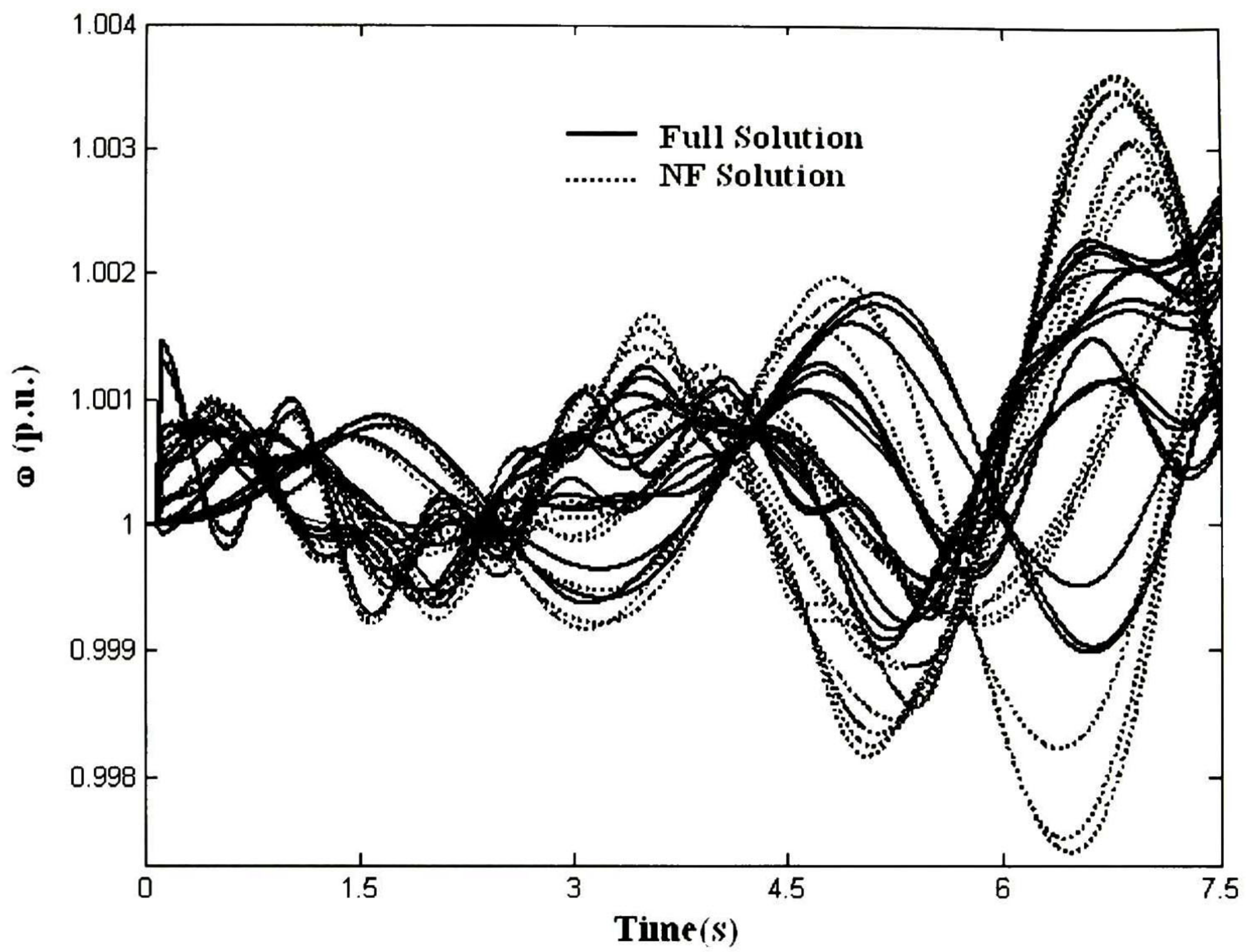


Figure 6.7. Comparison of relative rotor speed swings computed with conventional, and the structure preserving model.

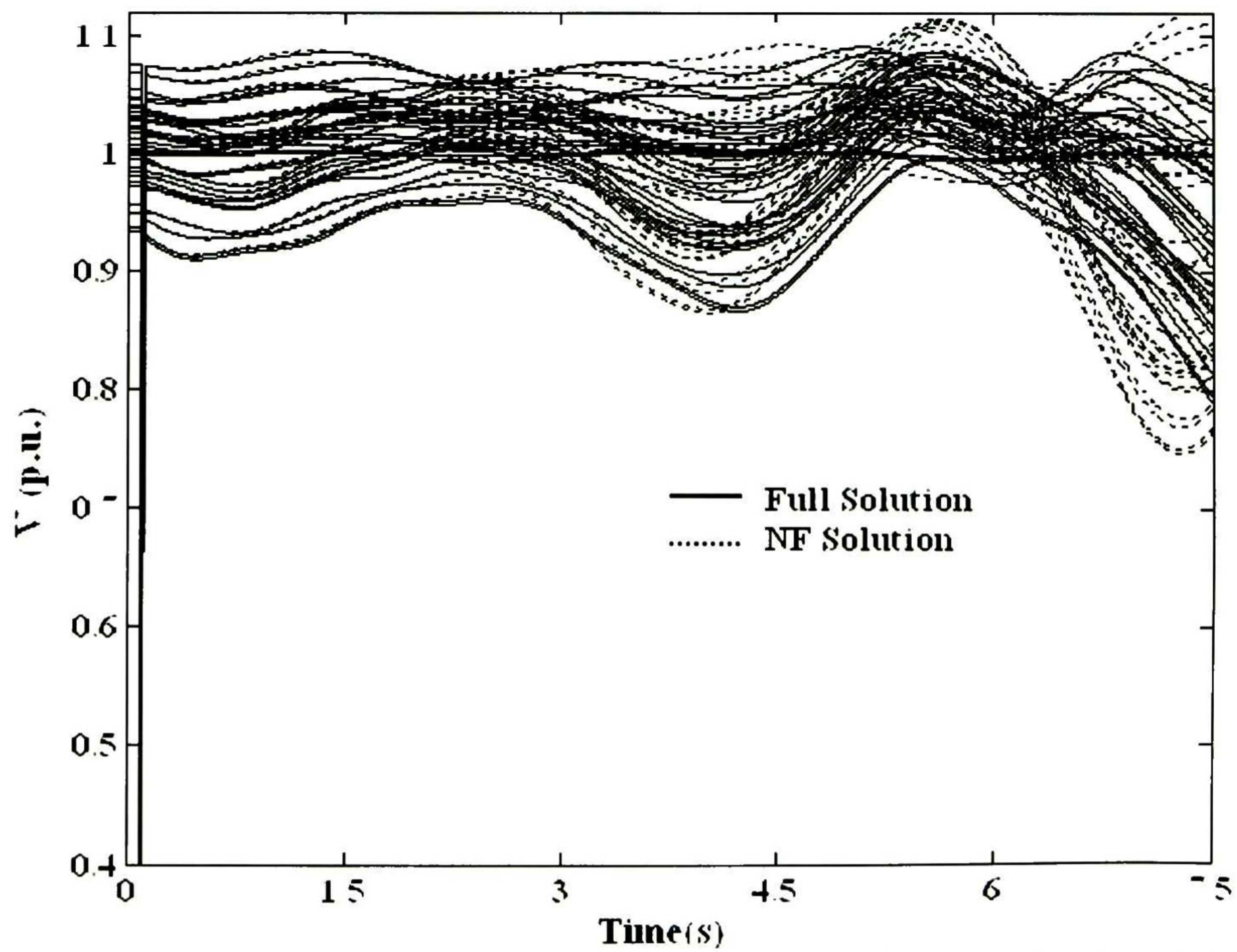


Figure 6.8. Comparison of bus voltage magnitude computed with conventional, and structure preserving model.

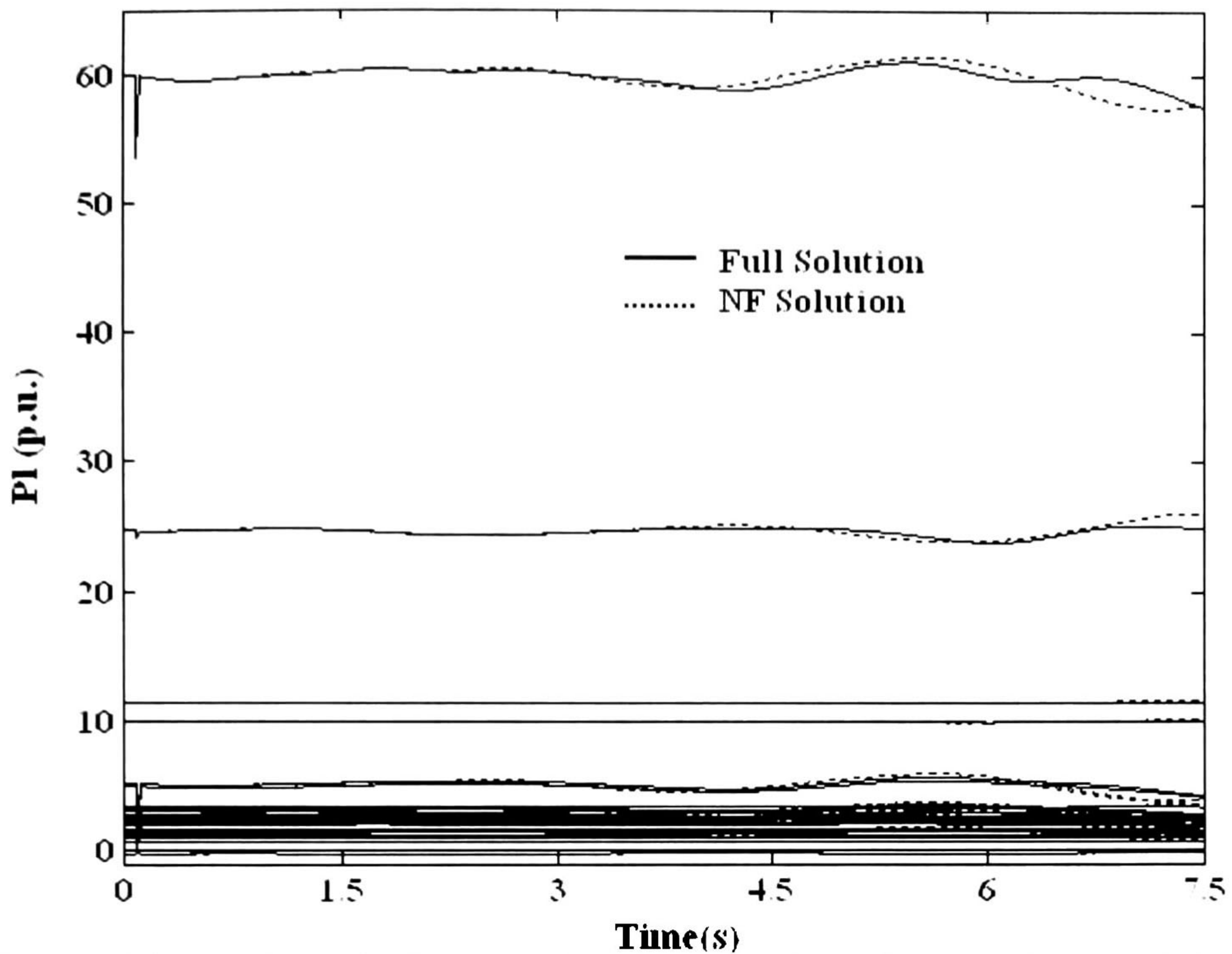


Figure 6.9. Comparison of active power load bus computed with conventional, and structure preserving model.

6.4 Voltage-Based Nonlinear Participation Factors

Further insight into the effect of voltage control devices on the inter-area oscillations may be obtained from the study of voltage-based nonlinear participation factors in Eq. 6.2c.

Tables 6.8 and 6.9 list the dominant nonlinear participation factors, $P_{2V_{qj}}$ and $P_{2V_{qkl}}$ associated with the slowest inter-area mode 31. For completeness the load-based participation factors are also included. Figure 6.6, in turn, shows the corresponding critical buses identified by normal form analysis. The factors are normalized with respect to the largest component.

Here, a large participation factor indicates a high involvement of the bus in the swing dynamics of the mode of concern. Table 6.6 summarizes the results of this analysis and also includes the relative order of importance of the loads.

Table 6.8. Dominant voltage and load based nonlinear participation factors

Order of importance	Bus	$P_{2v_{ij}}$	Bus	$P_{2L_{ij}}$
1	7	1.000	52	1.000
2	8	0.875	8	0.333
3	4	0.589	4	0.306
4	17	0.566	20	0.302
5	54	0.525	37	0.226
6	27	0.433	15	0.200
7	25	0.414	16	0.200
8	16	0.375	51	0.193
9	3	0.299	3	0.183
10	2	0.222	24	0.180
11	26	0.215	29	0.168
12	11	0.214	27	0.166
13	13	0.209	21	0.162
14	4	0.174	7	0.150
15	61	0.158	23	0.145
...	28	0.126
23	50	0.033	41	0.100

Table 6.9. Dominant voltage-based nonlinear participation factors, $P_{2V_{qkl}}$

Order of importance	Perturbed bus	Relative Participation	Nonlinearly interacting buses
1	21	1.000	22,23,17,19
2	22	0.824	22,23,24,15,21,58
3	23	0.820	22,23,21,24,15
4	19	0.772	21,23,24,25,15,28,56,19,20
5	20	0.716	56,19,20,57
6	28	0.324	28,29,3,29,61
7	29	0.194	28,29,3,29
8	60	0.072	54,55
9	55	0.044	54,55,12
10	58	0.038	22,23
11	52	0.031	52,68
12	16	0.029	16,24
13	41	0.018	41,42,66,67
14	68	0.016	52,68
15	6	0.013	5,6

Several observations can be made from these results. Referring to Fig. 6.10, we note that the dynamic patterns associated with the dominant contributions to the critical inter-area mode are located close to machines having the largest participation in the critical mode (machines G5,G7,G9 and G6 in Area 1) and machine G16 in Area 4. This suggests that FACTS controllers located at the most participating buses might be used to enhance damping of the inter-area mode 31.

From this study, transmission buses in Area 1 (buses 15,17,19 among others) and bus 50 in Area 5 are singled out as potential candidate locations to place FACTS controllers. As discussed later in this chapter, studies indicate that load modulation at these buses might have a significant influence on modal damping of the inter-area mode 31. Specifically, buses 52, 8, 4, and 9 are seen to have a significant participation in the inter-area mode.

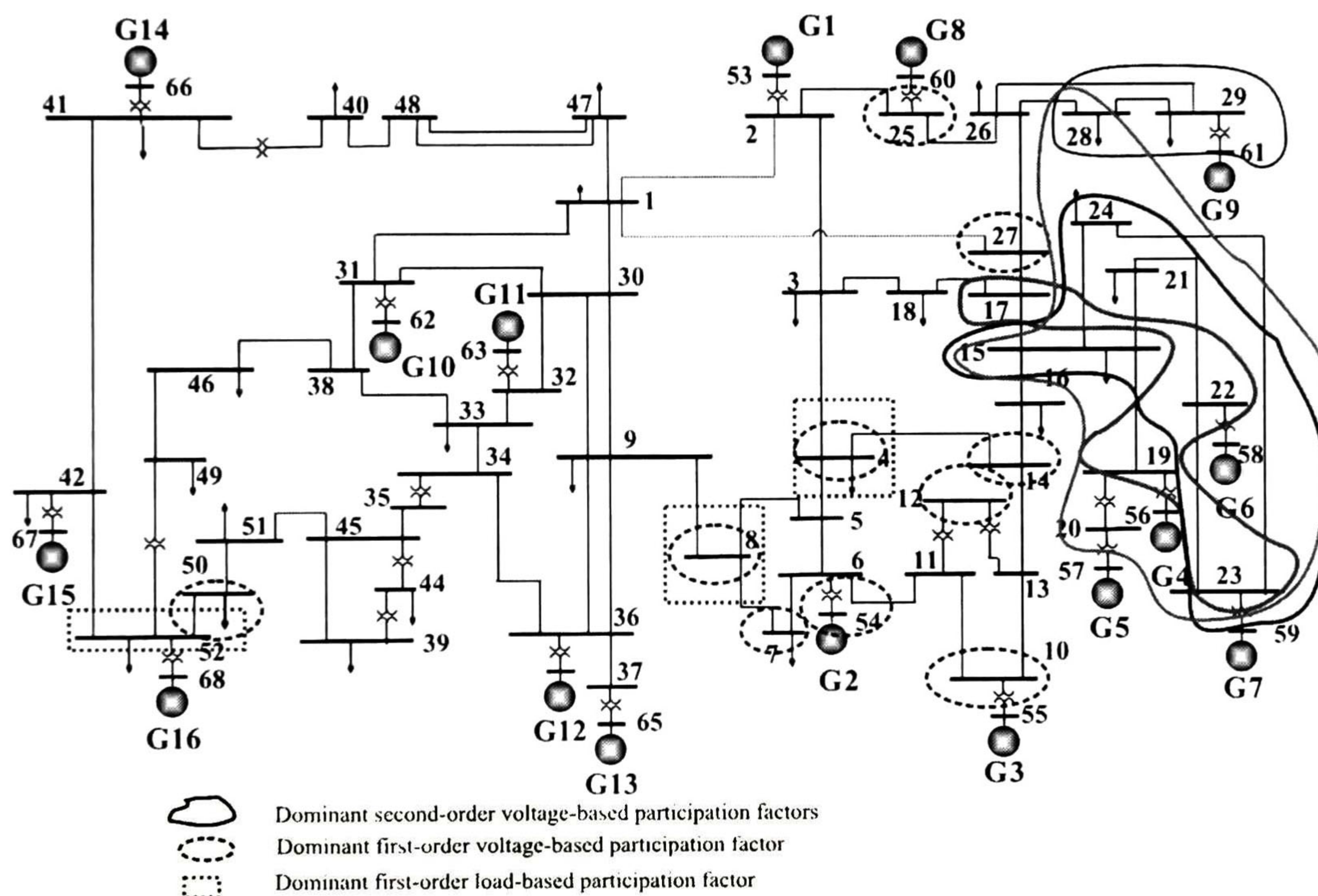


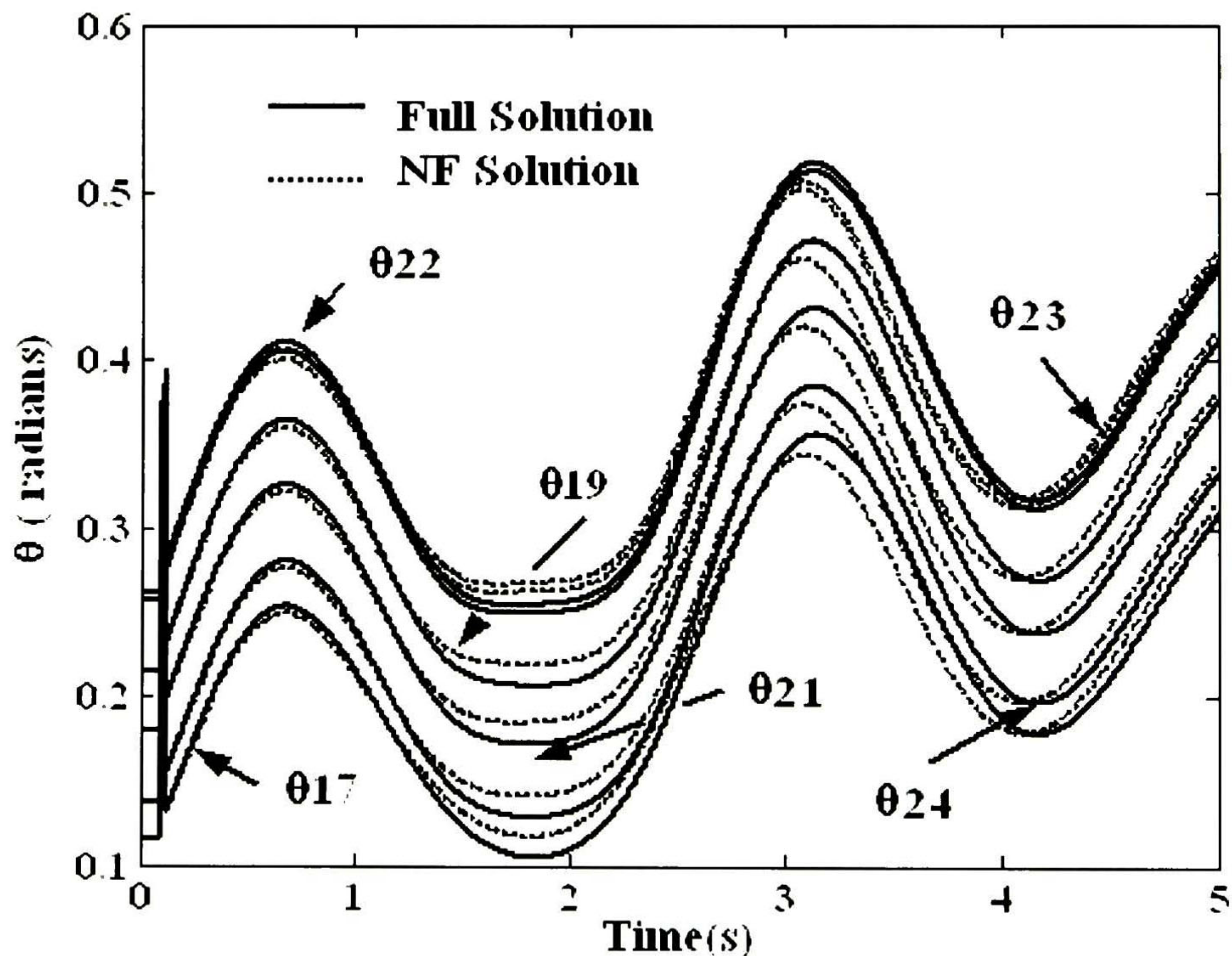
Figure 6.10. Approximate location of dominant second-order participations

Areas formed by second-order participation factors, on the other hand, indicate closely coupled clusters of buses. This information might be useful to study dynamic control interactions in systems with multiple compensation or interactions between controls and loads.

With the above findings in mind, linear and nonlinear time-domain simulations were conducted to verify the accuracy of the model. To verify the correctness of the results, a nonlinear perturbation was applied at selected

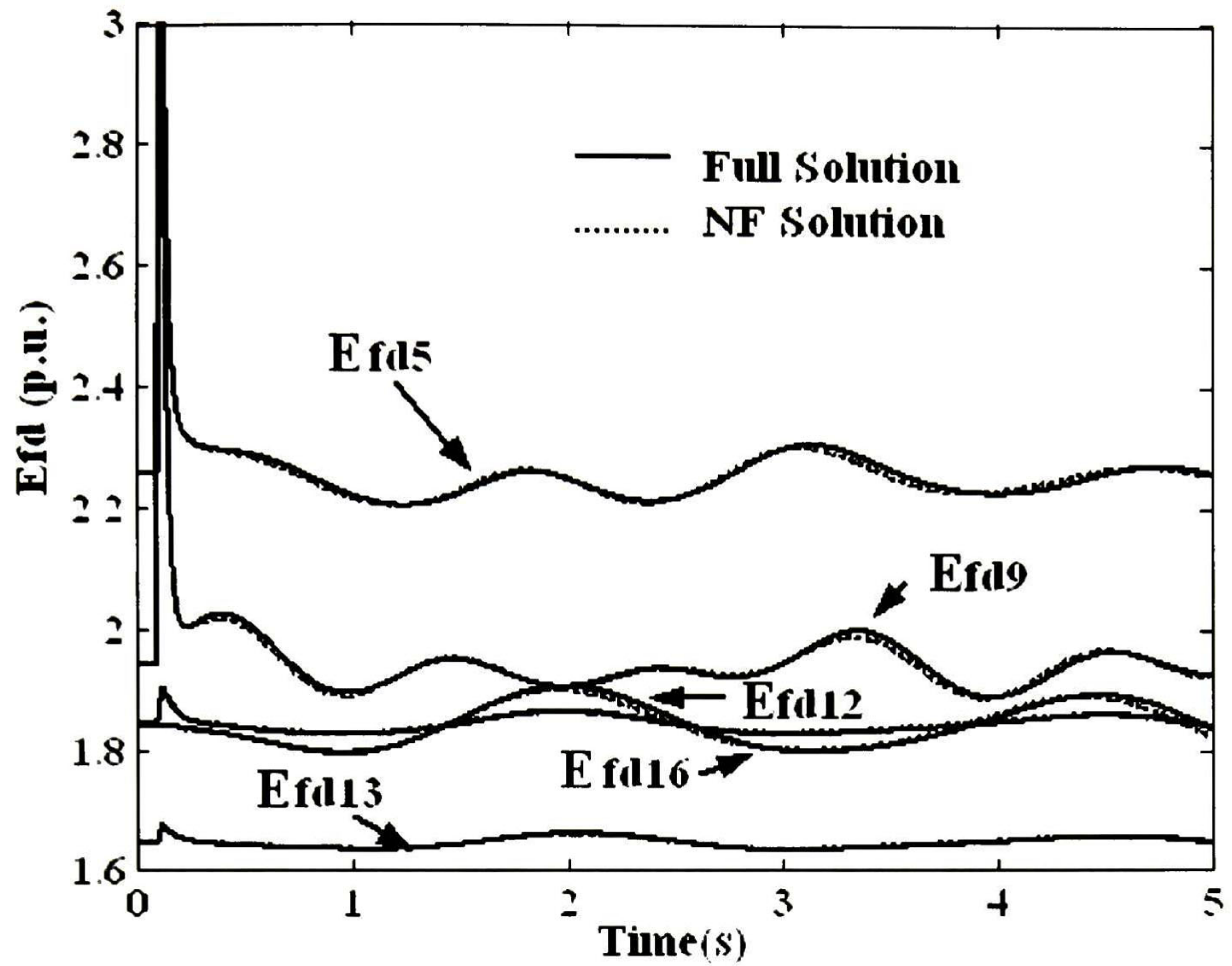
transmission lines. The disturbance considered to test the accuracy of the procedure for determining closed-form time-domain approximations to system behavior is three-phase fault at bus 1 cleared by opening line 1-27. For the purposes of this study, an SVC (-50/150 MVAR) was applied at bus 17, because of its closeness to the dominant bus 21 in Table 6.7. The general SVC control transfer function modeled in the simulation is given in [4].

Figure 6.11 shows the time evolution of selected signals from obtained using (6.2b). Again, the results are compared with the full system solution. In all cases, both approaches provide a consistent result, which shows the accuracy of the proposed techniques.

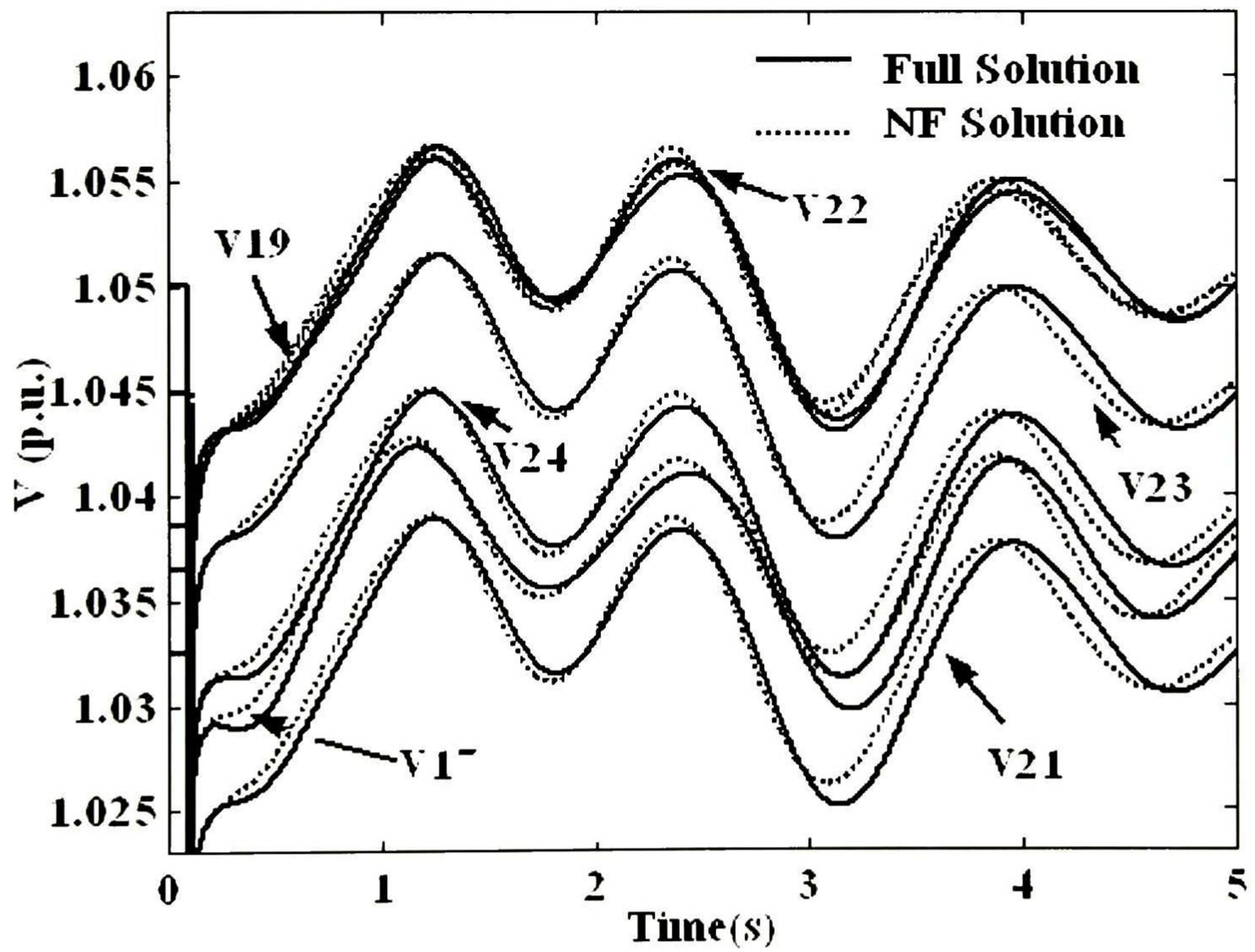


a) Phase deviations

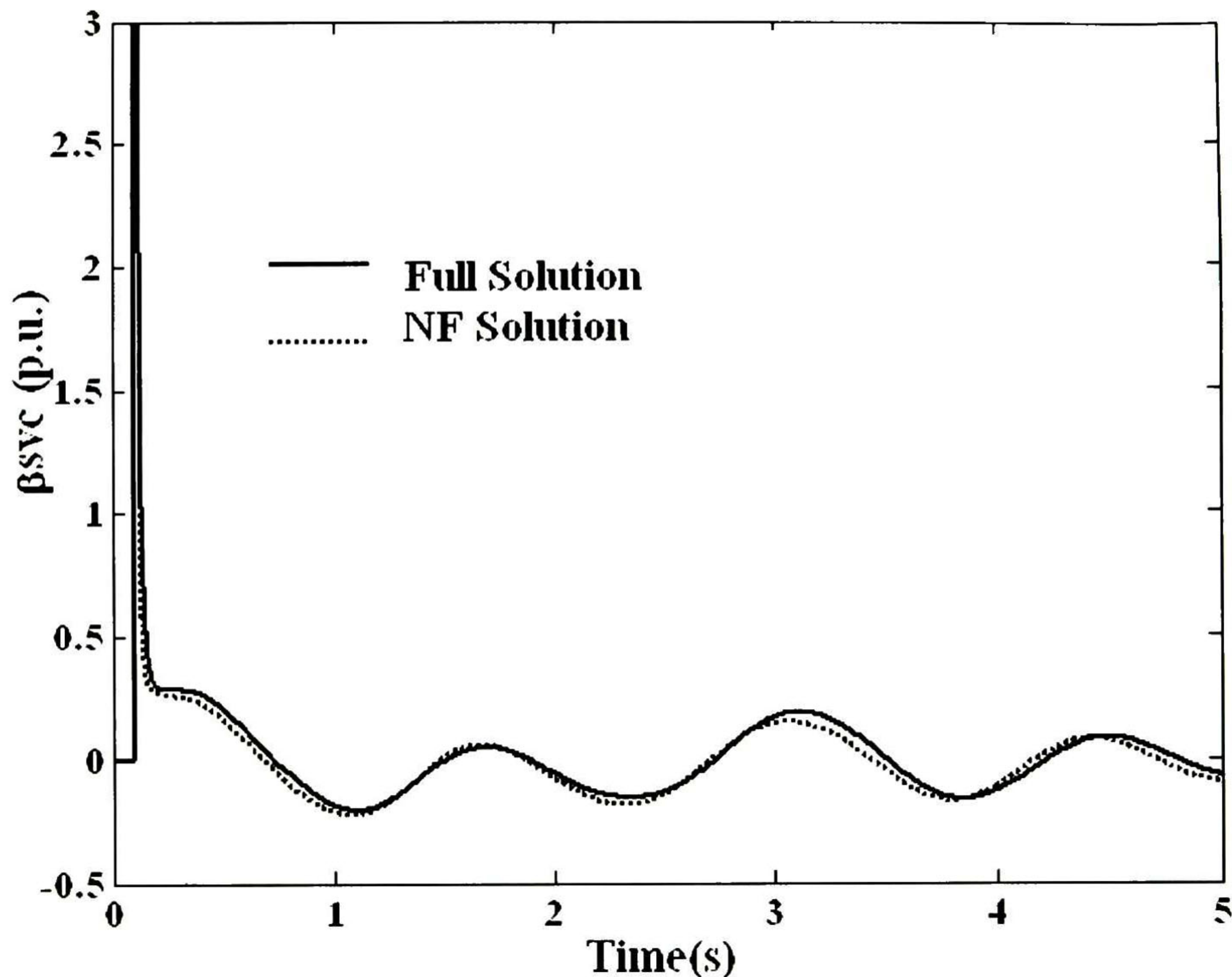
We now turn our attention to the accuracy of the system dynamics predicted by the normal form approximation.



b) Excitation output voltage deviations



c) Bus voltage magnitudes



d) SVC susceptance

Figure 6.11. Comparison of closed-form solutions of selected signals.

6.5 Conclusions

This chapter discusses the experience in the analysis of the network contribution to system behavior. Emphasis has been placed on the analysis of load characteristics and SVC voltage support, but the procedures are general and could be extended to include other devices. Because this information accounts for network and dynamic states, the approach can be used to study both, voltage and angle (wide-area) stability.

Application of nonlinear dynamic analysis has been shown to be a valuable way to study the impact of network variables on intersystem oscillations. Potential applications of the method include the analysis of voltage stability and the study of nonlinear dynamic interactions involving multiple controllers and loads. Numerical issues associated with the two-time scale model approximation are also being investigated.

Efforts have also been made in assessing the potential applicability of these techniques to identify critical system parameters.

References

- [1] G. Rogers, *Power System Oscillations*, The Kluwer International Series in Engineering, Norwell MA: Kluwer Academic Publishers, 2000
- [2] I. Martínez, A. R. Messina, and V. Vittal, "Normal Form Analysis of Complex System Models: A Structure-Preserving Approach", *IEEE Transactions on Power Systems*, vol. 22, pp. 1908-1915, Nov 2007
- [3] W. Brandon, B. W. Gordon and S. Liu, "A singular perturbation approach for modeling differential-algebraic systems", *Journal of Dynamic Systems, Measurement and Control*, vol. 120, pp. 541-545, Dec 1998
- [4] E. Barocio and A.R. Messina, "Normal form analysis of stressed power systems: incorporation of SVC models", *Electrical Power and Energy Systems*, vol. 25, pp. 79-90, Jan 2003
- [5] S. Liu, A. R. Messina and V. Vittal, "Assessing placement of controllers and nonlinear behavior using normal form analysis", *IEEE Trans. on Power Systems*, vol. 20, pp. 1486-1495, Aug 2005

Chapter 7

General Conclusions and Suggestions for Future Work

7.1 General Conclusions

In this work, a systematic procedure based on normal form theory and singular perturbation techniques has been proposed to investigate power system nonlinear behavior. The technique is general and can be used to analyze several physical phenomena or systems described by differential-algebraic equations. Also, because of their general structure, these models can be used in conjunction with many control methodologies and numerical integration packages.

A systematic methodology, based on normal form theory has been proposed for determining the effects of higher-order terms on the power system representation on system performance. While the conceptual framework developed provides a rigorous based for determining the effects of weak nonlinearities on system response, study experience shows that this technique may be used to asses large-scale disturbances.

Structure-preserving models offer a formal option to analyze system behavior which allows the detailed inclusion of network characteristics. This is particularly advantageous in the study of power systems with embedded FACTS controllers and the evaluation of the effects on system dynamic performance.

Analytical experience with test power networks suggest that stressed power systems exhibit a multi-time-scale behavior that must be accounted for. Reduced-order representations are error-prone and may obscure or preclude the analysis of the influence of network characteristics. Analysis of small and

medium size test power systems illustrates that this technique may accurately represent nonlinear system behavior. The encouraging results presented here, however, have been obtained through numerical investigations based on simplified system representations. They also indicate the need for future investigations which more completely treat the role of control devices on the transmission system on system behavior. Studies are being conducted to address the above issues.

A third-order normal form representation of the power system has been adopted as a first approximation to system behavior. Study experience shows that, under some circumstances, higher order representations might be needed.

Network characteristics and control strategies may have a profound influence on system wide-behavior. This is a subject that has not been addressed in analytical work using nonlinear formulations and deserves further investigation.

7.2 Suggestions for Future Work

Few systematic approaches to assess power system behaviour that preserve network structure have been reported. A number of issues, hence, remain open for research.

The future areas of work related to the analysis of effects nonlinear in the power system can be grouped into six main categories:

1. Much work is needed on generalized criteria to determine the optimal singular parameter ε . While the selection of this parameter has not been found to be critical for the test systems under consideration, more general criteria are needed for the analysis of more complex system representations
2. The construction of higher-order normal form representations in more complex systems. In particular, the numerical examples show that the algorithms for normal form analysis of small and medium size systems are feasible. All of the algorithms require the analysis of sparse linear models. The analysis of large power system models requires efficient analysis techniques. In particular advantage should be taken from the sparse nature of the system representation. Issues regarding the construction of the normal form representation should also be addressed.
3. The use of modal sensitivity techniques to quantify the influence of network behavior on the inter-area mode phenomenon should be expanded.

4. The extension of the developed techniques to investigate voltage stability problems.
5. Placement of FACTS controllers is vital to any coordination strategies. Approximate techniques to identify the best locations of FACTS controllers that take into account nonlinear effects are highly desirable. Examination of the impacts of more general control strategies on system-wide behavior are left to further research.
6. Faster and more efficient techniques to identify the most disturbed buses and loads are required. One of the primary applications of this approach is the identification of critical, most disturbed system zones and the evaluation of remedial measures based on aggressive network control. Moreover, the potential use of the method to detect and quantify adverse interactions between system controllers should be investigated.

In addition, various mathematical issues remain to be resolved, especially concerning the analysis of structure-preserving models and the identification of more general techniques to quantify nonlinearity and mode coupling.

Appendix A

A.1 Single-Machine Infinite-Bus Test System Data.

Machine parameters

The machine and network parameters expressed on 2220 MVA base are as follows

$H=3.5$ MWs/MVA, $D=10$ p.u., $X'_d=0.30$ p.u.

Transmission system parameters

$X_r=0.15$ p.u, $X_l=0.50$ p.u.

Initial operating conditions

$P=0.90$ p.u., $Q=-0.30$ p.u. (overexcited), $E_f=1.00\angle 36^\circ$, $E_B=0.995\angle 0^\circ$,

$P_{max}=1.1762$, $\delta^s = \delta^o = 49.92^\circ$, $\omega^o = 0$

Appendix B

The two-system data are as follows:

B.1 Base Case Condition (values in p.u on a 100 MVA base)

Table B.1 Load Data for Cases 1 and 2

Bus	Case 1		Case 2	
	Load (MW)	Load (MVAR)	Load (MW)	Load (MVAR)
5	11.20	1.80	9.20	3.80
6	11.80	1.80	13.80	3.80

Table B.2 Steady-state generator data – Case Study 1

Generator	Terminal voltage	Active power	Reactive power
1	1.020	6.644	-0.128
2	1.020	6.644	3.032
3	1.020	5.229	-0.190
4	1.020	5.000	2.377

Table B.3 Steady-state generator data - Case Study 2

Generator	Terminal voltage	Active power	Reactive power
1	1.0200	6.644	0.131
2	1.0136	6.644	4.998
3	1.0200	5.707	0.044
4	1.0146	5.000	5.001

B.2 Machine and Network Parameters

Table B.4 Generator data (All four generators)

x_d	x_q	x'_d	x'_q	T'_d	T'_q	BMVA
1.80	1.70	0.30	0.30	8.0	0.40	900

Table B.5 Generator damping and Inertia
(On machine base)

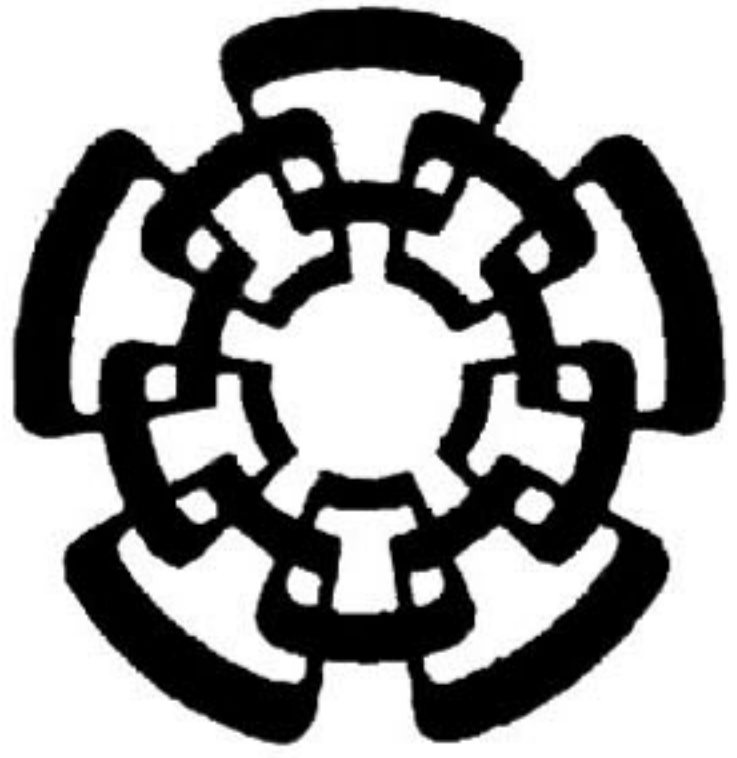
Generator	D	H
1	4.0	6.5
2	2.0	6.5
3	11.0	6.5
4	10.0	6.5

Table B.6 Line data

Bus #	Bus #	R	X
1	2	0.0025	0.025
2	5	0.0010	0.010
5	6	0.0220	0.220
3	4	0.0025	0.025
4	6	0.0010	0.010

Table B.7 Exciter data

Bus #	K_A	T_A	$V_{R_{MIN}}$	$V_{R_{Max}}$
1	180	0.01	-5.0	5.0
2	100	0.01	-5.0	5.0
3	130	0.01	-5.0	5.0
4	220	0.01	-5.0	5.0



CENTRO DE INVESTIGACIÓN Y DE ESTUDIOS AVANZADOS DEL I.P.N. UNIDAD GUADALAJARA

El Jurado designado por la Unidad Guadalajara del Centro de Investigación y de Estudios Avanzados del Instituto Politécnico Nacional aprobó la tesis

Análisis de Sistemas de Potencia que Preservan la Estructura del Modelo Usando Formas Normales

del (la) C.

Irma MARTÍNEZ CARRILLO

el día 11 de Enero de 2008.

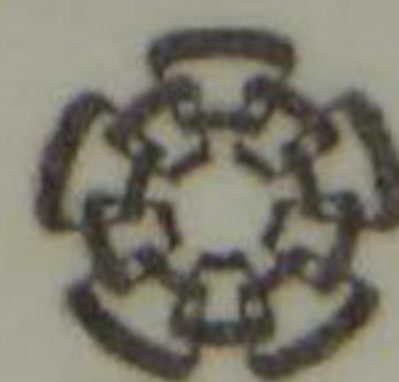
Dr. Arturo Román Messina
Investigador CINVESTAV 3C
CINVESTAV Unidad Guadalajara

Dr. Luis Ernesto López Mellado
Investigador CINVESTAV 3B
CINVESTAV Unidad Guadalajara

Dr. Federico Sandoval Ibarra
Investigador CINVESTAV 3A
CINVESTAV Unidad Guadalajara

Dr. Claudio Rubén Fuerte Esquivel
Profesor
Universidad Michoacana de San
Nicolás de Hidalgo, Facultad de
Ingeniería Eléctrica

Dr. Emilio Barocio Espejo
Profesor Investigador Titular C
Universidad de Guadalajara



CINVESTAV
BIBLIOTECA CENTRAL



SSIT000006324